INTERNATIONAL STANDARD

ISO 6336-1

Second edition
2006-09-01

Corrected version
2007-04-01

Calculation of load capacity of spur and helical gears —

Part 1:
Basic principles, introduction and general influence factors

Calcul de la capacité de charge des engrenages cylindriques à dentures droite et hélicoïdale —

Partie 1: Principes de base, introduction et facteurs généraux d'influence

Reference number
ISO 6336-1:2006(E)

PDF disclaimer

This PDF file may contain embedded typefaces. In accordance with Adobe's licensing policy, this file may be printed or viewed but shall not be edited unless the typefaces which are embedded are licensed to and installed on the computer performing the editing. In downloading this file, parties accept therein the responsibility of not infringing Adobe's licensing policy. The ISO Central Secretariat accepts no liability in this area.

Adobe is a trademark of Adobe Systems Incorporated.

Details of the software products used to create this PDF file can be found in the General Info relative to the file; the PDF-creation parameters were optimized for printing. Every care has been taken to ensure that the file is suitable for use by ISO member bodies. In the unlikely event that a problem relating to it is found, please inform the Central Secretariat at the address given below.

ISO copyright office
Case postale 56 • CH-1211 Geneva 20
Tel. + 41 22 749 01 11
Fax + 41 22 749 09 47
E-mail copyright@iso.org
Web www.iso.org

Published in Switzerland

Contents

Page

Foreword

ISO (the International Organization for Standardization) is a worldwide federation of national standards bodies (ISO member bodies). The work of preparing International Standards is normally carried out through ISO technical committees. Each member body interested in a subject for which a technical committee has been established has the right to be represented on that committee. International organizations, governmental and non-governmental, in liaison with ISO, also take part in the work. ISO collaborates closely with the International Electrotechnical Commission (IEC) on all matters of electrotechnical standardization.

International Standards are drafted in accordance with the rules given in the ISO/IEC Directives, Part 2.

The main task of technical committees is to prepare International Standards. Draft International Standards adopted by the technical committees are circulated to the member bodies for voting. Publication as an International Standard requires approval by at least 75 % of the member bodies casting a vote.

Attention is drawn to the possibility that some of the elements of this document may be the subject of patent rights. ISO shall not be held responsible for identifying any or all such patent rights.

ISO 6336-1 was prepared by Technical Committee ISO/TC 60, *Gears*, Subcommittee SC 2, *Gear capacity calculation*.

This second edition cancels and replaces the first edition (ISO 6336-1:1996), Clauses 6, 7 and 9 of which have been technically revised. It also incorporates the Amendments ISO 6336-1:1996/Cor.1:1998 and ISO 6336-1:1996/Cor.2:1999.

ISO 6336 consists of the following parts, under the general title *Calculation of load capacity of spur and helical gears*:

— *Part 1: Basic principles, introduction and general influence factors*

— *Part 2: Calculation of surface durability (pitting)*

— *Part 3: Calculation of tooth bending strength*

— *Part 5: Strength and quality of materials*

— *Part 6: Calculation of service life under variable load*

This corrected version incorporates the following corrections:

— the lines in Figure 17 have been corrected;

— Figure 19 has been replaced with the correct figure for the wheel blank factor;

— in Equation (90), C_R has been inserted;

— missing parentheses have been added in Equation (B.2);

— the cross-reference following Equation (D.9) has been changed to correspond to that Equation.

Introduction

This and the other parts of ISO 6336 provide a coherent system of procedures for the calculation of the load capacity of cylindrical involute gears with external or internal teeth. ISO 6336 is designed to facilitate the application of future knowledge and developments, also the exchange of information gained from experience.

Design considerations to prevent fractures emanating from stress raisers in the tooth flank, tip chipping and failures of the gear blank through the web or hub will need to be analyzed by general machine design methods.

Several methods for the calculation of load capacity, as well as for the calculation of various factors, are permitted (see 4.1.12). The directions in ISO 6336 are thus complex, but also flexible.

Included in the formulae are the major factors which are presently known to affect gear tooth pitting and fractures at the root fillet. The formulae are in a form that will permit the addition of new factors to reflect knowledge gained in the future.

Calculation of load capacity of spur and helical gears —

Part 1: Basic principles, introduction and general influence factors

1 Scope

This part of ISO 6336 presents the basic principles of, an introduction to, and the general influence factors for, the calculation of the load capacity of spur and helical gears. Together with ISO 6336-2, ISO 6336-3, ISO 6336-5 and ISO 6336-6, it provides a method by which different gear designs can be compared. It is not intended to assure the performance of assembled drive gear systems. It is not intended for use by the general engineering public. Instead, it is intended for use by the experienced gear designer who is capable of selecting reasonable values for the factors in these formulae based on knowledge of similar designs and awareness of the effects of the items discussed.

The formulae in ISO 6336 are intended to establish a uniformly acceptable method for calculating the pitting resistance and bending strength capacity of cylindrical gears with straight or helical involute teeth.

ISO 6336 includes procedures based on testing and theoretical studies such as those of Hirt [1], Strasser [2] and Brossmann [3]. The results of rating calculations made by following this method are in good agreement with previously accepted gear calculations methods (see References [4] to [8]) for normal working pressure angles up to 25° and reference helix angles up to 25°).

For larger pressure angles and larger helix angles, the trends of products $Y_\text{F}\,Y_\text{S}\,Y_\beta$ and, respectively, $Z_\text{H}\,Z_\varepsilon\,Z_\beta$ are not the same as those of some earlier methods. The user of ISO 6336 is cautioned that when the methods in ISO 6336 are used for other helix angles and pressure angles, the calculated results will need to be confirmed by experience.

The formulae in ISO 6336 are not applicable when any of the following conditions exist:

— spur or helical gears with transverse contact ratios less than 1,0;

— spur or helical gears with transverse contact ratios greater than 2,5;

— interference between tooth tips and root fillets;

— teeth are pointed;

— backlash is zero.

The rating formulae in ISO 6336 are not applicable to other types of gear tooth deterioration such as plastic yielding, scuffing, case crushing, welding and wear, and are not applicable under vibratory conditions where there may be an unpredictable profile breakdown. The bending strength formulae are applicable to fractures at the tooth fillet, but are not applicable to fractures on the tooth working surfaces, failure of the gear rim, or failures of the gear blank through web and hub. ISO 6336 does not apply to teeth finished by forging or sintering. It is not applicable to gears which have a poor contact pattern.

The procedures in ISO 6336 provide rating formulae for the calculation of load capacity, based on pitting and tooth root breakage. At pitch line velocities below 1 m/s the gear load capacity is often limited by abrasive wear (see other literature for information on the calculation for this).

2 Normative references

The following referenced documents are indispensable for the application of this document. For dated references, only the edition cited applies. For undated references, the latest edition of the referenced document (including any amendments) applies.

ISO 53:1998, *Cylindrical gears for general and heavy engineering — Standard basic rack tooth profile*

ISO 1122-1:1998, *Vocabulary of gear terms — Part 1: Definitions related to geometry*

ISO 1328-1:1995, *Cylindrical gears — ISO system of accuracy — Part 1: Definitions and allowable values of deviations relevant to corresponding flanks of gear teeth*

ISO 4287:1997, *Geometrical Product Specifications (GPS) — Surface texture: Profile method — Terms, definitions and surface texture parameters*

ISO 4288:1996, *Geometrical Product Specifications (GPS) — Surface texture: Profile method — Rules and procedures for the assessment of surface texture*

ISO 6336-2, *Calculation of load capacity of spur and helical gears — Part 2: Calculation of surface durability (pitting)*

ISO 6336-3, *Calculation of load capacity of spur and helical gears — Part 3: Calculation of tooth bending strength*

ISO 6336-5, *Calculation of load capacity of spur and helical gears — Part 5: Strength and quality of materials*

ISO 6336-6, *Calculation of load capacity of spur and helical gears — Part 6: Calculation of service life under variable load*

3 Terms, definitions, symbols and abbreviated terms

For the purposes of this document, the terms, definitions, symbols and abbreviated terms given in ISO 1122-1 and the following symbols apply.

NOTE Symbols are based on, and are extensions of, the symbols given in ISO 701 and ISO 1328-1. Only symbols for quantities used for the calculation of the particular factors treated in ISO 6336 are given, together with the preferred units.

Table 1 — Symbols used in ISO 6336-1, ISO 6336-2, ISO 6336-3 and ISO 6336-5

Symbol	Description	Unit
Principal symbols and abbreviations		
A, B, C, D, E	points on path of contact (pinion root to pinion tip, regardless of whether pinion or wheel drives, only for geometrical considerations)	—
a	centre distance [a]	mm
α	pressure angle (without subscript, at reference cylinder)	°
B	total face width of double helical gear including gap width	mm
b	face width	mm
β	helix angle (without subscript, at reference cylinder)	°
C	constant, coefficient	—
	relief of tooth flank	µm
c	constant	—
γ	auxiliary angle	°
D	diameter (design)	mm
d	diameter (without subscript, reference diameter)	mm
δ	deflection	µm
E	modulus of elasticity	N/mm^2
Eh	material designation for case-hardened wrought steel	—
Eht	case depth, see ISO 6336-5	mm
e	auxiliary quantity	—
ε	contact ratio, overlap ratio, relative eccentricity (see Clause 7)	—
ζ	roll angle	°
F	composite and cumulative deviations	µm
	force or load	N
f	deviation, tooth deformation	µm
G	shear modulus	N/mm^2
GG	material designation for grey cast iron	—
GGG	material designation for nodular cast iron (perlitic, bainitic, ferritic structure)	—
GTS	material designation for black malleable cast iron (perlitic structure)	—
g	path of contact	mm
ϑ	temperature	°C
HB	Brinell hardness	—
HRC	Rockwell hardness (C scale)	—
HR 30N	Rockwell hardness (30 N scale) (see ISO 6336-5)	—
HV	Vickers hardness	—
HV 1	Vickers hardness at load F = 9,81 N (see ISO 6336-5)	—
HV 10	Vickers hardness at load F = 98,10 N (see ISO 6336-5)	—
h	tooth depth (without subscript, root circle to tip circle)	mm
η	effective dynamic viscosity of the oil wedge at the mean temperature of wedge	mPa s
IF	material designation for flame or induction hardened wrought special steel	—
i	transmission ratio	—
	bin	—
J	Jominy hardenability (see ISO 6336-5)	—
K	constant, factors concerning tooth load	—

Table 1 (*continued*)

Symbol	Description	Unit
L	lengths (design)	mm
l	bearing span	mm
Γ	parameter on the line of action	—
M	moment of a force	Nm
	mean stress ratio	—
ME	symbols identifying material and heat-treatment requirements (see ISO 6336-5)	—
MQ		—
ML		—
m	module	mm
	mass	kg
μ	coefficient of friction	—
N	number, exponent, resonance ratio	—
NT	material designation for nitrided wrought steel, nitriding steel	—
NV	material designation for through-hardened wrought steel, nitrided, nitrocarburized	—
n	rotational speed	s^{-1} or min^{-1}
	number of load cycles	
ν	Poisson's ratio	—
	kinematic viscosity of the oil	mm^2/s
P	transmitted power	kW
p	pitch	mm
	number of planet gears	—
	slope of the Woehler-damage line	—
q	auxiliary factor	—
	flexibility of pair of meshing teeth (see Clause 9)	(mm·µm)/N
	material allowance for finish machining (see ISO 6336-3)	mm
r	radius (without subscript, reference radius)	mm
ρ	radius of curvature	mm
	density (for steel, $\rho = 7{,}83 \times 10^{-6}$)	kg/mm^3
S	safety factor	—
St	material designation for normalized base steel ($\sigma_B < 800$ N/mm^2)	—
s	tooth thickness, distance between mid-plane of pinion and the middle of the bearing span	mm
σ	normal stress	N/mm^2
T	torque	Nm
	tolerance	µm
τ	shear stress	N/mm^2
	angular pitch	mm
u	gear ratio (z_2 / z_1) $\geqslant 1$ [a]	—
U	Miner sum	—
V	material designation for through-hardened wrought special steel, alloy or carbon ($\sigma_B \geqslant 800$ N/mm^2)	—
v	tangential velocity (without subscript, at the reference circle = tangential velocity at pitch circle)	m/s
w	specific load (per unit face width, F_t / b)	N/mm
ψ	auxiliary angle	°
x	profile shift coefficient	—

Table 1 (*continued*)

Symbol	Description	Unit
χ	running-in factor	—
Y	factor related to tooth root stress	—
y	running-in allowance (only with subscript α or β)	µm
Z	factor related to contact stress	—
z	number of teeth [a]	—
ω	angular velocity	rad/s
Subscripts to symbols		
—	reference values (without subscript)	
A	application	
	external shock loads	
a	addendum	
	tooth tip	
ann	annulus gear	
α	transverse contact	
	profile	
b	base circle	
	face width	
be	bearing	
β	helix	
	face width	
	crowning	
C	pitch point	
	profile and helix modification	
ca	case	
cal	calculated	
co	contact pattern	
γ	total (total value)	
D	speed transformation	
	reducing or increasing	
dyn	dynamic	
Δ	rough specimen	
E	elasticity of material	
	resonance	
e	outer limit of single pair tooth contact	
eff	effective value, real stress	
ε	contact ratio	
F	tooth root stress	
f	tooth root, dedendum	
G	geometry	
H	Hertzian stress (contact stress)	
i	internal	
	bin number	
k	values related to the notched test piece	

Table 1 (*continued*)

Symbol	Description
L	lubrication
lim	value of reference strength
M	mean stress influence
m	mean or average value (mean section)
ma	manufacturing
max	maximum value
min	minimum value
N	number (a specific number may be inserted after the subscript N in the life factor)
n	normal plane
	virtual spur gear of a helical gear
	number of revolutions
oil	oil
P	permissible value
	rack profile
p	pitch
	values related to the smooth polished test piece
par	parallel
pla	planet gear
R	roughness
r	radial
red	reduced
rel	relative
s	tooth thickness
	notch effect
sh	shaft
stat	static (load)
sun	sun pinion, sun gear
T	test gear
	values related to the standard reference test gear
t	transverse plane
th	theoretical
v	velocity
	losses
W	pairing of materials
w	working (this subscript may replace the prime)
X	dimension (absolute)
y	running-in
	any point on the tooth flank
z	sun
0	basic value
	tool
1	pinion
2	wheel

Table 1 (*continued*)

Symbol	Description	
1..9	general numbering	
I(II)	end relief	
	reference (nonreference) face	
′	single-flank (subscript w possible) single-pair tooth contact	
″	double-flank contact (simultaneous contact between working and non-working flanks)	
Combined symbols		**Unit**
α_{en}	form-factor pressure angle, pressure angle at the outer point of single pair tooth contact of virtual spur gears	°
α_n	normal pressure angle	°
α_t	transverse pressure angle	°
α'_t or α_{wt}	pressure angle at the pitch cylinder	°
α_{Fen}	load direction angle, relevant to direction of application of load at the outer point of single pair tooth contact of virtual spur gears	°
α_{Pn}	normal pressure angle of the basic rack for cylindrical gears	°
B^*	constant (see equations in Clause 7)	—
b_{cal}	calculated face width	mm
b_{c0}	length of tooth bearing pattern at no load (contact marking)	mm
b_{red}	reduced face width (face width minus end reliefs)	mm
b_s	web thickness	mm
b_B	face width of one helix on a double helical gear	mm
$b_{I(II)}$	length of end relief	mm
β_b	base helix angle	°
β_e	form-factor helix angle, helix angle at the outer point of single tooth contact	°
C_a	tip relief	µm
C_{ay}	tip relief by running-in	µm
C_B	basic rack factor (same rack for pinion and wheel)	—
C_{B1}	basic rack factor (pinion)	—
C_{B2}	basic rack factor (wheel)	—
C_M	correction factor (see Clause 9)	—
C_R	gear blank factor (see Clause 9)	—
$C_{ZL,\ ZR,\ Zv}$	factors for determining lubricant film factors (see ISO 6336-2)	—
C_β	crowning height	µm
$C_{I(II)}$	end relief	µm
c_γ	mean value of mesh stiffness per unit face width	N/(mm·µm)
$c_{\gamma\alpha}$	mean value of mesh stiffness per unit face width (used for K_v, $K_{H\alpha}$, $K_{F\alpha}$)	N/(mm·µm)
$c_{\gamma\beta}$	mean value of mesh stiffness per unit face width (used for $K_{H\beta}$, $K_{F\beta}$)	N/(mm·µm)
c'	maximum tooth stiffness per unit face width (single stiffness) of a tooth pair	N/(mm·µm)
c'_{th}	theoretical single stiffness	N/(mm·µm)
D_{be}	bearing bore diameter (plain bearings)	mm
D_{sh}	journal diameter (plain bearings)	mm
d_a	tip diameter	mm
d_b	base diameter	mm
d_e	diameter of circle through outer point of single pair tooth contact	mm

Table 1 (*continued*)

Symbol	Description	Unit
d_f	root diameter	mm
d_{f2}	root diameter of internal gear	mm
d_{Nf}	root form diameter	mm
d_{sh}	external diameter of shaft, nominal for bending deflection	mm
d_{shi}	internal diameter of a hollow shaft	mm
d_{soi}	diameter at start of involute	mm
d_w	pitch diameter	mm
$d_{1,2}$	reference diameter of pinion (or wheel)	mm
$\delta_{1,2}$	deformation of bearing (1, 2) in direction of load	µm, mm
$\delta_{b\ th}$	combined deflection of mating teeth assuming even load distribution over the face width	µm
δ_g	difference in feeler gauge thickness measurement of mesh misalignment f_{ma}	µm
δ_S	elongation on fracture	%
ε_α	transverse contact ratio	—
$\varepsilon_{\alpha n}$	virtual contact ratio, transverse contact ratio of a virtual spur gear	—
ε_β	overlap ratio	—
ε_γ	total contact ratio, $\varepsilon_\gamma = \varepsilon_\alpha + \varepsilon_\beta$	—
ε_1	addendum contact ratio of the pinion, $\varepsilon_1 = CE/p_{bt}$	—
ε_2	addendum contact ratio of the wheel, $\varepsilon_2 = AC/p_{bt}$	—
ζ_{aw}	roll angle from working pitch point to tip diameter	°
ζ_{fw}	roll angle from root form diameter to working pitch point	°
$F_{be\ r}$	radial force on bearing	N
F_{bn}	(nominal) load, normal to the line of contact	N
F_{bt}	nominal transverse load in plane of action (base tangent plane)	N
F_m	mean transverse tangential load at the reference circle relevant to mesh calculations, $F_m = (F_t K_A K_v)$	N
$F_{m\ T}$	mean transverse tangential part load at reference circle	N
F_{max}	maximum tangential tooth load for the mesh calculated	N
F_t	(nominal) transverse tangential load at reference cylinder per mesh	N
F_{tH}	determinant tangential load in a transverse plane for $K_{H\alpha}$ and $K_{F\alpha}$, $F_{tH} = F_t K_A K_v K_{H\beta}$	N
F_α	total profile deviation	µm
F_β	total helix deviation	µm
$F_{\beta 6}$	tolerance on total helix deviation for ISO accuracy grade 6	µm
$F_{\beta x}$	initial equivalent misalignment (before running-in)	µm
$F_{\beta x\ cv}$	initial equivalent misalignment for the determination of the crowning height (estimate)	µm
$F_{\beta x\ T}$	equivalent misalignment measured under a partial load	µm
$F_{\beta y}$	effective equivalent misalignment (after running-in)	µm
f_{be}	component of equivalent misalignment [b] due to bearing deformation	µm
f_{ca}	component of equivalent misalignment [b] due to case deformation	µm
$f_{f\alpha}$	profile form deviation (the value for the total profile deviation F_α may be used alternatively for this, if tolerances complying with ISO 1328-1 are used)	µm
f_{ma}	mesh misalignment [b] due to manufacturing deviations	µm
f_{pt}	transverse single pitch deviation	µm

Table 1 (*continued*)

Symbol	Description	Unit
f_{par}	non-parallelism of pinion and wheel axes (manufacturing deviation) [b]	µm
f_{pb}	transverse base pitch deviation (the values of f_{pt} may be used for calculations in accordance with ISO 6336, using tolerances complying with ISO 1328-1)	µm
f_{sh}	component of equivalent misalignment [b] due to deformations of pinion and wheel shafts	µm
f_{shT}	component of misalignment due to shaft and pinion deformation measured at a partial load	µm
f_{sh0}	shaft deformation under specific load [b]	µm·mm/N
$f_{H\beta}$	helix slope deviation (the value for the total helix deviation F_β may be used alternatively for this, if tolerances complying with ISO 1328-1 are used)	µm
$f_{H\beta 6}$	tolerance on helix slope deviation for ISO accuracy grade 6	µm
g_α	length of path of contact	mm
h_{aP}	addendum of basic rack of cylindrical gears	mm
h_{fP}	dedendum of basic rack of cylindrical gears	mm
h_{f2}	dedendum of tooth of an internal gear	mm
h_{min}	minimum lubricant film thickness	mm
h_{Fe}	bending moment arm for tooth root stress relevant to load application at the outer point of single pair tooth contact	mm
h_t	tooth height	mm
J^*	moment of inertia per unit face width	kg·mm²/mm
K'	constant of the pinion offset	—
K_v	dynamic factor	—
K_A	application factor	—
$K_{F\alpha}$	transverse load factor (root stress)	—
$K_{F\beta}$	face load factor (root stress)	—
$K_{H\alpha}$	transverse load factor (contact stress)	—
$K_{H\beta}$	face load factor (contact stress)	—
K_γ	mesh load factor (takes into account the uneven distribution of the load between meshes for multiple transmission paths)	—
l_a	effective length of roller (roller bearings)	mm
m^*	relative individual gear mass per unit face width referenced to line of action	kg/mm
m_n	normal module	mm
m_{red}	reduced gear pair mass per unit face width referenced to the line of action	kg/mm
m_t	transverse module	mm
N_F	exponent	—
N_i	number of cycles to failure for bin i	—
N_L	number of load cycles	—
N_S	resonance ratio in the main resonance range	—
$n_{1,2}$	rotation speed of pinion (or wheel)	min^{-1} or s^{-1}
n_i	number of cycles for bin i	—
n_E	resonance speed	min^{-1}
p_{bn}	normal base pitch	mm
p_{bt}	transverse base pitch	mm
q'	minimum value for the flexibility of a pair of meshing teeth	(mm·µm)/N
q_{pr}	protuberance of the tool (see ISO 6336-3)	mm
q_s	notch parameter, $q_s = s_{Fn} / 2\rho_F$	—

Table 1 (*continued*)

Symbol	Description	Unit
q_{sk}	notch parameter of the notched test piece	—
q_{sT}	notch parameter of the standard reference test gear, $q_{sT} = 2,5$	—
q_{α}	auxiliary factor	—
Ra	arithmetic mean roughness value, $Ra = 1/6\ Rz$	µm
Rz	mean peak-to-valley roughness (as specified in ISO 4287 and ISO 4288)	µm
Rz_{k}	mean peak-to-valley roughness of the notched, rough test piece	µm
Rz_{T}	mean peak-to-valley roughness of the standard reference test gear, $Rz_{T} = 10$	µm
r_{b}	base radius	mm
ρ_{fP}	root fillet radius of the basic rack for cylindrical gears	mm
ρ_{g}	radius of grinding notch	mm
ρ_{red}	radius of relative curvature	mm
ρ_{C}	radius of relative curvature at the pitch surface	mm
ρ_{F}	tooth root radius at the critical section	mm
ρ'	slip-layer thickness	mm
S_{F}	safety factor for tooth breakage	—
S_{H}	safety factor for pitting	—
s_{c}	film thickness of marking compound used in contact pattern determination	µm
s_{pr}	residual fillet undercut, $s_{pr} = q_{pr} - q$	mm
s_{Fn}	tooth root chord at the critical section	mm
s_{R}	rim thickness	mm
$\sigma_{k\ lim}$	nominal notched-bar stress number (bending)	N/mm^2
$\sigma_{p\ lim}$	nominal plain-bar stress number (bending)	N/mm^2
σ_{B}	tensile strength	N/mm^2
σ_{F}	tooth root stress	N/mm^2
σ_{Fi}	tooth root stress for bin i	N/mm^2
$\sigma_{F\ lim}$	nominal stress number (bending)	N/mm^2
σ_{FE}	allowable stress number (bending), $\sigma_{FE} = \sigma_{F\ lim}\ Y_{ST}$	N/mm^2
σ_{FG}	tooth root stress limit	N/mm^2
σ_{FP}	permissible tooth root stress	N/mm^2
σ_{F0}	nominal tooth root stress	N/mm^2
σ_{H}	contact stress	N/mm^2
σ_{Hi}	contact stress for bin i	N/mm^2
$\sigma_{H\ lim}$	allowable stress number (contact)	N/mm^2
σ_{HG}	pitting stress limit	N/mm^2
σ_{HP}	permissible contact stress	N/mm^2
σ_{H0}	nominal contact stress	N/mm^2
σ_{S}	yield stress	N/mm^2
σ_{i}	stress for bin i	N/mm^2
$\sigma_{0,2}$	proof stress (0,2 % permanent set)	N/mm^2
$T_{1,2}$	nominal torque at the pinion (or wheel)	N m
T_{eq}	equivalent torque	N m
T_{i}	torque for bin i	N m
T_{n}	nominal torque	N m

Table 1 (*continued*)

Symbol	Description	Unit
t_g	maximum depth of grinding notch	mm
U	sum of individual damage parts	—
w_m	mean specific load (per unit face width)	N/mm
w_t	tangential load per unit tooth width, including overload factors	N/mm
$x_{1,2}$	profile shift coefficient of pinion (or wheel)	—
χ^*	relative stress gradient in the root of a notch	mm^{-1}
χ_β	factor characterizing the equivalent misalignment after running-in	—
χ^*_p	relative stress gradient in a smooth polished test piece	mm^{-1}
Y_{DT}	deep tooth factor	—
Y_F	tooth form factor, for the influence on nominal tooth root stress with load applied at the outer point of single pair tooth contact	—
Y_M	mean stress influence factor	—
Y_{Nk}	life factor for tooth root stress, relevant to the notched test piece	—
Y_{Np}	life factor for tooth root stress, relevant to the plain polished test piece	—
Y_{NT}	life factor for tooth root stress for reference test conditions	—
Y_R	tooth root surface factor (relevant to the plain polished test piece)	—
$Y_{R\ rel\ k}$	relative roughness factor, the quotient of the gear tooth root surface factor of interest divided by the notch test piece factor, $Y_{R\ rel\ k} = Y_R/Y_{Rk}$	—
$Y_{R\ rel\ T}$	relative surface factor, the quotient of the gear tooth root surface factor of interest divided by the tooth root surface factor of the reference test gear, $Y_{R\ rel\ T} = Y_R/Y_{RT}$	—
Y_S	stress correction factor, for the conversion of the nominal tooth root stress, determined for application of load at the outer point of single pair tooth contact, to the local tooth root stress	—
Y_{Sg}	stress correction factors for teeth with grinding notches	—
Y_{Sk}	stress correction factor, relevant to the notched test piece	—
Y_{ST}	stress correction factor, relevant to the dimensions of the reference test gears	—
Y_X	size factor (tooth root)	—
Y_β	helix angle factor (tooth root)	—
Y_δ	notch sensitivity factor of the actual gear (relative to a polished test piece)	—
$Y_{\delta k}$	sensitivity factor of a notched test piece, relative to a smooth polished test piece	—
$Y_{\delta T}$	sensitivity factor of the standard reference test gear, relative to the smooth polished test piece	—
$Y_{\delta\ rel\ k}$	test relative notch sensitivity factor, the quotient of the gear notch sensitivity factor of interest divided by the notched test piece factor, $Y_{\delta\ rel\ k} = Y_\delta/Y_{\delta k}$	—
$Y_{\delta\ rel\ T}$	relative notch sensitivity factor, the quotient of the gear notch sensitivity factor of interest divided by the standard test gear factor, $Y_{\delta\ rel\ T} = Y_\delta/Y_{\delta T}$	—
y_α	running-in allowance for a gear pair	µm
y_β	running-in allowance (equivalent misalignment)	µm
Z_v	velocity factor	—
Z_B, Z_D	single pair tooth contact factors for the pinion, for the wheel	—
Z_E	elasticity factor	$\sqrt{N/mm^2}$
Z_H	zone factor	—
Z_L	lubricant factor	—
Z_N	life factor for contact stress	—
Z_{NT}	life factor for contact stress for reference test conditions	—

Table 1 (*continued*)

Symbol	Description	Unit
Z_R	roughness factor affecting surface durability	—
Z_W	work hardening factor	—
Z_X	size factor (pitting)	—
Z_β	helix angle factor (pitting)	—
Z_ε	contact ratio factor (pitting)	—
z_n	virtual number of teeth of a helical gear	—
$z_{1,2}$	number of teeth of pinion (or wheel) [a]	—
$\omega_{1,2}$	angular velocity of pinion (or wheel)	rad/s

[a] For external gears a, z_1 and z_2 are positive; for internal gearing, a and z_2 have a negative sign, z_1 has a positive sign.
[b] The components in the plane of action are determinant.

4 Basic principles

4.1 Application

4.1.1 Scuffing

Formulae for scuffing resistance on cylindrical gear teeth are not included in ISO 6336. At the present time there is insufficient agreement concerning the method for designing cylindrical gears to resist scuffing failure.

4.1.2 Wear

Very little attention and concern have been devoted to the study of gear tooth wear. This subject primarily concerns gear teeth with low surface hardness or gears with improper lubrication. No attempt has been made to cover the subject in ISO 6336.

4.1.3 Micropitting

ISO 6336 does not cover micropitting, which is an additional type of surface distress that may occur on gear teeth.

4.1.4 Plastic yielding

ISO 6336 does not extend to stress levels greater than those permissible at 10^3 cycles or less, since stresses in this range may exceed the elastic limit of the gear tooth in bending or in surface compressive stress. Depending on the material and the load imposed, a single stress cycle greater than the limit level at $< 10^3$ cycles could result in plastic yielding of the gear tooth.

4.1.5 Particular categories

Pitting resistance and bending strength rating systems for a particular category of cylindrical gearing may be established by selecting proper values for the factors used in these general formulae.

4.1.6 Specific applications

For the design of gears it is very important to recognize that requirements for different fields of application vary considerably. Use of ISO 6336 procedures for specific applications demands a realistic and knowledgeable appraisal of all applicable considerations, particularly:

- the allowable stress of the material and the number of load repetitions,
- the consequences of any percentage of failure (failure rate), and
- the appropriate safety factor.

The following three application fields exemplify the requirements of the above-mentioned characteristics.

4.1.6.1 Vehicle final drive gears

For vehicle final drive gears, which are relatively low speed, coarse pitch teeth, are chosen for adequate strength. As a consequence, pinions have small numbers of teeth (z_1 of about 14), whereas a value z_1 of about 28 would be chosen for a comparatively high speed gear of similar size. Thus, the tooth bending strength of the former would be about twice that of the latter.

The computed reliability of vehicle gears can be as low as 80 % to 90 % whereas that of high speed industrial gears should be at least 99 %.

In general, the material used in high volume vehicle gear production may be of more uniform quality than that used for gears produced in small numbers.

Comparison of applied gear designs has indicated that for about 10 000 cycles, the load transmitted by truck final drive gears is about four times greater than that transmitted by aircraft or space vehicle gears, where the material, quality, size and design are the same.

For low speed vehicle gears which are intended to have short lives (less than 100 000 cycles), small amounts of plastic deformation, pitting and abrasive wear can usually be tolerated. Consequently, the levels of surface stress which are permissible are substantially higher than would be permissible for long life, high speed gears.

4.1.6.2 Main drive for aircraft and space vehicles

For main drives of aircraft and space vehicles, which are found in helicopter rotor drives and the main pump drives of space vehicle boosters, gears of the highest quality material and accuracy are used. Such gears are extensively tested. For example, 10 to 20 transmissions of the same production series may be tested under operational conditions for the full design life. The tolerable wear rate is established on the basis of test results. Lubricant spray rate, position of injection points and direction of spray is optimized.

For these reasons, higher loading is permissible for a design life up to 100 times longer (in cycles of tooth loading), and speeds about 10 times greater than those of a typical vehicle transmission. The probability of damage in such cases shall not exceed 0,1 % to 1 %. Overall loading cannot be as high as for vehicle gears, since neither surface wear nor minor damage can be tolerated.

4.1.6.3 Industrial high speed gears

For industrial high speed gears, where the pitch line velocities exceed 50 m/s, the pinions are often designed with 30 or more teeth with the objective of minimizing the risk of scuffing and wear. A typical gear pair would consist of a pinion with 45 teeth and a wheel with 248.

Industrial high speed gears should be better than 99 % reliable for a normal life of more than 10^{10} cycles. Extensive prototype testing is normally excluded because of the cost. As a consequence, the load capacity ratings of high speed gears tend to be conservative with relatively high safety factors.

4.1.7 Safety factors

It is necessary to distinguish between the safety factor relative to pitting, S_H, and that relative to tooth breakage, S_F.

For a given application, adequate gear load capacity is demonstrated by the computed values of S_H and S_F being greater than or equal to the values $S_{H\,min}$ and $S_{F\,min}$, respectively.

Certain minimum values for safety factors shall be determined. Recommendations concerning these minimum values are made in ISO 6336, but values are not proposed.

An appropriate probability of failure and the safety factor shall be carefully chosen to meet the required reliability at a justifiable cost. If the performance of the gears can be accurately appraised through testing of the actual unit under actual load conditions, a lower safety factor and more economical manufacturing procedures may be permissible:

$$\text{Safety factor} = \frac{\text{Modified allowable stress number}}{\text{Calculated stress}}$$

Safety factors based on load are permitted. When they are based on load the safety factor equals the specific calculated load capacity divided by the specific operating load transmitted. When the factor is based on load, this shall be stated clearly.

NOTE Safety factors based on load (power) relative to tooth bending are proportional to S_F. Safety factors based on load (power) relative to pitting are proportional to S_H^2.

In addition to the general requirements mentioned and the special requirements for surface durability, pitting, (see ISO 6336-2) and tooth bending strength (see ISO 6336-3), the safety factors shall be chosen after careful consideration of the following influences.

- Reliability of material data: ISO 6336-applicable materials, for which data are given in ISO 6336-5, and their abbreviations, are listed in Table 2. The allowable stress numbers used in the calculation are valid for a given probability of failure; the material values in ISO 6336-5 are valid for 1 % probability of damage. This risk of damage reduces with the increase of the safety factor and vice versa.
- Reliability of load values used for calculation: if loads or the response of the system to vibration, are estimated rather than measured, a larger safety factor should be used.
- Variations in gear geometry due to manufacturing tolerances.
- Variations in alignment.
- Variations in material due to process variations in chemistry, cleanliness and microstructure (material quality and heat treatment).
- Variations in lubrication and its maintenance over the service life of the gears.

Depending on the reliability of the assumptions on which the calculations are based (e.g. load assumptions) and according to the reliability requirements (consequences of damage occurrence), a corresponding safety factor is to be chosen.

Where gears are produced under a specification or a request for proposal (quotation), in which the gear supplier is to provide gears or assembled gear drives having specified calculated capacities (ratings) in accordance with ISO 6336, the value of the safety factor for each mode of failure (pitting, tooth breakage) is to be agreed upon between the parties.

Table 2 — Materials

Material	Type	Abbreviation
Normalized low carbon steels / cast steels	Wrought normalized low carbon steels	St
	Cast steels	St (cast)
Cast iron materials	Black malleable cast iron (perlitic structure)	GTS (perl.)
	Nodular cast iron (perlitic, bainitic, ferritic structure)	GGG (perl., bai., ferr.)
	Grey cast iron	GG
Through-hardened wrought steels	Carbon steels, alloy steels	V
Through-hardened cast steels	Carbon steels, alloy steels	V(cast)
Case-hardened wrought steels		Eh
Flame or induction hardened wrought or cast steels		IF
Nitrided wrought steels / nitriding steels / through-hardening steels, nitrided	Nitriding steels	NT(nitr.)
	Through hardening steels	NV (nitr.)
Wrought steels, nitrocarburized	Through hardening steels	NV (nitrocar.)

4.1.8 Testing

The most reliable known approach to the appraisal of overall system performance is that of testing a proposed new design. Where sufficient field or test experience is available, satisfactory results can be obtained by extrapolation of previous tests or field data.

When suitable test results or field data are not available, values for the rating factors should be chosen conservatively.

4.1.9 Manufacturing tolerances

Evaluation of rating factors should be based on the minimum accuracy grade limits specified for the component parts in the manufacturing process.

4.1.10 Implied accuracy

Where empirical values for rating factors are given by curves, curve fitting equations are provided to facilitate computer programming. The constants and coefficients used in curve fitting often have significant digits in excess of those appropriate to the reliability of the empirical data.

4.1.11 Other considerations

In addition to the factors considered in ISO 6336 influencing pitting resistance and bending strength, other interrelated system factors can have a significant influence on overall transmission performance. The following factors are particularly significant.

4.1.11.1 Lubrication

The ratings determined by these formulae are valid only if the gear teeth are operated with a lubricant of proper viscosity and additives for the load, speed and surface finish, and if there is a sufficient quantity of lubricant supplied to the gear teeth and bearings to lubricate and maintain an acceptable operating temperature.

4.1.11.2 Misalignment and deflection of foundations

Many gear systems depend on external supports such as machinery foundations to maintain alignment of the gear mesh. If these supports are poorly designed, initially misaligned, or become misaligned during operation through elastic or thermal deflection or other influences, overall gear system performance will be adversely affected.

4.1.11.3 Deflections

Deflections of gear teeth, gear blanks, gear shafts, bearings and housings affect performance and distribution of total tooth load over meshing flanks. Since these deflections vary with load, it is impossible to obtain optimum tooth contact at different loads in those transmissions that encounter variable load. When gear tooth flanks are not modified, the face load factor increases with increasing deflection, thereby lowering rated capacity.

4.1.11.4 System dynamics

The method of analysis used in ISO 6336 provides a dynamic factor in the formulae by derating the gears for increased loads caused by gear tooth inaccuracies and for harmonic effects. In general, simplified values are given for easy application. The dynamic response of the system results in additional gear tooth loads due to the relative motions of the connected masses of the driver and the driven equipment. The application factor, K_{A}, is intended to account for the operating characteristics of the driving and driven equipment. It must be recognized, however, that if the operating roughness of the driver, gearbox or driven equipment causes an excitation with a frequency that is near to one of the system's major natural frequencies, resonant vibrations can cause severe overloads which could be several times higher than the nominal load.

For critical service applications, it is recommended that a vibration analysis be performed. This analysis shall include the total system of driver, gearbox, driven equipment, couplings, mounting conditions and sources of excitation. Natural frequencies, mode shapes and the dynamic response amplitudes should be calculated. The resulting load spectrum cumulative fatigue effect calculation, if necessary or required, is given in ISO 6336-6.

4.1.11.5 Contact pattern

The teeth of most cylindrical gears are modified in both profile and helix directions during the manufacturing operation to accommodate deflection of the mountings and thermal distortions. This results in a localized contact pattern during roll testing under light loads. Under design load, the contact should spread over the tooth flank without any concentration of the pattern at the edges. This influence shall be taken into account by the corresponding load distribution factor.

4.1.11.6 Corrosion

Corrosion of gear tooth surfaces can significantly reduce the bending strength and pitting resistance of the teeth. Quantifying the extent of these reductions is beyond the scope of ISO 6336.

4.1.12 Influence factors

The influence factors presented in ISO 6336 are derived from results of research and field service. It is convenient to distinguish between the following.

a) Factors which are determined by gear geometry or which have been established by convention. They shall be calculated in accordance with the equations given in ISO 6336.

b) Factors which account for several influences and which are dealt with as independent of each other, but which may nevertheless influence each other to a degree for which no numerical value can be assigned. These include the factors K_{A}, K_{v}, $K_{\mathrm{H}\alpha}$, $K_{\mathrm{H}\beta}$ or $K_{\mathrm{F}\alpha}$ and the factors influencing allowable stress.

The factors K_v, $K_{H\beta}$ and $K_{H\alpha}$ also depend on the magnitudes of the profile and helix modifications. Profile and helix modifications are only effective if they are significantly larger than the manufacturing deviations. For this reason, the influence of the profile and helix modifications may only be taken into consideration if the gear manufacturing deviations do not exceed specific limit values. The minimum required gear manufacturing accuracy is stated, together with reference to ISO 1328-1, for each factor.

The influence factors can be determined by various methods. These are qualified, as necessary, by adding subscripts A through C to the symbols. Unless otherwise specified, e.g. in an application standard, the more accurate of the methods is to be preferred for important transmissions. In cases of dispute, when proof of accuracy and reliability is supplied, Method A is superior to Method B, and Method B to Method C.

It is recommended that supplementary subscripts be used whenever the method used for evaluation of a factor would not be readily identifiable.

In some applications it could be necessary to choose between factors which have been determined using alternative methods (e.g. the alternatives for the determination of the equivalent misalignment). When necessary, the relevant method can be indicated by extending the subscript, e.g. $K_{H\beta\text{-B1}}$.

ISO 6336 is primarily intended for verifying the load capacity of gears for which essential calculation data are available by way of detail drawings, or in similar form.

The data available at the primary design stage is usually restricted. It is therefore necessary, at this stage, to make use of approximations or empirical values for some factors.

For given fields of application or for rough calculations, it is often permissible to substitute unity or some other constant for some factors. In doing so, it is necessary to verify that a good margin of safety is assured. Otherwise, the safety factor shall be adequately increased.

More precise evaluation is possible when manufacture and inspection is completed, for then data obtained by direct measurement are available.

Contractual provisions relating to the nature of the calculation proof shall be agreed in advance between manufacturer and purchaser.

4.1.12.1 Method A

Method A factors are derived from the results of full scale load tests, precise measurements or comprehensive mathematical analysis of the transmission system on the basis of proven operating experience, or any combination of these. All gear and loading data shall be available. In such cases the accuracy and reliability of the method used shall be demonstrated and the assumptions clearly stated.

In general, and for the following reasons, Method A is seldom used:

— the relevant relationships have not been more extensively researched than those in Methods B and C;

— details of the operating conditions are incomplete;

— suitable measuring equipment is not available;

— the costs of analysis and measurements exceed their value.

4.1.12.2 Method B

Method B factors are derived with sufficient accuracy for most applications. Assumptions involved in their determination are listed. In each case, it is necessary to assess whether or not these assumptions apply to the conditions of interest. Additional subscripts should be inserted when necessary, e.g. $K_{v\text{-B}}$.

4.1.12.3 Method C

Method C is where simplified approximations are specified for some factors. The assumptions under which they have been determined are listed. On each occasion an assessment should be made as to whether or not these assumptions apply to the existing conditions. The additional subscript C shall be used when necessary, e.g. $K_{\text{v-C}}$.

4.1.13 Numerical equations

It is necessary to apply the numerical equations specified in ISO 6336 with the stated units. Any exceptions are specially noted.

4.1.14 Succession of factors in course of calculation

The factors K_v, $K_{\text{H}\beta}$ or $K_{\text{F}\beta}$ and $K_{\text{H}\alpha}$ or $K_{\text{F}\alpha}$ depend on a nominal tangential load. They are also to some extent interdependent and shall therefore be calculated successively as follows:

a) K_v with the load $F_\text{t}\,K_\text{A}$;

b) $K_{\text{H}\beta}$ or $K_{\text{F}\beta}$ with the load $F_\text{t}\,K_\text{A}\,K_\text{v}$;

c) $K_{\text{H}\alpha}$ or $K_{\text{F}\alpha}$ with the load $F_\text{t}\,K_\text{A}\,K_\text{v}\,K_{\text{H}\beta\,(\text{F}\beta)}$ [1].

When a gear drives two or more mating gears, it is necessary to multiply by ($K_\text{A}\,K_\gamma$) instead of K_A; also see 4.2.

4.1.15 Determination of allowable values of gear deviations

The allowable values of gear deviation shall be determined in accordance with ISO 1328-1.

4.2 Tangential load, torque and power

When assessing the load acting on gear teeth, all loads affecting the gearing shall be considered.

In the case of double helical gears, it is assumed that the total tangential load is divided equally between the two helices. If this is not the case, for examples as a consequence of externally applied axial loads, this shall be taken into consideration. The two halves of the helix should be treated as two helical gears arranged in parallel.

Concerning multiple-path transmissions, the total tangential load is not quite evenly distributed to the various load paths (irrespective of design, tangential velocity or accuracy of manufacture). Allowance is made for this by means of the mesh load factor K_γ (see also 4.1.14). If possible, K_γ should preferably be determined by measurement; alternatively, its value may be estimated from the literature.

If the operating speed is near to a resonance speed, a careful study is necessary. See Clauses 5 and 6.

4.2.1 Nominal tangential load, nominal torque and nominal power

The nominal tangential load F_t is determined in the transverse plane at the reference cylinder. It is derived from the nominal torque or power transmitted by the gear pair.

The load capacity rating of gears is effectively based on the input torque to the driven machine. This is the torque corresponding to the heaviest regular working condition. Alternatively, the nominal torque of the prime

1) $K_{\text{H}\beta}$ is also to be used in the evaluation of $K_{\text{F}\alpha}$, since for tooth bending it is $K_{\text{H}\beta}$ which represents the determinant load due to uneven distribution of F_t over the face width (see 7.2.1).

mover can be used as a basis if it corresponds to the torque requirement of the driven machine, or some other suitable basis can be chosen.

F_t is defined as the nominal tangential load per mesh, i.e. for the mesh under consideration. T and P are defined accordingly. In the following equations, $n_{1,2}$ is given in revolutions per minute.

$$F_t = \frac{2\,000\,T_{1,2}}{d_{1,2}} = \frac{19\,098 \times 1000\,P}{d_{1,2}\,n_{1,2}} = \frac{1000\,P}{v} \tag{1}$$

$$T_{1,2} = \frac{F_t\,d_{1,2}}{2\,000} = \frac{1000\,P}{\omega_{1,2}} = \frac{9\,549\,P}{n_{1,2}} \tag{2}$$

$$P = \frac{F_t\,v}{1\,000} = \frac{T_{1,2}\,\omega_{1,2}}{1\,000} = \frac{T_{1,2}\,n_{1,2}}{9\,549} \tag{3}$$

$$v = \frac{d_{1,2}\,\omega_{1,2}}{2\,000} = \frac{d_{1,2}\,n_{1,2}}{19\,098} \tag{4}$$

$$\omega_{1,2} = \frac{2\,000\,v}{d_{1,2}} = \frac{n_{1,2}}{9{,}549} \tag{5}$$

4.2.2 Equivalent tangential load, equivalent torque and equivalent power

When the transmitted load is not uniform, consideration should be given not only to the peak load and its anticipated number of cycles, but also to intermediate loads and their numbers of cycles. This type of load is classed as a *duty cycle* and may be represented by a load spectrum. In such cases, the cumulative fatigue effect of the duty cycle is considered in rating the gear set. A method of calculating the effect of the loads under this condition is given in ISO 6336-6.

4.2.3 Maximum tangential load, maximum torque and maximum power

This is the maximum tangential load $F_{t\,max}$ (or corresponding torque T_{max}, corresponding power P_{max}) in the variable duty range. Its magnitude can be limited by a suitably responsive safety clutch. $F_{t\,max}$, T_{max} and P_{max} are required to determine the safety from pitting damage and from sudden tooth breakage due to loading corresponding to the static stress limit.

5 Application factor K_A

The factor K_A adjusts the nominal load F_t in order to compensate for incremental gear loads from external sources. These additional loads are largely dependent on the characteristics of the driving and driven machines, as well as the masses and stiffness of the system, including shafts and couplings used in service.

For applications such as marine gears and others subjected to cyclic peak torque (torsional vibrations) and designed for infinite life, the application factor can be defined as the ratio between the peak cyclic torques and the nominal rated torque. The nominal rated torque is defined by the rated power and speed. It is the torque used in the load capacity calculations.

If the gear is subjected to a limited number of known loads in excess of the amount of the peak cyclic torques, this influence may be covered directly by means of cumulative fatigue or by means of an increased application factor, representing the influence of the load spectrum.

It is recommended that the purchaser and manufacturer/designer agree on the value of the application factor.

5.1 Method A — Factor $K_{A\text{-}A}$

K_A is determined in this method by means of careful measurements and a comprehensive analysis of the system, or on the basis of reliable operational experience in the field of application concerned. See 4.2.2.

5.2 Method B — Factor $K_{A\text{-}B}$

If no reliable data, obtained as described in 5.1, are available, even as early as the first design phase, it is possible to use the guideline values for K_A as described in ISO 6336-6.

6 Internal dynamic factor K_v

The internal dynamic factor makes allowance for the effects of gear tooth accuracy grade as related to speed and load. High accuracy gearing requires less derating than low accuracy gearing.

It is generally accepted that the internal dynamic load on the gear teeth is influenced by both design and manufacturing.

The internal dynamic factor makes allowance for the effects of gear tooth accuracy and modifications as related to speed and load:

$$K_v = \frac{\text{Total mesh torque at operating speed}}{\text{Mesh torque with "perfect" gears}}$$

$$K_A \cdot K_v = \frac{\text{Total mesh torque at operating speed}}{\text{Nominal transmitted (design) mesh torque}}$$

“Perfect” gears are defined as having zero quasi-static transmission error at the nominal transmitted (design) mesh torque. They can only exist for a single load and, with proper modifications, have zero dynamic effects [e.g. zero transmission error (perfect conjugate action), zero excitation, no fluctuation at tooth mesh frequency and no fluctuation at rotational frequencies]. With zero excitation from the gears, there is zero response at any speed.

6.1 Parameters affecting internal dynamic load and calculations

6.1.1 Design

The design parameters include the following:

- pitchline velocity;
- tooth load;
- inertia and stiffness of the rotating elements;
- tooth stiffness variation;
- lubricant properties;
- stiffness of bearings and case structure;
- critical speeds and internal vibration within the gear itself.

6.1.2 Manufacturing

The manufacturing considerations include the following:

- pitch deviations;
- runout of reference surfaces with respect to the axis of rotation;
- tooth flank deviations;
- compatibility of mating gear tooth elements;
- balance of parts;
- bearing fit and preload.

6.1.3 Transmission perturbance

Even when the input torque and speed are constant, significant vibration of the gear masses, and resultant dynamic tooth loads, can exist. These loads result from the relative displacements between the mating gears as they vibrate in response to an excitation known as transmission error. The ideal kinematics of a gear pair require a constant ratio between the input and output rotations. Transmission error is defined as the departure from uniform relative angular motion of a pair of meshing gears. It is influenced by all deviations from the ideal gear tooth form and spacing due to the design and manufacture of the gears, and to the operational conditions under which the gears shall perform. The latter include the following.

a) Pitch line velocity: the frequencies of excitation depend on the pitch line velocity and module.

b) Gear mesh stiffness variations as the gear teeth pass through the meshing cycle: this source of excitation is especially pronounced in spur gears. Spur and helical gears with total contact ratios greater than 2,0 have less stiffness variation.

c) Transmitted tooth load: since deflections are load-dependent, gear tooth profile modifications can be designed to give uniform velocity ratio only for one magnitude of load. Loads different from the design load will give increased transmission error.

d) Dynamic unbalance of the gears and shafts.

e) Application environment: excessive wear and plastic deformation of the gear tooth profiles increase the transmission error. Gears shall have a properly designed lubrication system, enclosure and seals to maintain a safe operating temperature and a contamination-free environment.

f) Shaft alignment: gear tooth alignment is influenced by load and thermal deformations of the gears, shafts, bearings and housing.

g) Excitation induced by tooth friction.

6.1.4 Dynamic response

The effects of dynamic tooth loads are influenced by the following:

- mass of the gears, shafts, and other major internal components;
- stiffness of the gear teeth, gear blanks, shafts, bearings and housings;
- damping, the principal sources of which are the shaft bearings and seals, while other sources include hysteresis of the gear shafts and viscous damping at sliding interfaces and shaft couplings.

6.1.5 Resonance

When excitation frequencies (such as tooth meshing frequency and its harmonics) coincide or nearly coincide with a natural frequency of vibration of the gearing system, the resonant forced vibration can cause high dynamic tooth loading. When the magnitude of internal dynamic load at a speed involving resonance becomes large, operation near this speed should be avoided.

a) Gear blank resonance

The gear blanks of high speed, lightweight gearing can have natural frequencies within the operating speed range. If the gear blank is excited by a frequency which is close to one of its natural frequencies, the resonant deflections could cause high dynamic tooth loads. Also, there is the possibility of plate or shell mode vibrations which can cause the gear blank to fail. The dynamic factors K_v (from the following Methods B and C) do not take account of gear blank resonance.

b) System resonance

The gearbox is only one component of a system comprised of a power source, gearbox, driven equipment and interconnecting shafts and couplings. The dynamic response of this system depends on the configuration of the system. In certain cases a system could possess a natural frequency close to the excitation frequency associated with an operating speed. Under such resonant conditions, the operation shall be worked out carefully as mentioned above. For critical drives, a detailed analysis of the entire system is recommended. This should also be taken into account when determining the effects on the application factor.

6.2 Principles and assumptions

In accordance with the specifications of 4.1.12, methods for determining K_v are given in 6.3, from Method A ($K_{v\text{-}A}$) to Method C ($K_{v\text{-}C}$).

Given optimum profile modification appropriate to the loading, a large overlap ratio, even distribution of load over the face width, highly accurate teeth and high specific tooth loading, the value of the dynamic factor approaches 1,0.

In gear trains which include multiple mesh gears such as idler gears and epicyclic gearing, planet and sun gears, there are several natural frequencies. These can be higher or lower than the natural frequency of a single gear pair which has only one mesh. When such gears run in the supercritical range, resonance of higher natural frequencies occur and may lead to a higher dynamic factor.

Transverse vibrations of the shaft-gear systems will also influence the dynamic load. Transverse compliance of a shaft-gear system can result in coupled vibrations where the pinion and/or wheel combine torsional and lateral vibrations. This results in more natural frequencies than the one formed by just a pinion and wheel and may lead to a higher dynamic factor K_v.

In the case of high specific loading, high values of $(K_A F_t) / b$, high values of $(v z_1 / 100)\sqrt{u^2 / (1+u^2)}$, and having the corresponding accuracy of gear cutting, tooth tips and/or roots should be suitably relieved.

6.3 Methods for determination of dynamic factor

6.3.1 Method A — Factor $K_{v\text{-}A}$

The maximum tooth loads, including the internally generated dynamic additional loads and the uneven distribution of loads as described in Clause 8, are determined in Method A by measurement or by a comprehensive dynamic analysis of the general system. Under these circumstances K_v (just as $K_{H\alpha}$ and $K_{F\alpha}$) is assumed to have a value of 1,0.

K_v can also be assessed by measuring the tooth root stresses of the gears when transmitting load at working speed and at a lower speed, then comparing the results.

The factor K_v may be determined by a comprehensive analytical procedure which is supported by experience of similar designs. Guidance on procedures can be found in the literature.

Reliable values of the dynamic factor, K_v, can best be predicted by a mathematical model which has been satisfactorily verified by measurement.

6.3.2 Method B — Factor $K_{v\text{-}B}$

For this method the simplifying assumption is made that the gear pair consists of an elementary single mass and spring system comprising the combined masses of pinion and wheel, the stiffness being the mesh stiffness of the contacting teeth. It is also assumed that each gear pair functions as a single stage gear pair, i.e. the influence of other stages in a multiple-stage gear system is ignored. This assumption is permissible if the torsional stiffness of the shafts connecting the wheel of one stage with the pinion of the next is relatively low. See 6.4.2 for the procedure dealing with very stiff shafts.

In accordance with this assumption, loads due to torsional vibration of the shafts and coupled masses are not covered by K_v. These latter loads should be included with other externally applied loads (e.g. with the application factor).

It is further assumed, in the evaluation of dynamic factors by Method B, that damping at the gear mesh has an average value. (Other sources of damping such as friction at component interfaces, hysteresis, bearings, couplings, etc., are not taken into consideration.) Because of these additional sources of damping, the actual dynamic tooth loads are normally somewhat smaller than those calculated by this method. This does not apply in the range of main resonance (see 6.4.4).

Calculation of K_v by this method serves no useful purpose when the value $(v\, z_1 / 100)\sqrt{u^2 / (1+u^2)}$ is less than 3 m/s. Method C is sufficiently accurate for all cases in this range.

6.3.3 Method C — Factor $K_{v\text{-}C}$

Method C is derived from Method B by introducing the following additional simplifying assumptions.

a) The running speed range is subcritical.

b) Steel solid disc wheels.

c) The pressure angle $\alpha_t = 20°$; $f_{pb} = f_{pt} \cos 20°$ according to ISO/TR 10064-1.

d) Helix angle $\beta = 20°$ for helical gearing (refers to c', $c_{\gamma\alpha}$).

e) Total contact ratio $\varepsilon_\gamma = 2{,}5$ for helical gearing.

f) Tooth stiffness (see 9.3):

   — For spur gears, $c' = 14$ N/(mm·µm), $c_{\gamma\alpha} = 20$ N/(mm·µm);

   — For helical gears, $c' = 13{,}1$ N/(mm·µm), $c_{\gamma\alpha} = 18{,}7$ N/(mm·µm).

g) Tip relief $C_a = 0$ µm and tip relief after running-in $C_{ay} = 0$ µm.

h) Effective deviation $f_{pb\ eff} = f_{f\alpha\ eff}$.

i) For assumed values for f_{pb}, y_p and $f_{pb\ eff}$, see Equations (18) and (19) and Table 3.

The features described in 6.4.1 a) have not been taken into consideration in the application of Method C. The influence of specific loading is taken into account.

Table 3 — Assumed mean values of effective base pitch deviation, $f_{pb\ eff}$, for factor $K_{v\text{-}C}$

	Accuracy grades as specified in ISO 1328-1									
	3	4	5	6	7	8	9	10	11	12
$f_{pb\ eff}$	2,8	5,1	9,8	19,5	35	51	69	100	134	191

6.4 Determination of dynamic factor using Method B: $K_{v\text{-}B}$

According to the preconditions and assumptions given in 6.3.2, Method B is suited for all types of transmission (spur and helical gearing with any basic rack profile and any gear accuracy grade) and, in principle, for all operating conditions. However, there are restrictions for certain fields of application and operation which will be noted in each case and should be taken into account.

The resonance ratio N (ratio of the running speed to the resonance speed) is determined as described in 6.4.2 [2)]. The entire running speed range can be divided into three sectors — subcritical, main resonance and supercritical. Formulae are provided for calculating K_v in each sector.

NOTE The dynamic factors calculated from the equations in 6.4.3 to 6.4.6 correspond to the experimentally determined mean dynamic tooth load values. In the subcritical and main resonance ranges, values of K_v derived from measurement data usually deviate from the calculated values by up to +10 %. Even greater deviations can occur when there are other natural frequencies in the gear and shaft system. See 6.4.1 a), 6.4.3, and 6.4.4.

6.4.1 Running speed ranges

a) Subcritical range ($N < 1$) [3)]

In this sector, resonances can exist if the tooth mesh frequency coincides with $N = 1/2$ and $N = 1/3$. Under such circumstances the dynamic loads can exceed the values calculated using Equation (13). The risk of this is slight for precision helical or spur gears, if the latter have suitable profile modification (gears to accuracy grade 5 of ISO 1328-1 or better).

When the contact ratio of spur gears is small or if the accuracy is low, K_v can be just as great as in the main resonance speed range. If this occurs, the design or operating parameters should be altered.

Resonances at $N = 1/4$, 1/5, ... are seldom troublesome because the associated vibration amplitudes are usually small.

When the specific loading $(F_t K_A)/b < 50$ N/mm, a particular risk of vibration exists (under some circumstances, with separation of working tooth flanks) — above all for spur or helical gears of coarse accuracy grade running at higher speed.

b) Main resonance range ($N = 1$)

Operation in this range should generally be avoided, especially for spur gears with unmodified tooth profiles, or helical gears of accuracy grade 6 or coarser as specified in ISO 1328-1. Helical gears of high accuracy with a high total contact ratio can function satisfactorily in this sector. Spur gears of grade 5 or better as specified in ISO 1328-1 shall have suitable profile modification.

c) Supercritical range ($N > 1$)

The same limitations on gear accuracy grade as in b) apply to gears operating in this speed range. Resonance peaks can occur at $N = 2$, 3 ... in this range. However, in the majority of cases vibration amplitudes are small, since excitation loads with lower frequencies than meshing frequency are usually small.

2) When it is known in advance that gears will operate in the supercritical sector, there is no need to evaluate the resonance speed. As a consequence, the dynamic factor can be directly determined in accordance with 6.4.5.

3) For a definition of N, see Equation (9). In practice, the calculated resonance sector is broadened to ensure a safe margin. See Equations (10) and (11) and the preamble thereto.

For some gears in this speed range, it is also necessary to consider dynamic loads due to transverse vibration of the gear and shaft assemblies (see 6.3.2). If the critical frequency is near the frequency of rotation, the associated effective value of K_v can exceed the value calculated using Equation (21) by up to 100 %. This condition should be avoided.

6.4.2 Determination of resonance running speed (main resonance) of a gear pair [3)]

This is as follows:

$$n_{E1} = \frac{30\,000}{\pi\, z_1} \sqrt{\frac{c_{\gamma\alpha}}{m_{red}}} \tag{6}$$

where

m_{red} is the relative mass of a gear pair, i.e. of the mass per unit face width of each gear, referred to its base radius or to the line of action

$$m_{red} = \frac{m_1^* \, m_2^*}{m_1^* + m_2^*} = \frac{J_1^* \, J_2^*}{J_1^* \, r_{b2}^2 + J_2^* \, r_{b1}^2} \tag{7}$$

where

$$m_{1,2}^* = \frac{J_{1,2}^*}{r_{b1,2}^2} \tag{8}$$

and r_b is the base radius

See 6.4.8 for the method of calculating an approximate value of m_{red}. See Clause 9 for the stiffness $c_{\gamma\alpha}$.

Method A is to be preferred for less common transmission designs. A method for deriving approximate values is specified for the following cases:

a) pinion on large diameter shaft;

b) two neighbouring gears rigidly joined together;

c) one big wheel driven by two pinions;

d) simple planetary gears;

e) idler gears.

The ratio of pinion speed to resonance speed is termed the “resonance ratio”, N (n_1 is in revolutions per minute):

$$N = \frac{n_1}{n_{E1}} = \frac{n_1\, \pi\, z_1}{30\,000} \sqrt{\frac{m_{red}}{c_{\gamma\alpha}}} \tag{9}$$

The resonance running speed n_{E1} may be above or below the running speed calculated from Equation (6) because of stiffnesses which have not been included (the stiffness of shafts, bearings, housings, etc.) and as a result of damping. For reasons of safety, the resonance ratio in the main resonance range, N_S, is defined by the following upper limit.

$$N_S < N \leqslant 1{,}15 \tag{10}$$

The lower limit of resonance ratio N_S is determined:

a) at loads such that $(F_t\ K_A)\ /\ b$ is less than 100 N/mm, as

$$N_S = 0{,}5 + 0{,}35\sqrt{\frac{F_t\ K_A}{100\ b}} \qquad (11)$$

b) for loads where $(F_t\ K_A\ /\ b) \geqslant 100$ N/mm, as

$$N_S = 0{,}85 \qquad (12)$$

For resonance ratio, N, in the main resonance range, see Figure 1.

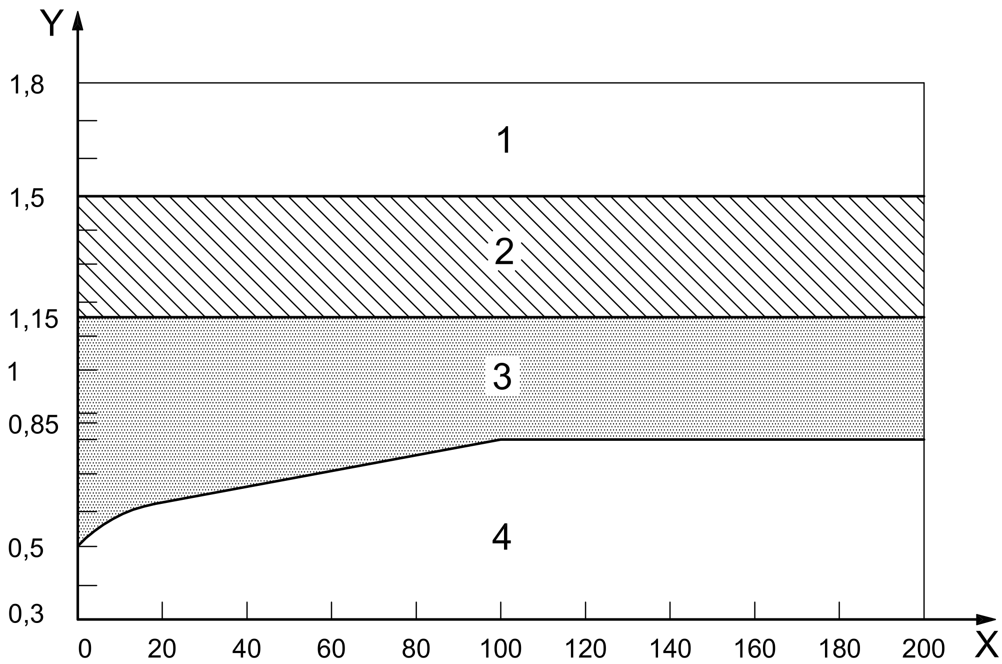

Key

X specific loading, $\frac{F_t\ K_A}{b}$, N/mm

Y resonance ratio, N

1 supercritical range

2 intermediate range

3 main resonance range

4 subcritical range

Figure 1 — Resonance range

Thus the following ranges result for the calculation of K_v.

a) Subcritical range, $N \leqslant N_S$ (see 6.4.3).

b) Main resonance range, $N_S < N \leqslant 1{,}15$ (see 6.4.4). This field should be avoided. Refined analysis by Method A is recommended for K_v.

c) Intermediate range, $1{,}15 < N \leqslant 1{,}5$ (see 6.4.6). Refined analysis by Method A is recommended.

d) Supercritical range, $N \geqslant 1{,}5$ (see 6.4.5).

6.4.3 Dynamic factor in subcritical range ($N \leqslant N_S$)

See 6.4.1 a) for special features; the majority of industrial gears operate in this range.

$$K_v = (N\,K) + 1 \tag{13}$$

$$K = (C_{v1}\,B_p) + (C_{v2}\,B_f) + (C_{v3}\,B_k) \tag{14}$$

where

C_{v1} allows for pitch deviation effects and is assumed to be constant at $C_{v1} = 0{,}32$ (see Figure 2);

C_{v2} allows for tooth profile deviation effects and can be read from Figure 3 or determined in accordance with Table 4;

C_{v3} allows for the cyclic variation effect in mesh stiffness and can be read from Figure 3 or determined in accordance with Table 4.

Table 4 — Equations for calculation of factors C_{v1} to C_{v7} and C_{ay} for determination of $K_{v\text{-}B}$, Method B (equations relate to curves in Figures 2 and 3)

	$1 < \varepsilon_\gamma \leqslant 2$	$\varepsilon_\gamma > 2$	
C_{v1}	0,32	0,32	
C_{v2}	0,34	$\dfrac{0{,}57}{\varepsilon_\gamma - 0{,}3}$	
C_{v3}	0,23	$\dfrac{0{,}096}{\varepsilon_\gamma - 1{,}56}$	
C_{v4}	0,90	$\dfrac{0{,}57 - 0{,}05\,\varepsilon_\gamma}{\varepsilon_\gamma - 1{,}44}$	
C_{v5}	0,47	0,47	
C_{v6}	0,47	$\dfrac{0{,}12}{\varepsilon_\gamma - 1{,}74}$	
	$1 < \varepsilon_\gamma \leqslant 1{,}5$	$1{,}5 < \varepsilon_\gamma \leqslant 2{,}5$	$\varepsilon_\gamma > 2{,}5$
C_{v7}	0,75	$0{,}125 \sin[\pi(\varepsilon_\gamma - 2)] + 0{,}875$	1,0
$C_{ay} = \dfrac{1}{18}\left(\dfrac{\sigma_{Hlim}}{97} - 18{,}45\right)^2 + 1{,}5$			
NOTE When the material of the pinion (1) is different from that of the wheel (2), C_{ay1} and C_{ay2} are calculated separately, then $C_{ay} = 0{,}5\,(C_{ay1} + C_{ay2})$.			

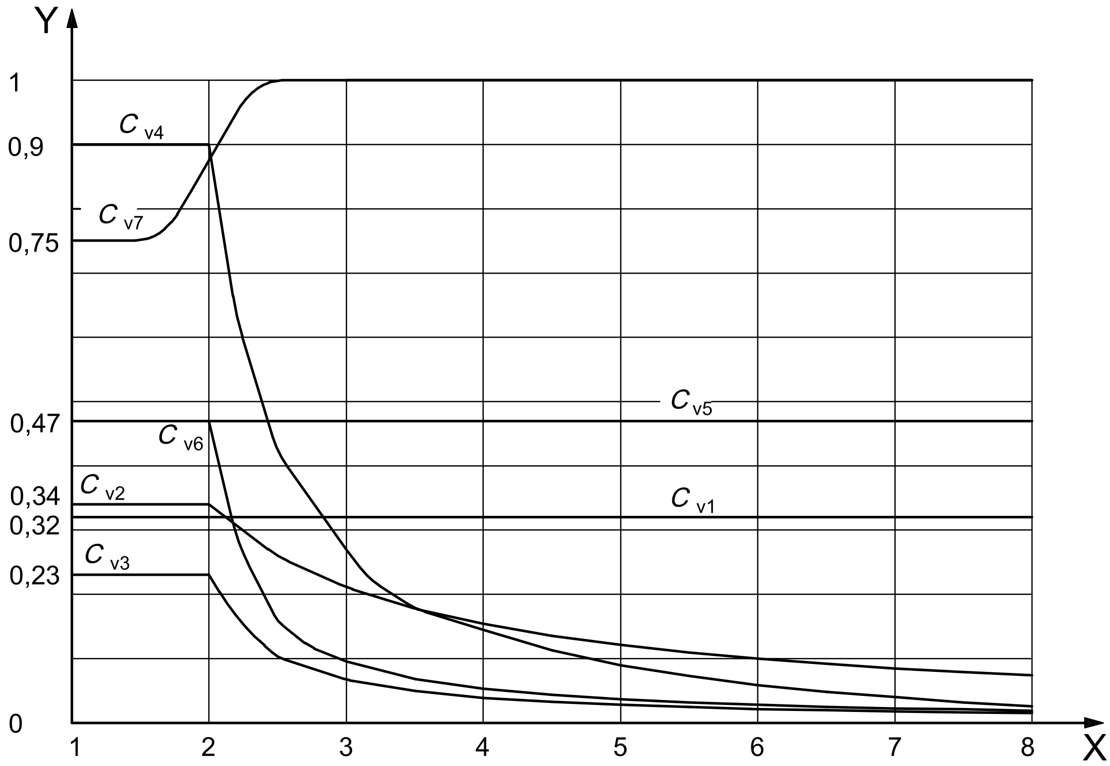

Key

X contact ratio, ε_γ

Y factor, C_v

NOTE For the equations used for calculation, see Table 4.

Figure 2 — Values of C_{v1} to C_{v7} for determination of K_{v-B} (Method B)

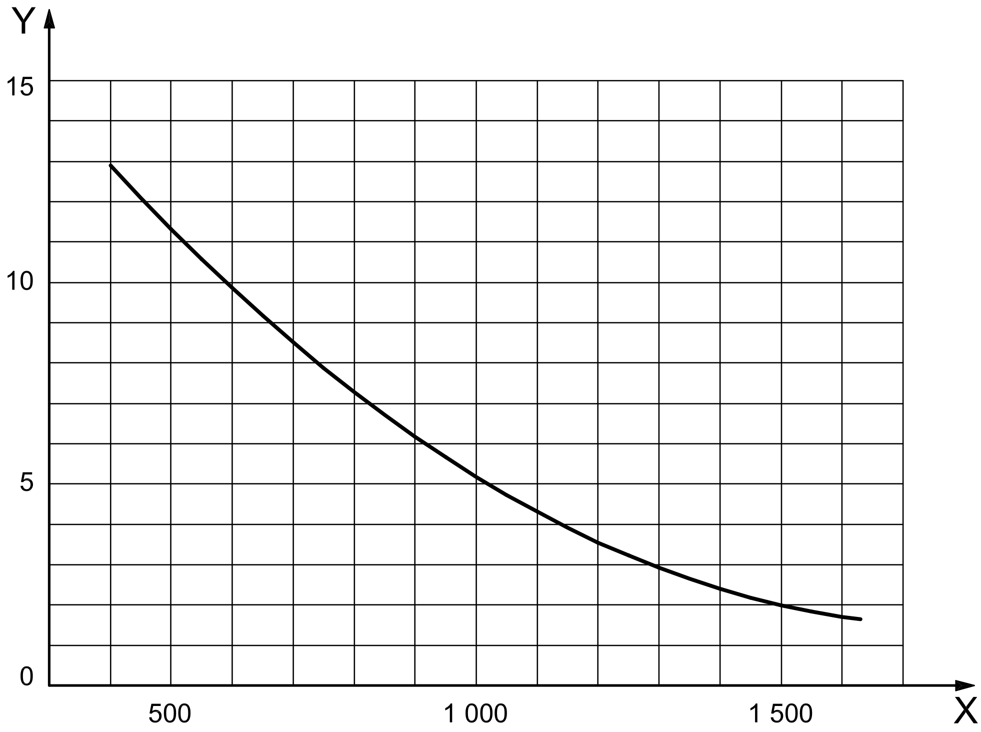

Key

X allowable stress number, σ_{Hlim}, N/mm^2

Y tip relief, C_{ay}, µm

NOTE When the pinion material (1) is different from the wheel (2) then $C_{ay} = 0{,}5\ (C_{ay1} + C_{ay2})$.

Figure 3 —Tip relief C_{ay} produced by running-in (see Table 3 for calculation)

B_p, B_f and B_k are non-dimensional parameters to take into account the effect of tooth deviations and profile modifications on the dynamic load [4].

$$B_p = \frac{c' \, f_{pb\,eff}}{K_A \, (F_t/b)} \tag{15}$$

$$B_f = \frac{c' \, f_{f\alpha\,eff}}{K_A \, (F_t\,/\,b)} \tag{16}$$

$$B_k = \left| 1 - \frac{c' \, C_a}{K_A \, (F_t\,/\,b)} \right| \tag{17}$$

The effective single pitch and profile deviations are those of the “run-in” pinion and wheel. Initial deviations are generally modified during early service (running-in). The values of $f_{pb\,eff}$ and $f_{f\alpha\,eff}$ are determined by deducting estimated running-in allowances (y_p and y_f) as follows:

$$f_{pb\,eff} = f_{pb} - y_p \tag{18}$$

$$f_{\alpha\,eff} = f_{f\alpha} - y_f \tag{19}$$

4) Equation (17) is not suitable for the determination of an “optimum” tip relief C_a. The amount C_a of tip relief may only be used in Equation (17) for gears of quality grades in the range 0 to 5 as specified in ISO 1328-1. For gears in the range 6 to 12, $B_k = 1{,}0$. Also see 4.1.1.2.

Considerations of probability suggest that, in general, magnitudes of transmission deviation will not be greater than the allowable values of f_{pb} and $f_{f\alpha}$ for the wheel, which are the larger. They are therefore used in Equations (18) and (19) respectively; these are usually the values for the largest wheel.

In the event that neither experimental nor service data on relevant material running-in characteristics are available (Method A), it can be assumed that $y_p = y_\alpha$, with y_α from Figure 17 or 18 or 8.3.5.1. y_f can be determined in the same way as y_α when the profile deviation $f_{f\alpha}$ is used instead of base pitch deviation f_{pb}.

C_a is the design amount for profile modification (tip relief at the beginning and end of tooth engagement).

A value C_{ay} resulting from running-in is to be substituted for C_a in Equation (17) in the case of gears without a specified profile modification. The value of C_{ay} can be obtained from Figure 3 or calculated according to Table 4.

See Clause 9 for single tooth stiffness c'.

6.4.4 Dynamic factor in main resonance range ($N_S < N \leqslant 1,15$)

Subject to restriction (see 6.4.1 b), this factor is equal to

$$K_v = (C_{v1}\, B_p) + (C_{v2}\, B_f) + (C_{v4}\, B_k) + 1 \tag{20}$$

See 6.4.3 for details regarding C_{v1}, C_{v2}, B_p, B_f and B_k.

C_{v4} takes into account resonant torsional oscillations of the gear pair, excited by cyclic variation of the mesh stiffness. Its value can be taken from Figure 2 or calculated as indicated in Table 4.

NOTE The dynamic factor at this speed is strongly influenced by damping. The real value of the dynamic factor can deviate from the calculated value [see Equation (20)] by up to 40 %. This is especially true for spur gears with incorrectly designed profile modification.

6.4.5 Dynamic factor in supercritical range ($N \geqslant 1,5$)

Most high precision gears used in turbine and other high speed transmissions operate in this sector; see 6.4.1 c) for features.

$$K_v = (C_{v5}\, B_p) + (C_{v6}\, B_f) + C_{v7} \tag{21}$$

In this range, the influences on K_v of C_{v5} and C_{v6} correspond to those of C_{v1} and C_{v2} on K_v in the subcritical range. See 6.4.3 for data on these factors and on B_p and B_f.

C_{v7} takes into account the component of load which, due to mesh stiffness variation, is derived from tooth bending deflections during substantially constant speed.

C_{v5}, C_{v6} and C_{v7} can be obtained from Figure 2 or calculated according to Table 3.

6.4.6 Dynamic factor in intermediate range ($1,15 < N < 1,5$)

In this range, the dynamic factor is determined by linear interpolation between K_v at $N = 1,15$ as specified in and K_v at $N = 1,5$ as specified in 6.4.5.

$$K_v = K_{v(N=1,5)} + \frac{K_{v(N=1,15)} - K_{v(N=1,5)}}{0,35}(1,5 - N) \tag{22}$$

See 6.4.4 and 6.4.5 for details and explanatory notes.

6.4.7 Resonance speed determination for less common gear designs

The resonance speed determination for less common gear designs should be made with the use of Method A. However, other methods may be used to approximate the effects. Some examples are as follows.

6.4.7.1 Pinion shaft with diameter at mid-tooth depth, d_{m1}, about equal to shaft diameter

The resonance speed tends to decrease because the pinion mass is supplemented by the shaft mass.

Nevertheless, the resonance speed can be calculated in the normal way, using the mass of the pinion (toothed portion) and the normal mesh stiffness $c_{\gamma\alpha}$.

6.4.7.2 Two rigidly connected coaxial gears

The mass of the larger of the connected gears is to be included. The mass of the smaller gear can often be ignored. This gives a useable approximation when the diameters of the connected gears are markedly different (see also 6.4.2).

6.4.7.3 One large wheel driven by two pinions

See also 6.3.2. As the mass of the wheel is normally much greater than the masses of the pinions, each mesh can be considered separately, i.e.

— as a pair comprising the first pinion and the wheel, and

— as a pair comprising the second pinion and the wheel.

6.4.7.4 Planetary gears

Because of the many transmission paths which include stiffnesses other than mesh stiffness, the vibratory behaviour of planetary gears is very complex. The calculation of dynamic load factors using simple formulae, such as Method B, is generally quite inaccurate. Nevertheless, Method B modified as follows can be used for a first estimate of K_v. This estimate should, if possible, be verified by means of a subsequent detailed theoretical or experimental analysis, or on the basis of operating experience. See also the comments in 6.3.2.

a) Planet gear — Ring gear rigidly connected to the gear case

In this case, the mass of the ring gear can be assumed to be infinite, the ring gear works as a rigid connection of the vibrating system. Under the presupposition that the vibrating system is decoupled from the other driving elements (connection with low stiffness against torsion), the remaining system consisting of sun and planets including the tooth contact between the sun and the planet and respectively, between the planet and the ring gear, possesses two resonance frequencies. These can be determined in similar fashion to Equation (6) using two reduced masses $m_{red,1}$, $m_{red,2}$, where, instead of $c_{\gamma\alpha}$, the single tooth contact stiffness of a planet is to be used and the tooth number of the sun for z_1. The reduced masses $m_{red,1}$ and $m_{red,2}$ can be determined as follows:

$$m_{red,1} = \frac{m^*_{pla}\, m^*_{sun}}{\left(p\, m^*_{pla}\right) + m^*_{sun}} \tag{23}$$

$$m_{red,2} = m^*_{pla} \tag{24}$$

with

$$m^*_{pla} = \frac{\pi}{8} \frac{d^4_{m\,pla}}{d^4_{b\,pla}} \left(1 - q^4_{pla}\right) \rho_{pla} \tag{25}$$

where

m^*_{sun} is the moment of inertia per unit face width of the sun gear, divided by $r^2_{b\ sun}$, where $r_{b\ sun} = d_{b\ sun} / 2$;

m^*_{pla} is the moment of inertia per unit face width of a planet gear, divided by $r^2_{b\ pla}$, where $r_{b\ pla} = d_{b\ pla} / 2$;

p is the number of planet gears in the gear stage under consideration;

$d_{m\ pla}$ see Equation (31);

q_{pla} see Equation (32);

ρ_{pla} is the density.

It has to be observed that F_t in Equations (15) to (17) is equal to the whole peripheral load of the sun divided by the number of planets p. The dynamic factor $K_{v,1/2}$ can be estimated using the resonance speed $n_{E,1/2}$ calculated with $m_{red,1/2}$; for further calculation the larger of the two factors $K_{v,1/2}$ is to be used.

b) Rotating ring gear

In this case, it is mostly necessary to make a detailed analysis of the vibrating system. Only in the special case of much greater reduced masses of the sun m^*_{sun} and the ring gear m^*_{carr} the calculation described in 6.4.7.3 can be assumed:

$$m^*_{carr} = \frac{\pi}{8} \frac{d^4_{m\ carr}}{d^4_{b\ carr}} \left(1 - q^4_{carr}\right) \rho_{carr} \tag{26}$$

where

m^*_{carr} is the moment of inertia per unit face width of the ring gear, divided by $r^2_{b\ carr}$, where $r_{b\ carr} = d_{b\ carr} / 2$;

$d_{m\ carr}$ in analogy to Equation (31);

q_{pla} in analogy to Equation (32).

6.4.7.5 Idler gears

The following calculation procedure is an extension of the approximate two mass model and falls under the limitations of 6.3.2.

For the calculation of the resonant frequencies of an idler gear, it is necessary to use a mechanical model with several degrees of freedom. Using the presuppositions made in Method B or C [5)], this model can be reduced to three degrees of freedom. With the system of equations belonging to this substituting model, two resonant frequencies (resonant speeds $n_{E,1/2}$) can be calculated:

$$n_{E1,2} = \frac{30\,000}{\pi\ z_1} \sqrt{\frac{1}{2}\left(B \pm \sqrt{B^2 - 4\,C}\right)} \tag{27}$$

5) These presuppositions are a connection with low stiffness of torsion to the other driving elements and a high flexural strength of the gear shafts.

with

$$B = c_{\gamma\alpha,1/2}\left(\frac{1}{m_1^*}+\frac{1}{m_2^*}\right)+c_{\gamma\alpha,2/3}\left(\frac{1}{m_2^*}+\frac{1}{m_3^*}\right) \tag{28}$$

$$C = c_{\gamma\alpha,1/2}\ c_{\gamma\alpha,2/3}\frac{m_1^*+m_2^*+m_3^*}{m_1^*\ m_2^*\ m_3^*} \tag{29}$$

where

$m^*_{1/2/3}$ are the moments of inertia per unit face width of the smaller gear (pinion), the idler gear and the larger gear, related to the path of contact;

$c_{\gamma\alpha,1/2}$ is the mesh stiffness of the combination driving gear — idler gear;

$c_{\gamma\alpha,2/3}$ is the mesh stiffness of the combination idler gear — driven gear.

For calculation of the mesh stiffness, see Clause 9.

K_v may be determined by Method B using N as the least favorable ratio, i.e. the N-ratio which results in the highest K_v has to be considered.

6.4.8 Calculation of reduced mass of gear pair with external teeth

Approximate values of reduced mass which are sufficiently accurate can be derived from the following equations:

$$m_{red} = \frac{\pi}{8}\left(\frac{d_{m1}}{d_{b1}}\right)^2 \frac{d_{m1}^2}{\dfrac{1}{\left(1-q_1^4\right)\rho_1}+\dfrac{1}{\left(1-q_2^4\right)\rho_2\, u^2}} \tag{30}$$

where

d_{b1} is the base diameter;

$$d_{m1,m2} = \frac{d_{a1,a2}+d_{f1,f2}}{2} \tag{31}$$

$$q_1 = \frac{d_{i1}}{d_{m1}};\ q_2 = \frac{d_{i1}}{d_{m2}} \tag{32}$$

See Figure 4.

Equations (30) to (32) apply to external double helical, external single helical and external spur gears. They ignore the masses of web and hub because of their negligible influence on the moment of inertia.

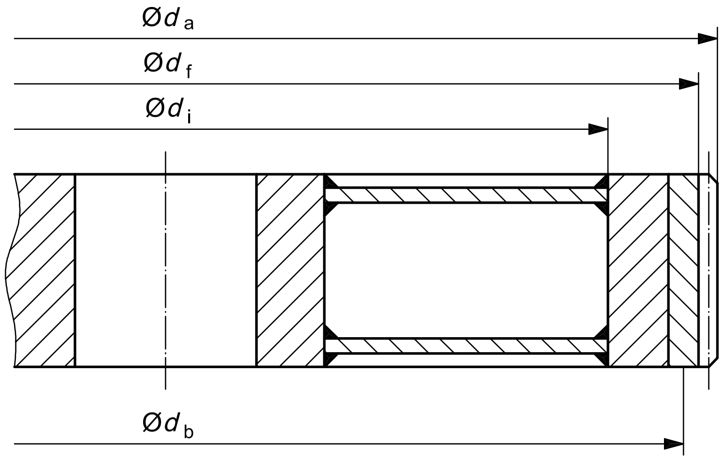

Figure 4 — Definitions of the various diameters

For pinions and wheels of solid construction:

$$1 - q_1^4 = 1; 1 - q_2^4 = 1 \quad (33)$$

The calculation of $(1 - q_1^4)$ or $(1 - q_2^4)$ for a gear rim whose rim width differs from the face width is only valid where the masses of the rim are directly connected to the gear rim. More distant masses on the same shaft are ignored, since the stiffness of the interconnecting shaft is generally of minor significance compared to tooth stiffness.

6.5 Determination of dynamic factor using Method C: $K_{\text{v-C}}$

In conjunction with the conditions and assumptions described in 6.3.3, Method C supplies average values which can be used for industrial transmissions and gear systems with similar requirements in the following fields of application:

a) subcritical running speed range, i.e. $(v\,z_1/100)\sqrt{u^2/(1+u^2)} < 10$ m/s, where the restrictions in 6.3.3 a) apply accordingly;

b) external and internal spur gears;

c) basic rack profile as specified in ISO 53;

d) straight and helical spur gears with $\beta \leqslant 30°$;

e) pinion with relatively low number of teeth, $z_1 < 50$;

f) solid disc wheels or heavy steel gear rim [6)].

Method C can also generally be used, with restrictions for the following fields of application:

g) all types of cylindrical gears, if $(v\,z_1/100)\sqrt{u^2/(1+u^2)} < 3$ m/s;

h) lightweight gear rim [6)];

---

6) If the rim is very light or if helical gears have a very large overlap ratio, values obtained from Figure 5 or 6 are too unfavourable. Thus, calculated values tend to be safe. The same applies when gears are made of cast iron.

i) helical gears where $\beta > 30°$ [6)].

K_v can be read from graphs (see 6.5.1) or computed (see 6.5.2). The method gives similar values.

6.5.1 Graphical values of dynamic factor using Method C

$$K_v = (f_F\ K_{350}\ N) + 1 \tag{34}$$

f_F takes into account the influence of the load on the dynamic factor, K_{350}, the influence of the gear accuracy grade at the specific loading of 350 N/mm and N is the resonance ratio [see Equation (9)].

The curves for gear accuracy grade in Figures 5 and 6 extend only to the value $(v\ z_1 / 100)\sqrt{u^2 / (1+u^2)} = 3$ m/s, which is not generally exceeded for this accuracy grade.

a) For helical gears with overlap ratio $\varepsilon_\beta \geqslant 1$ (also approximately for $\varepsilon_\beta > 0{,}9$), the correction factor f_F shall be in accordance with Table 5 and $(K_{350}\ N)$ shall be in accordance with Figure 5.

b) For spur gears, the correction factor f_F shall be in accordance with Table 6 and $(K_{350}\ N)$ shall be in accordance with Figure 6.

c) For helical gears with overlap ratio $\varepsilon_\beta < 1$, the value K_v is determined by linear interpolation between values in accordance with a) and b):

$$K_v = K_{v\alpha} - \varepsilon_\beta (K_{v\alpha} - K_{v\beta}) \tag{35}$$

where

$K_{v\alpha}$ is the dynamic factor for spur gears using b);

$K_{v\beta}$ is the dynamic factor for helical gears using a).

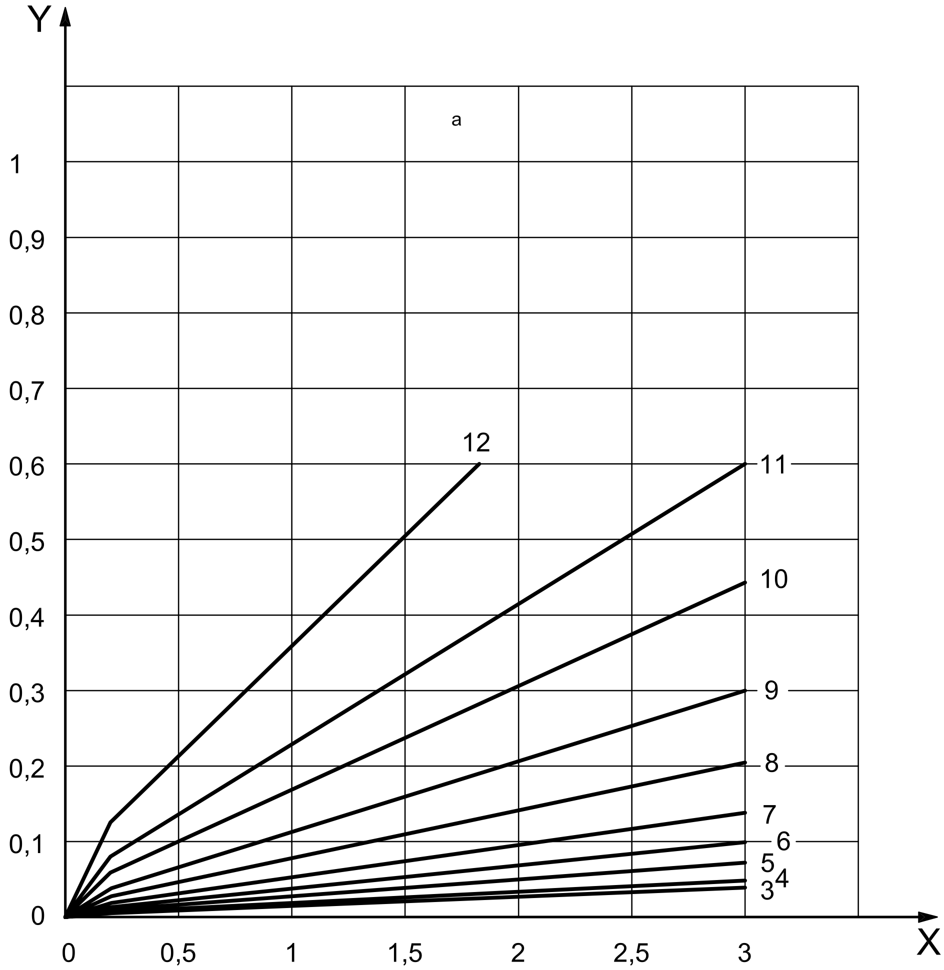

Key

X $(v\, z_1 / 100) \sqrt{u^2 / (1+u^2)}$

Y $K_{350}\, N$

a Gear accuracy in accordance with ISO 1328-1, helical gears.

Figure 5 — Values of $K_{350}\, N$ for helical gears with $\varepsilon_\beta \geqslant 1$

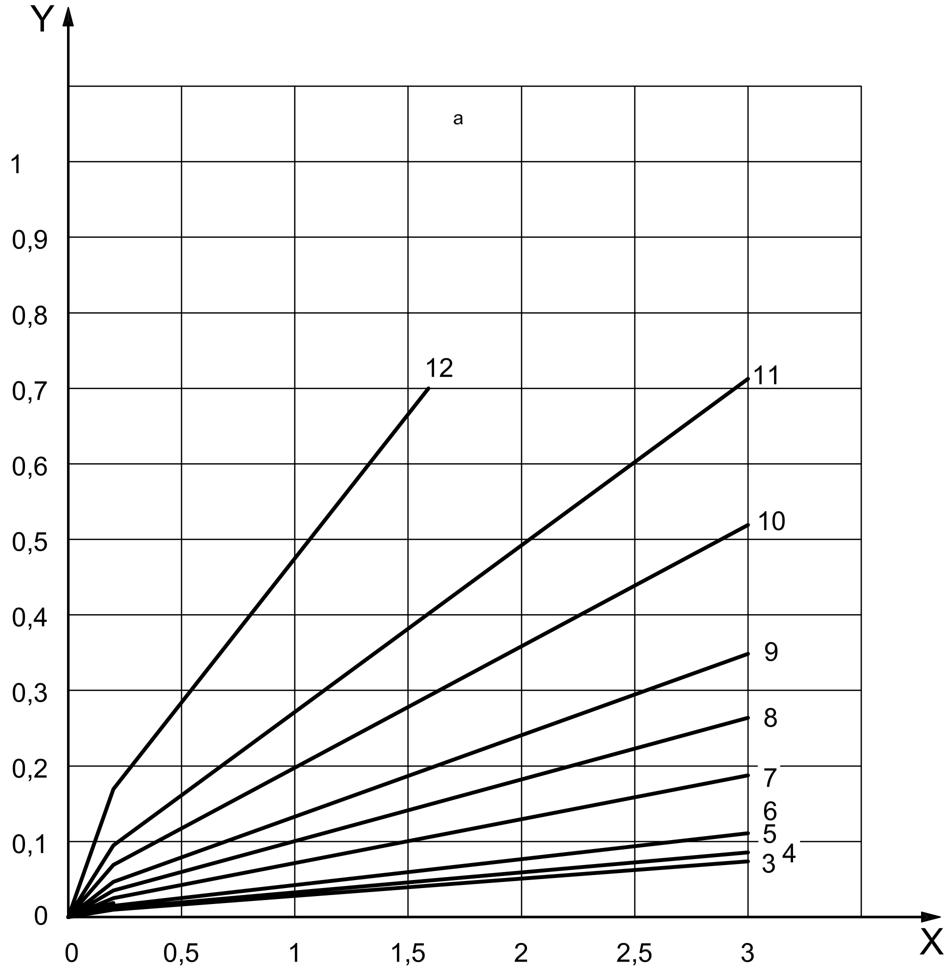

Key

X $(v\,z_1/100)\sqrt{u^2/(1+u^2)}$

Y $K_{350}\,N$

a Gear accuracy in accordance with ISO 1328-1, spur gears.

Figure 6 — Value of $K_{350}\,N$ for spur gears

Table 5 — Load correction factor f_F for helical gears

Gear accuracy grade [a]	Load correction factor f_F $(F_t K_A)/b$ N/mm							
	⩽ 100	200	350	500	800	1 200	1 500	2 000
3	1,96	1,29	1	0,88	0,78	0,73	0,70	0,68
4	2,21	1,36	1	0,85	0,73	0,66	0,62	0,60
5	2,56	1,47	1	0,81	0,65	0,56	0,52	0,48
6	2,82	1,55	1	0,78	0,59	0,48	0,44	0,39
7	3,03	1,61	1	0,76	0,54	0,42	0,37	0,33
8	3,19	1,66	1	0,74	0,51	0,38	0,33	0,28
9	3,27	1,68	1	0,73	0,49	0,36	0,30	0,25
10	3,35	1,70	1	0,72	0,47	0,33	0,28	0,22
11	3,39	1,72	1	0,71	0,46	0,32	0,27	0,21
12	3,43	1,73	1	0,71	0,45	0,31	0,25	0,20

NOTE Interpolate for intermediate values.

[a] Gear accuracy grade in accordance with ISO 1328-1.

Table 6 — Load correction factor f_F for spur gears

Gear accuracy grade [a]	Load correction factor f_F $(F_t K_A)/b$ N/mm							
	⩽ 100	200	350	500	800	1 200	1 500	2 000
3	1,61	1,18	1	0,93	0,86	0,83	0,81	0,80
4	1,81	1,24	1	0,90	0,82	0,77	0,75	0,73
5	2,15	1,34	1	0,86	0,74	0,67	0,65	0,62
6	2,45	1,43	1	0,83	0,67	0,59	0,55	0,51
7	2,73	1,52	1	0,79	0,61	0,51	0,47	0,43
8	2,95	1,59	1	0,77	0,56	0,45	0,40	0,35
9	3,09	1,63	1	0,75	0,53	0,41	0,36	0,31
10	3,22	1,67	1	0,73	0,50	0,37	0,32	0,27
11	3,30	1,69	1	0,72	0,48	0,35	0,30	0,24
12	3,37	1,71	1	0,72	0,47	0,33	0,27	0,22

NOTE Interpolate for intermediate values.

[a] Gear accuracy grade in accordance with ISO 1328-1.

6.5.2 Determination by calculation of dynamic factor using Method C

a) For spur gears and helical gears with overlap ratio $\varepsilon_\beta \geqslant 1$ (also approximately for $\varepsilon_\beta > 0{,}9$)

$$K_\mathrm{v} = 1 + \left(\frac{K_1}{K_\mathrm{A} \dfrac{F_\mathrm{t}}{b}} + K_2 \right) \frac{v\, z_1}{100} K_3 \sqrt{\frac{u^2}{1+u^2}} \quad (36)$$

where numerical values for K_1 and K_2 shall be as specified in Table 7, and K_3 shall be in accordance with Equation (37). If $(F_\mathrm{t}\, K_\mathrm{A})\, /b$ is less than 100 N/mm, this value is assumed to be equal to 100 N/mm. See 6.4.1 a).

$$\text{If} \quad \frac{v\, z_1}{100} \sqrt{\frac{u^2}{1+u^2}} \leqslant 0{,}2 \quad K_3 = 2{,}0$$

$$\text{If} \quad \frac{v\, z_1}{100} \sqrt{\frac{u^2}{1+u^2}} > 0{,}2 \quad K_3 = -0{,}357 \frac{v\, z_1}{100} \sqrt{\frac{u^2}{1+u^2}} + 2{,}071 \quad (37)$$

b) For helical gears with overlap ratio $\varepsilon_\beta < 1$:

The value K_v is determined by linear interpolation between values determined for spur gears ($K_{\mathrm{v}\alpha}$) and helical gears ($K_{\mathrm{v}\beta}$) in accordance with 6.5.1 c). See Equation (35).

Table 7 — Values of factors K_1 and K_2 for calculation of $K_{\mathrm{v\text{-}C}}$, by Equation (36)

	K_1 Accuracy grades as specified in ISO 1328-1										K_2 All accuracy grades
	3	4	5	6	7	8	9	10	11	12	
Spur gears	2,1	3,9	7,5	14,9	26,8	39,1	52,8	76,6	102,6	146,3	0,019 3
Helical gears	1,9	3,5	6,7	13,3	23,9	34,8	47,0	68,2	91,4	130,3	0,008 7

7 Face load factors $K_{\mathrm{H}\beta}$ and $K_{\mathrm{F}\beta}$

7.1 Gear tooth load distribution

The face load factor takes into account the effects of the non-uniform distribution of load over the gear face width on the surface stress ($K_{\mathrm{H}\beta}$) and on the tooth root stress ($K_{\mathrm{F}\beta}$).

See 7.2.1 and 7.2.2 for definitions of the face load factors.

The extent to which the load is unevenly distributed depends on the following influences:

a) the gear tooth manufacturing accuracy — lead, profile and spacing;

b) alignment of the axes of rotation of the mating gear elements;

c) elastic deflections of gear unit elements — shafts, bearings, housings and foundations which support the gear elements;

d) bearing clearances;

e) hertzian contact and bending deformations at the tooth surface including variable tooth stiffness;

f) thermal deformations due to operating temperature (especially important for gears with large face widths);

g) centrifugal deflections due to operating speed;

h) helix modifications including tooth crowning and end relief;

i) running-in effects;

j) total tangential tooth load (including increases due to application factor K_A and dynamic factor K_v);

k) additional shaft loads (e.g. from belt or chain drives);

l) gear geometry.

7.2 General principles for determination of face load factors $K_{H\beta}$ and $K_{F\beta}$

Uneven load distribution along the face width is caused by an equivalent mesh misalignment in the plane of action, comprising load-induced elastic deformation of gears and housing, and displacements of bearing journals; also by manufacturing deviations and thermal distortions.

When combined, the housing and gear manufacturing deviations, deflections of the housing and displacements of journal bearings, always result in a straight line deviation within the plane of action. Elastic deformations of shafts and gear bodies always result in non-linear deviations, as well as the deformations produced by thermal distortion resulting from uneven temperature distribution over the face width. The undulations and the flank form deviation are superimposed on the resulting mesh alignment. The unevenness of load distribution is reduced by running-in in accordance with the running-in effects characteristic of the material combination.

7.2.1 Face load factor for contact stress $K_{H\beta}$

$K_{H\beta}$ takes into account the effect of the load distribution over the face width on the contact stress and is defined as follows:

$$K_{H\beta} = \frac{\text{maximum load per unit face width}}{\text{average load per unit face width}} = \frac{(F/b)_{\text{max}}}{F_m/b}$$

The tangential loads at the reference cylinder are used for an approximate calculation, i.e. using the transverse specific loading [$F_m/b = (F_t\ K_A\ K_v)/b$] at the reference cylinder and the corresponding maximum local loading.

7.2.2 Face load factor for tooth root stress $K_{F\beta}$

$K_{F\beta}$ takes into account the effect of the load distribution over the face width on the stresses at the tooth root. It depends on the variables which are determined for $K_{H\beta}$ and also on the face width to tooth depth ratio, b/h.

7.3 Methods for determination of face load factor — Principles, assumptions

Several methods in accordance with the specifications of 4.1.12 are given in 7.3.1 to 7.3.3 for the determination of the face load factors.

Careful analysis is recommended when the face/diameter ratio, b/d, of the pinion is greater than 1,5 for through hardened gears and greater than 1,2 for surface hardened gears.

When equivalent misalignments due to mechanical and thermal deformations are compensated for by helix modification (possibly varying over the face width), a nearly uniform load distribution over the face width can be achieved for a given operating condition, if there is a high degree of manufacturing accuracy. In this case the value of the face load factor approaches unity. See Annex B for guidance data on face crowning and tip relief. See 4.1.12 for accuracy grade limitations.

7.3.1 Method A — Factors $K_{H\beta\text{-A}}$ and $K_{F\beta\text{-A}}$

By this method, the load distribution over the face width is determined by means of a comprehensive analysis of all influence factors. The load distribution over the face width of gears under load can be assessed from measured values of tooth root strain, during operation at working temperature or, with limitations, by a critical examination of the tooth bearing pattern.

Data to be given in the delivery specification or drawing include

a) maximum (permissible) face load factor, or

b) maximum permissible total mesh misalignment under operating load and temperature, for which the face load factor can be derived using a precise calculation method where it is also necessary that all other relevant influences be known.

7.3.2 Method B — Factors $K_{H\beta\text{-B}}$ and $K_{F\beta\text{-B}}$

By this method, the load distribution along the face width is determined by means of computer aided calculations. This method depends on the elastic deflections under load, the static displacements and on the stiffness of the whole elastic system (see 7.4). The load distribution in a gear mesh and the deformations of the elastic system affect each other. Therefore, one of the following methods must be used:

— iterative method (Dudley/Winter);

— influence factors.

7.3.3 Method C — Factors $K_{H\beta\text{-C}}$ and $K_{F\beta\text{-C}}$

By using this method, account is taken of those components of equivalent misalignment due to pinion and pinion-shaft deformations and also those due to manufacturing deviations. Means of evaluating approximate values of the variables include calculation, measurement and experience, either individually or in combination (see 7.6). As explained in 7.2.1, Method C involves the assumption that gear body elastic deflections produce, in the mesh, a linearly increasing separation over the face width of the working tooth flanks (see Annex D for further information). That equivalent misalignment, inclusive of manufacturing deviations, involves similar separation of working flanks, which is implicit in this assumption.

Figures 7 and 8 illustrate the influences of equivalent misalignment, according to these assumptions, and the tooth load, on the load distribution.

7.4 Determination of face load factor using Method B: $K_{H\beta\text{-B}}$

7.4.1 Number of calculation points

The load distribution is calculated for exactly 10 increments along the face width.

7.4.2 Definition of $K_{H\beta}$

$K_{H\beta}$ is defined as the maximum load intensity (local load per unit length increment of face width) compared to the mean load (F_m/b). The basic model of the gear mesh is a spur tooth pair having the same number of teeth, transverse module and face width of the gear pair being analysed.

$$K_{H\beta} = \frac{(F/b)_{max}}{(F_m/b)} \qquad (38)$$

7.4.3 Stiffness and elastic deformations

The effective stiffness used for the calculation of the load distribution is the stiffness of the whole elastic system. Examples are given in Annex E. It is the addition of the following elastic elements:

- gear mesh;
- gear body;
- stiffness of shaft / hub connections, pinion and gear shaft;
- stiffness of the bearings;
- stiffness of the housing;
- stiffness of the foundation.

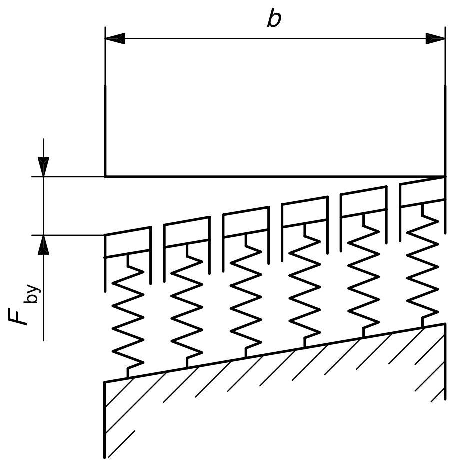

a) Without load

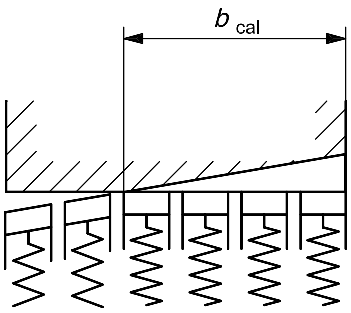

b) Low load and/or large value of equivalent misalignment (large value of $F_{\beta y}$)

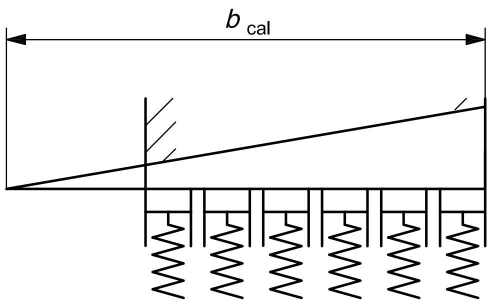

c) High load and/or small value of equivalent misalignment (small value of $F_{\beta y}$)

Figure 7 — Distribution of load along face width with linear equivalent misalignment (illustration of principle)

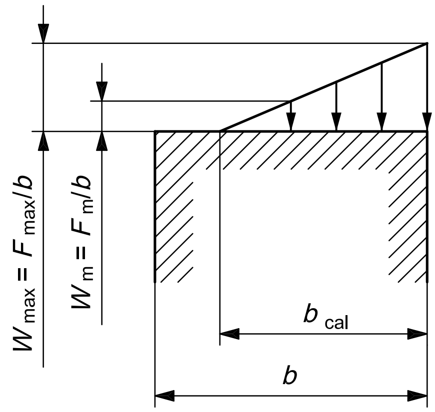

a) Low load and/or large value of $F_{\beta y}$, $b_{cal}/b \leqslant 1$

$$W_{max} = \frac{F_{max}}{b} = \frac{2\,F_m}{b} \cdot \frac{b}{b_{cal}}$$

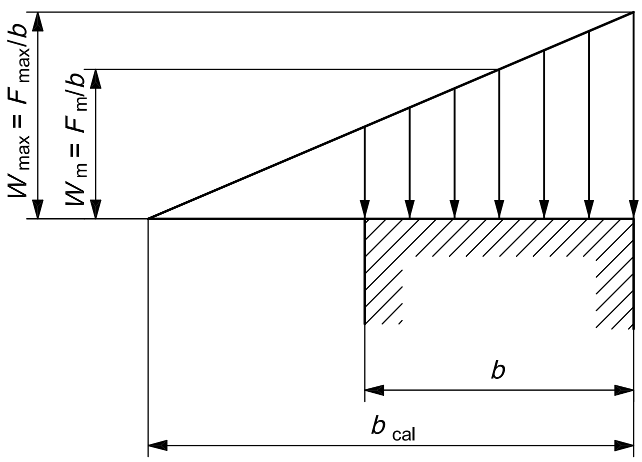

b) High load and/or small value of $F_{\beta y}$, $b_{cal}/b > 1$

$$W_{max} = \frac{F_{max}}{b} = \frac{F_m}{b} \cdot \frac{b_{cal}}{b_{cal} - \frac{b}{2}}$$

Figure 8 — Calculation of load per the unit face width $(F/b)_{max}$ with linear distribution of the load on the face width $F_m = (F_t\, K_A\, K_v)$

7.4.3.1 Gear mesh

The stiffness of each increment results from the method of calculating the deformations. The stiffness of each spring is the mean value of mesh stiffness $c_{\gamma\beta}$ according to Clause 9. The load is assumed to be in the zone of single tooth contact without load sharing. The load sharing between helical teeth is not considered. In certain gears such as thin rimmed gears, the stiffness can vary. Similarily, at ends of the face width the stiffness values can be less than in the centre face. These effects are ignored in Method B.

7.4.3.2 Gear body

The deformations of the gear body due to bending and torsion can be considered by regarding the gear body as a part of the shaft. Different diameters are used for calculating the bending and torsional deformation in the area of the gear mesh, which should be between the root and the tip diameter of the pinion/gear. The value for bending is the (tip diameter – root diameter)/2 plus root diameter. For torsion it is the root diameter plus 0,4 modules. The load is in the base tangent plane for bending.

7.4.3.3 Shaft / hub connection

For normally shrink-fitted gears or connections, the shaft is stiffened to a diameter midway (d_{mid}) between hub diameter and bore (d_{bore}), see Figure 9.

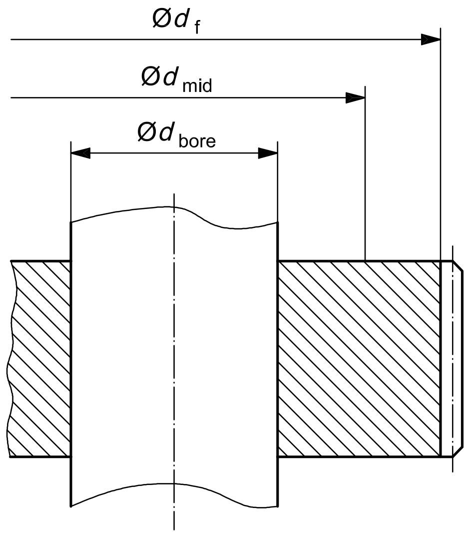

Figure 9 — Definitions of various diameters

7.4.3.4 Pinion and gear shaft

The bending deflections of the pinion and gear shaft (with variable inside and outside diameter) have to be calculated according to the linear bending theory. The bending deflections can be caused by all gear meshes and by all other external loads (belts, chains, couplings, etc.). The diameter in the tooth area to be used for bending is (tip diameter – root diameter)/2 plus root diameter. The load is in the base tangent plane for bending. The torsional deformation of the pinion and gear have only to be calculated in the area of the gear mesh. It has to be considered that the torque is decreasing along the face width. A diameter of root diameter plus 0,4 modules should be used.

7.4.3.5 Bearings

The elastic deformations of the bearings may be calculated by the input of stiffness values for the applied load. If exact stiffness values are not known, minimum and maximum values have to be chosen to verify the influence of the bearing deformations.

7.4.3.6 Housing

The elastic deformations of the housing may be determined by calculation or empirical means. In the case of tapered bearings, the axial deflection of the housing due to gear loads and external thrust loads must be considered in determing the bearing clearances and resulting shaft positions at the bearings.

7.4.3.7 Foundation

The elastic deformations of the foundation may be determined by calculation or empirical means.

7.4.4 Static displacements

7.4.4.1 Shaft working position in bearings

The operating bearing clearances must be considered, including the effects of manufacturing variations, thermal expansion, interference fits, axial clearance in tapered bearings and oil film thickness in plain bearings.

7.4.4.2 Manufacturing errors

Manufacturing variations (permissible variations in gears, housings, etc.) may be estimated from drawing tolerances or established manufacturing standards. The use of ISO 1328 for tooth alignment $f_{H\beta}$ is permitted for the estimate of total manufacturing variation, provided that contact checking at assembly is used to verify that its use is appropriate.

7.4.5 Assumptions

The methods used for determining the values of bearing deformations, bearing clearances, housing deformation and the values for manufacturing errors must be stated. If influence factors are neglected, it has to be justified that they are low enough in magnitude.

7.4.6 Computer program output

In order to verify the computer calculations, the output of the program must include the full list of input values and all relevant intermediate results. To understand the input assumptions and the output value of $K_{H\beta}$, the following data is required in tabular graphic form:

- deflections of the shafts (bending and twist);
- bearing forces;
- gear data;
- load distribution;
- load distribution factor.

7.5 Determination of face load factor using Method C: $K_{H\beta\text{-}C}$

The formulae for the calculations of elastic deflections of the pinion and pinion-shaft (f_{sh}) are simplified and are based on the following assumptions.

a) The deflections of the wheel and wheel shaft are not included in the basic calculations; normally these elements are sufficiently stiff so that their deflections can be ignored, but if it is required to include them they must be assessed independently and corresponding amounts added to f_{ma} with the correct sign.

b) Deformations of the gear case and of the bearings are not included in the basic calculations; normally these elements are sufficiently stiff so that their deflections can be ignored (noting that it is deflection differences which are important), but if it is required to include them they must be assessed independently and corresponding amounts added to f_{ma} with the correct sign.

c) No effect of bearing clearances is included. If the configuration is such that the clearances can result in significant shaft tilting, then this tilt must be assessed independently and corresponding amounts added to f_{ma} with the correct sign.

d) The torsional and bending deflection of a pinion with the actual load distribution are assumed to be not significantly different from those determined with loading distributed evenly over the face width. This assumption is valid for low calculated values of $K_{H\beta}$ and becomes increasingly less valid for higher values.

e) The bearings do not absorb any bending moments.

f) The pinion configuration is in accordance with Figure 13. Note that the restriction that the pinion is towards the centre of the shaft span ($0 \leqslant s / l \leqslant 0{,}3$) does not apply if suitable helix correction is used. Note also that the factor K' takes into account the stiffening effect of the pinion body.

g) The pinion shaft has constant diameter (d_{sh}), is solid (or hollow shaft with $d_{shi}/d_{sh} < 0{,}5$) or can at least be satisfactorily so approximated.

h) The shaft material is steel.

i) Any additional external loads acting on the pinion shaft (e.g. from shaft couplings) have a negligeable effect on the bending deflection of the shaft across the gear face width.

There are three commonly arising conditions which are not covered by the equations of 7.5.2.4 but which can be easily dealt with by slight variants on those equations.

— Where the ratio is unity of near unity and the torqued ends of the shaft are at opposite sides of the box (e.g. rod mill pinion), the torsional deflections of each gear are the same and in the opposite sense, thus compensating for each other, but the bending deflections add.

— Simple planetary gear trains: planet/annulus mesh. As with all idler gears, there is no torsional deflection on the pinion (planet) and the main bending deflection is usually that of the pin in the carrier (caused by loads of the meshing with both the sun and annulus gears).

— Simple planetary gear trains: sun/planet mesh. The torsional deflection of the sun gear is due to the multiple meshes but its bending deflection is zero. However, the deflection of the carrier can also be important at this mesh.

For further information on the derivation of the f_{sh} equations, see Annex D. Note in particular that so as to simplify the procedures for the evaluation of $K_{H\beta}$ by Method C, equivalent mesh misalignment due to elastic deflections is assumed to follow a straight line and that a correction constant (1,33) is introduced to compensate. With increasing curvature of the elastic deformation line, as occurs when gear pairs are heavily loaded or pinion face width to diameter ratios are large, or both, the assumptions may lead to increasing differences between calculated and actual distributions of the load; thus the accuracy of the calculated $K_{H\beta\text{-C}}$ becomes worse as its magnitude increases.

The face load factor $K_{H\beta\text{-C}}$ is calculated from the mean load intensity accross the face (F_m/b), the mesh stiffness ($c_{\gamma\beta}$), and an effective total mesh misalignment ($F_{\beta y}$). One of two equations is used Equation (39) or (41), depending upon whether the contact is calculated to extend across the full face width (see Figures 7 and 8).

Throughout this clause, in the case of double helical gears ($b = 2b_B$), and the smaller of the values for pinion or wheel shall be substituted for b or b_B — this being the width at the tooth roots excluding tooth end chamfering or rounding.

a) $b_{cal} / b \leqslant 1$ corresponding to $\frac{F_{\beta y} c_{\gamma\beta}}{2 F_m / b} \geqslant 1$:

$$K_{H\beta} = \sqrt{\frac{2 F_{\beta y} c_{\gamma\beta}}{F_m / b}} \geqslant 2 \tag{39}$$

$$b_{cal} / b = \sqrt{\frac{2 F_m / b}{F_{\beta y} c_{\gamma\beta}}} \tag{40}$$

b) $b_{cal} / b > 1$ corresponding to $\frac{F_{\beta y} c_{\gamma\beta}}{2 F_m / b} < 1$:

$$K_{H\beta} = 1 + \frac{F_{\beta y} c_{\gamma\beta}}{2 F_m / b} \tag{41}$$

$$b_{cal} / b = 0{,}5 + \frac{F_m / b}{F_{\beta y} c_{\gamma\beta}} \tag{42}$$

The value of effective misalignment to be used is obtained by combining two elements:

a) the effect of manufacturing error (of all relevant components) is included through f_{ma} in accordance with 7.5.3;

b) the effect of elastic deflections of the pinion and pinion-shaft are included through f_{sh} as in 7.5.2.4 to form an initial equivalent misalignment $F_{\beta x}$, which is then reduced by a running-in allowance to form $F_{\beta y}$.

The way in which the two elements are combined depends upon the helix modification (crowning, helix correction, end relief, or none) applied to the mesh (see 7.5.2.3).

7.5.1 Effective equivalent misalignment $F_{\beta y}$

The following equation can be used for common transmission designs:

$$F_{\beta y} = F_{\beta x} - y_\beta = F_{\beta x} \chi_\beta \tag{43}$$

where

$F_{\beta x}$ is the initial equivalent misalignment, i.e. the absolute value of the sum of deformations, displacements and manufacturing deviations of pinion and wheel, measured in the plane of action, and which can be determined in accordance with Method C (see 7.5.2.3).

7.5.2 Running-in allowance y_β and running-in factor χ_β

y_β is the amount by which the initial equivalent misalignment is reduced by running-in since operation was commenced. χ_β is the factor characterizing the equivalent misalignment after running-in. It is convenient to use χ_β in calculations, but only as long as y_β is proportional to $F_{\beta x}$. The important influences include

— pinion and wheel material,

— surface hardness,

— rotational speed at the reference circle,

- type of lubricant,
- surface treatment,
- abrasive in the oil, and
- initial equivalent misalignment $F_{\beta x}$ (as a result of deformations, displacements and manufacturing deviations).

y_β and χ_β do not take into account the effects of running-in operations obtained by manufacturing processes such as lapping. Removal of material by such means shall be taken into account in the value of f_{ma}.

In the absence of direct, assured data from experiment or operating experience (Method A), y_β can be determined in accordance with Method B given in 7.5.2.1 or 7.5.2.2.

7.5.2.1 Determination of y_β and χ_β by calculation

The values from Equations (44) to (51) reproduce the curves in Figures 10 and 11 (see Table 2 for abbreviations used).

a) For St, St (cast), V, V(cast), GGG (perl., bai.), GTS (perl.):

$$y_\beta = \frac{320}{\sigma_{H\,lim}} F_{\beta x} \tag{44}$$

$$\chi_\beta = 1 - \frac{320}{\sigma_{H\,lim}} \tag{45}$$

where $y_\beta \leqslant F_{\beta x}$ and $\chi_\beta \geqslant 0$ and where

for $v \leqslant 5$ m/s	there is no restriction;
for 5 m/s $< v \leqslant 10$ m/s	the upper limit of y_β is 25 600/$\sigma_{H\,lim}$, corresponding to $F_{\beta x} = 80$ µm;
for $v > 10$ m/s	the upper limit of y_β is 12 800/$\sigma_{H\,lim}$, corresponding to $F_{\beta x} = 40$ µm;
$\sigma_{H\,lim}$	is as specified in ISO 6336-5.

b) For GG, GGG (ferr.):

$$y_\beta = 0{,}55\ F_{\beta x} \tag{46}$$

$$\chi_\beta = 0{,}45 \tag{47}$$

where

for $v \leqslant 5$ m/s	there is no restriction;
for 5 m/s $< v \leqslant 10$ m/s	the upper limit of y_β is 45 µm, corresponding to $F_{\beta x} = 80$ µm;
for $v > 10$ m/s	the upper limit of y_β is 22 µm, corresponding to $F_{\beta x} = 40$ µm;

for Eh, IF, NT (nitr.), NV (nitr.), NV (nitrocar.)

$$y_\beta = 0{,}15\ F_{\beta x} \tag{48}$$

$$\chi_\beta = 0{,}85 \tag{49}$$

where for all velocities, the upper limit of y_β is 6 µm, corresponding to $F_{\beta x} = 40$ µm.

When the material of the pinion differs from that of the wheel, the values for the pinion ($y_{\beta 1}$ and $\chi_{\beta 1}$) and the values for the wheel ($y_{\beta 2}$ and $\chi_{\beta 2}$) are to be determined separately. Then, the average values of each (y_β and χ_β) from Equations (50) and (51), are used for the calculations:

$$y_\beta = \frac{y_{\beta 1} + y_{\beta 2}}{2} \tag{50}$$

$$\chi_\beta = \frac{\chi_{\beta 1} + \chi_{\beta 2}}{2} \tag{51}$$

7.5.2.2 Graphical values of y_β

The value y_β can be read from Figures 10 and 11 as a function of the initial equivalent misalignment $F_{\beta x}$ and the value of $\sigma_{H\,lim}$ for the material (see Table 2 for abbreviations used).

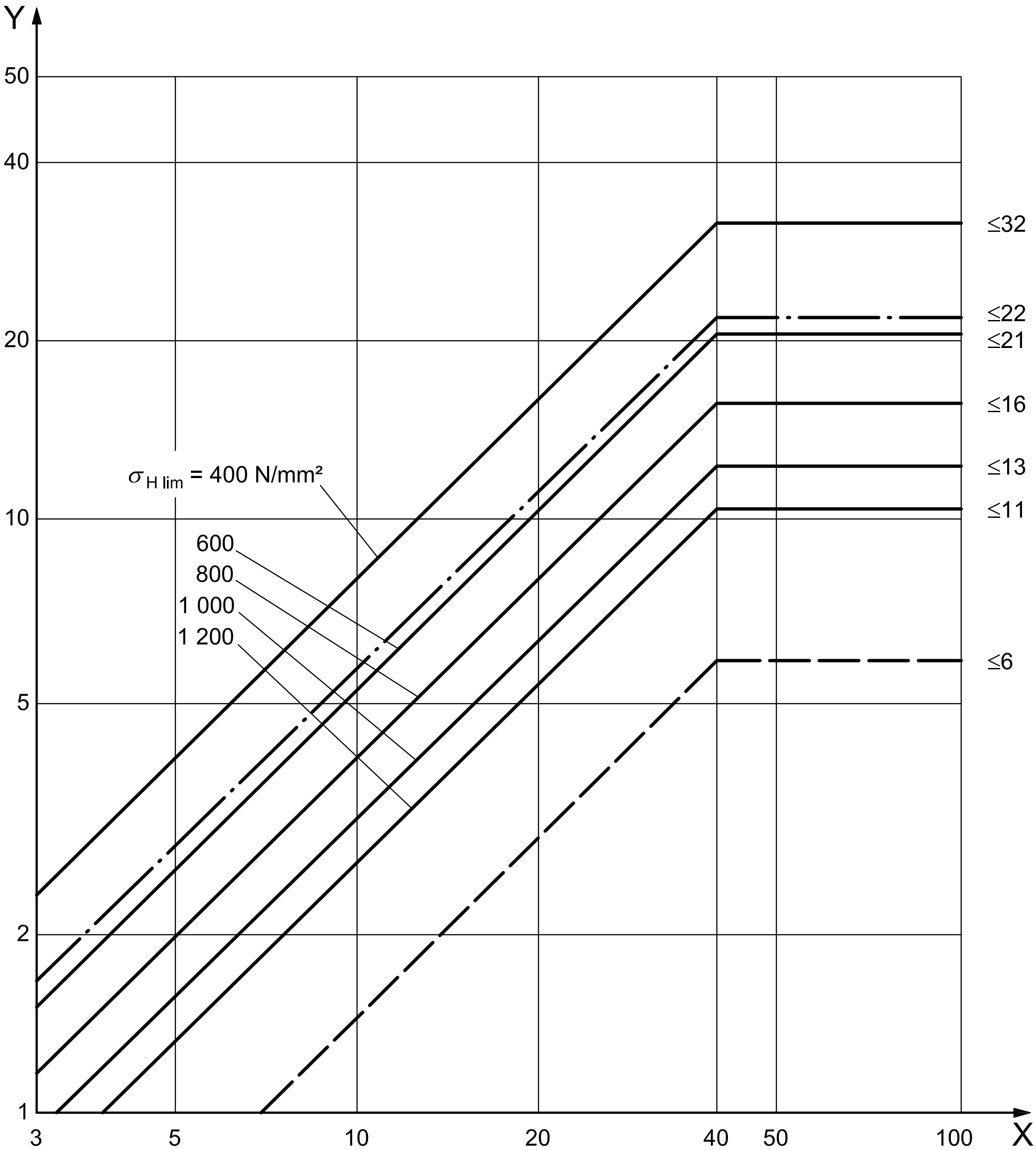

Key

X initial equivalent misalignment, $F_{\beta x}$, µm

Y running-in allowance, y_β, µm

solid line	St, St (cast), V, GGG (perl., bai.), GTS (perl.)	rotational velocity $v > 10$ m/s
dash-dot line	GG, GGG (ferr.)	rotational velocity $v > 10$ m/s
dashed line	Eh, IF, NT (nitr.), NV (nitr.), NV (nitrocar.)	all speeds

If the materials of the pinion and the wheel are different, y_β shall be determined in accordance with Equation (50).

Figure 10 — Running-in allowance for gear pair (see also Figure 11)

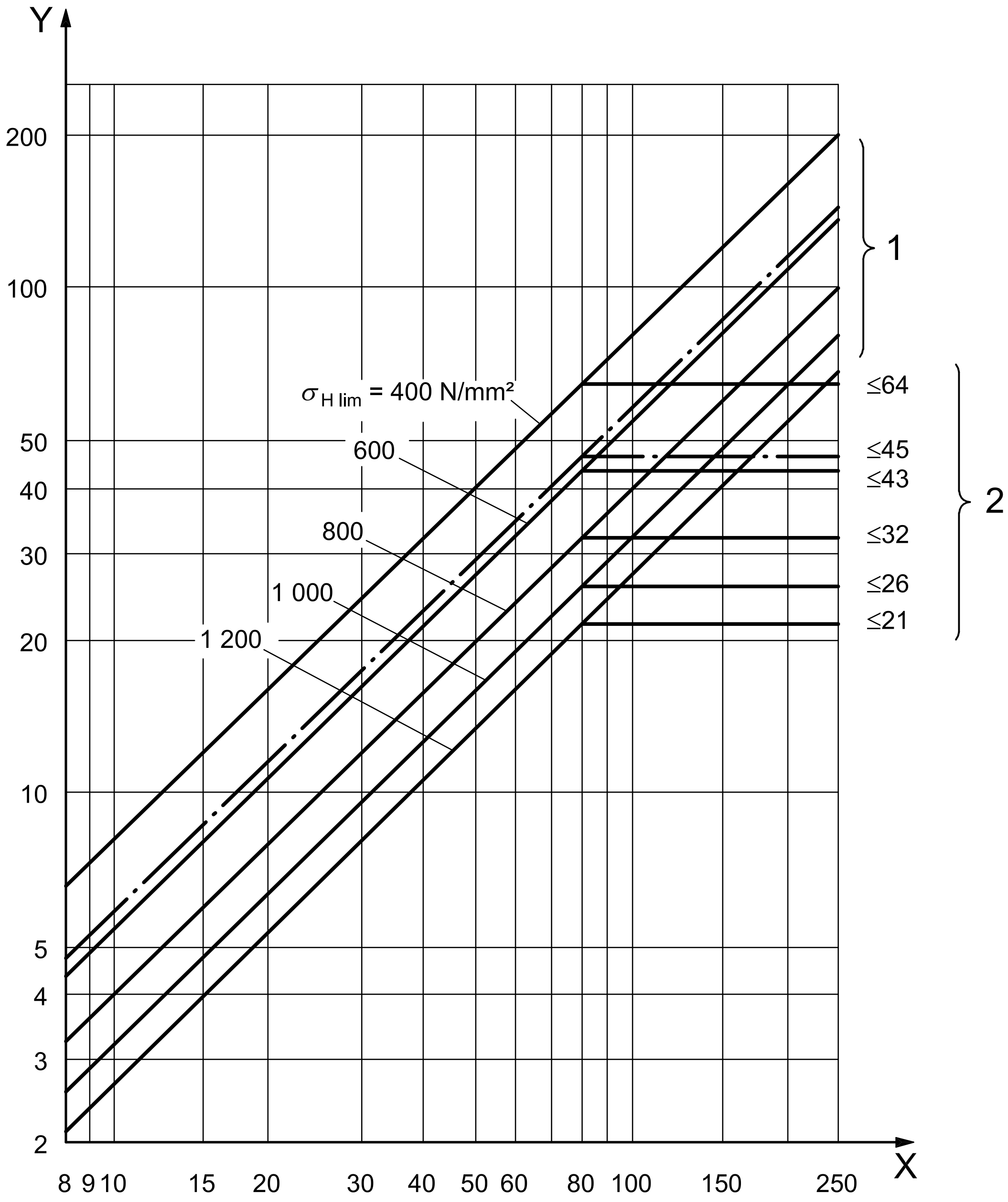

Key

X initial equivalent misalignment, $F_{\beta x}$, µm

Y running-in allowance, y_β, µm

1 circumferential speed at reference circle $v \leqslant 5$ m/s

2 circumferential speed at reference circle 5 m/s $< v \leqslant 10$ m/s

————	St, St (cast), V, GGG (perl., bai.), GTS (perl.)	rotational speed $v \leqslant 10$ m/s
— · —	GG, GGG (ferr.)	

If the materials of the pinion and the wheel are different, y_β shall be determined in accordance with Equation (50).

Figure 11 — Running-in allowance for a gear pair (see also Figure 10)

7.5.2.3 Determination of initial equivalent misalignment, $F_{\beta x}$ (see Annex D)

The value $F_{\beta x}$ is the absolute value of the sum of manufacturing deviations and pinion and shaft deflections, measured in the plane of action [see Caution in b)].

Of the components of deformations, displacement and deviation, only those in the plane of action are determinant for the calculation of $F_{\beta x}$.

a) Gear pairs of which the size and suitability of the contact pattern are not proven and the bearing pattern under load is imperfect [7)]:

See Annex D for an explanation of the factor 1,33 in Equation (52).

$$F_{\beta x} = 1{,}33\ B_1\ f_{sh} + B_2\ f_{ma};\ F_{\beta x} \geqslant F_{\beta x\,min} \tag{52}$$

with B_1 and B_2 taken from Table 8.

Allowance should be made in f_{ma} for the effects of adjustment measures (lapping, running-in at part load), crowning or end-relief, or similarly, for that of the position of the contact pattern.

b) Gear pairs with verification of the favourable position of the contact pattern (e.g. by modification of the teeth or adjustment of bearings) [7), 8)]

$$F_{\beta x} = \left| 1{,}33\ B_1\ f_{sh} - f_{H\beta 6} \right|;\ F_{\beta x} \geqslant F_{\beta x min} \tag{53}$$

with B_1 taken from Table 8.

Table 8 — Constants for use in Equations (52) and (53)

No.	Helix modification		Equation constants	
	Type	**Amount**	B_1	B_2
1	None	—	1	1
2	Central crowning only	$C_\beta = 0{,}5\ f_{ma}$ [a]	1	0,5
3	Central crowning only	$C_\beta = 0{,}5\ (f_{ma} + f_{sh})$ [a]	0,5	0,5
4 [b]	Helix correction only	Corrected shape calculated to match torque being analysed	0,1 [c]	1,0
5	Helix correction plus central crowning	Case 2 plus case 4	0,1 [c]	0,5
6	End relief	appropriate amount $C_{I(II)}$ [d]	0,7	0,7

[a] Appropriate crowning, C_β, see Annex D.

[b] Predominantly applied for applications with constant load conditions.

[c] Valid for very best practice of manufacturing, otherwise higher values appropriate.

[d] See Annex E.

7) Running clearances in rolling bearings should be very small under working conditions. Large clearances can contribute considerably to equivalent misalignment $F_{\beta x}$. When this is the case, a more accurate calculation using Equation (54), or a contact pattern check under load is recommended.

8) With a favourable position of the contact pattern, the elastic deformations and the manufacturing deviations compensate each other. See Figure 12 (compensatory).

A check shall be made to ascertain which of the helices of double-helical gears has the larger equivalent misalignment and, consequently, is determinate for $K_{H\beta}$.

By subtracting $f_{H\beta 5}$, which is the helix slope deviation tolerance for ISO quality 5 (see ISO 1328-1:1995), allowance is made for the compensatory roles of elastic deformation and manufacturing deviations. See Annex D for explanatory notes to Equation (53).

Subject to achieving the requisite contact patterns, $F_{\beta x}$ can be calculated using Equation (53) for gears which have been processed by lapping, running-in at part load or other adjustment means, as well as for gears with carefully designed crowning or end-relief. For crowned gears, the contact pattern centre shall be suitably offset from the mid-face position. Concerning double helical gears, it is necessary to ascertain whether the lesser deformed helix of the pinion has the largest value of $F_{\beta x}$.

CAUTION — When, apart from pinion body and pinion shaft deformations f_{shi}, those of the wheel/wheel shaft f_{sh2} and the gear case f_{ca}, and also the displacements of the bearings f_{be} are to be taken into consideration, Equations (52) and (53) are to be extended to become Equation (54) (see also 7.5.4 and 7.5.5):

$$F_{\beta x} = 1{,}33\, B_1\, f_{sh} + f_{sh2} + f_{ma} + f_{ca} + f_{be};\; f_m \geqslant f_{H\beta 5} \tag{54}$$

The signs of f_{sh2}, f_{ca} and f_{be} shall be carefully heeded; if precise information is not available, it is essential that positive signs are chosen (so that calculated values tend to be safe). Only the bending deflection, if any, of the wheel shaft, is likely to be of consequence to f_{sh2}; previously this amount was taken as the wheel shaft misalignment component of f_{be}. Nevertheless, in general the approximations according to Equations (52) and (53) are satisfactory.

The following influences shall be heeded, as a rule, the elastic deformations of “relatively flexible” spur gears tend to compensate for manufacturing misalignment. On the other hand, because of the axial component of F_m in single-helical gears, additional misalignment can be induced.

Special measures can be taken to secure even distribution of load over the face width. These include set-up bearings, lapping the gears, or running-in the gears as a specified process, in service. By way of a further example, a spur gear or a double-helical gear can be mounted directly on a spherical roller bearing and so be free to take up an attitude of mean, balanced alignment.

Uneven distribution of the body temperature of a large high speed gear can cause deformation near mid-face width resulting in heavy local loading. Either allowance for this deformation shall be included in $K_{H\beta}$, or it shall be compensated for by suitable helix modification.

Similar measures shall be taken when deformation is induced by a large centrifugal force.

Furthermore, the body temperature of a high speed helical pinion is usually higher than that of the mating wheel. This creates additional misalignment which shall be accounted for in the calculations.

c) For gears having ideal contact pattern, full helix modification, under load (for both helices of double helical gears):

$$F_{\beta x} = F_{\beta x\,min} \tag{55}$$

where $F_{\beta x\,min}$ is the greater of the two values:

$$F_{\beta x\,min} = (0{,}005\ \text{mm} \cdot \mu\text{m/N})\, \frac{F_m}{b},\ \text{or}\ F_{\beta x\,min} = 0{,}5\ f_{H\beta} \tag{56}$$

Helix modification is intended to compensate for the torsion and bending deflections of the pinion and wheel, also the deformations or displacements of other components under operating loads and, if known, the tooth alignment deviation of the mating wheel [9]).

$F_{\beta y}$ would be equal to 0 at the design loading of gear pairs having optimum helix modification, i.e. the face load factor $K_{H\beta}$ would be equal to 1. However, in the interest of safety, the minimum value in accordance with Equations (55) and (56) is to be used as the equivalent misalignment.

Similarly, Equation (53) can be used in designing suitable crowning.

See 7.5.2.4 for the determination of f_{sh}, the equivalent misalignment due to pinion and pinion shaft deflections. See 7.5.3 for the determination of mesh misalignment due to manufacturing deviations f_{ma}. See 7.5.2 for the determination of the running-in allowance y_β, i.e. the amount by which the equivalent misalignment is reduced.

For some common arrangements of gear pairs, guidance on the calculation of $F_{\beta x}$ is included in Figure 13 a) to e), in which particular regard is paid to the contact pattern position. A comprehensive analysis is recommended for other, more complex, arrangements.

7.5.2.4 Equivalent misalignment, f_{sh}

The value f_{sh} takes into account the components of equivalent misalignment resulting from bending and twisting of the pinion and pinion shaft, and its value may be determined as follows.

7.5.2.4.1 Approximate calculation of f_{sh}

The following calculation is sufficiently accurate for many common designs. The Equations (57) and (58) are based on the following conventions. The bending component is the product of the deflection at the middle point of the shaft, by point b, where the load F_m is assumed to be acting. The torsional component is calculated for a solid cylinder of diameter d_1, with the load distributed evenly over the face width. In reality, a smaller diameter is determinant; also, the load is not evenly distributed; however, the inaccuracies in the assumptions tend to balance each other out. The equation is valid when the elastic modulus and Poisson's ratio of the material are those of steel. Based on practical experience, Equations (57) and (58) also include a constant empirical term. Concerning hollow shafts, the deflection component f_{sh}, derived from either of these equations, is sufficiently accurate, provided that the bore diameter does not exceed 0,5 d_{sh}.

For both spur and single helical gears:

$$f_{sh} = \frac{F_m}{b} 0{,}023 \left[\left| B^* + K' \frac{l\, s}{d_1^2} \left(\frac{d_1}{d_{sh}} \right)^4 - 0{,}3 \right| + 0{,}3 \right] \left(\frac{b}{d_1} \right)^2 \qquad (57)$$

with B^* equal to 1 if the total power is transmitted through a single engagement.

See 7.2.1 for F_m/b.

For double helical gears:

$$f_{sh} = \frac{F_m}{b} 0{,}046 \left[\left| B^* + K' \frac{l\, s}{d_1^2} \left(\frac{d_1}{d_{sh}} \right)^4 - 0{,}3 \right| + 0{,}3 \right] \left(\frac{b_B}{d_1} \right)^2 \qquad (58)$$

9) Helix angle modification is an alteration of the helix angle, a consequence of which the axial pitch is also modified. The latter concept is useful when dealing with gears having large overlap ratios and consideration of axial pitch is often necessary.

with B^* equal to 1,5, if the total power is transferred by a single engagement.

See 7.2.1 for F_m/b.

If there is more than one power path, then only k % of input is through one gear mesh (e.g. as in the case of grooved-roller mill gears) and the following applies:

$B^* = 1 + 2\ (100 - k)/k$ for spur and single helical gears;

$B^* = 0{,}5 + (200 - k)/k$ for double helical gears.

The constant, K', makes allowances for the position of the pinion in relation to the torqued end. It can be taken from Figure 13.

A comprehensive analysis is recommended for other arrangements or where the values for s/l exceed those specified in Figure 13, and also where there are additional shaft loads, e.g. from belt pulleys or chain wheels.

Substitute the absolute value f_{sh} in Equations (52) and (53). See Figure 12 and 7.5.2.3 for information on the compensation of f_{sh} by f_{ma}.

7.5.2.4.2 Face width to be used in Equations (57) and (58) for crowned spur and helical gears

This type of helix modification is employed in order to compensate for manufacturing deviations and load-induced deformations of the gears, and in particular to relieve the tooth-endloading. Gears are usually crowned symmetrically about the mid-face width. See Annex D for recommendations on the extent of crowning.

If the height of the crowning is greater than that specified in Annex B, the reduced width $b_{(b)}$ is to replace the face width b in formulae used for calculating load capacity (see Annex B, Figure B.1). This is determined from values of $C_{\beta(b)}$ calculated in accordance with Equation (B.1) or (B.2). It is to be assumed that the tooth ends outside $b_{(b)}$ are not bearing any load.

7.5.2.4.3 Face width to be used in Equations (57) and (58) for spur and helical gears with end relief

This type of helix modification is used to protect the tooth ends from the overloading caused by equivalent misalignment. Usually, the relief applied is the same at both ends of the teeth. See Annex B for a recommendation, on the amount of end relief.

If the amount of end relief is greater than is specified in Annex B, a reduced width $b_{(b)}$ shall replace the face width b in formulae used for calculating load capacity (see Figure B.2). This is determined from values of $C_{I(II)(b)}$ calculated in accordance with Equations (B.3) or (B.4). It is to be assumed that the tooth ends outside $b_{(b)}$ are not bearing any load.

Figure	Position of contact pattern	Determination of $F_{\beta x}$
a)	Contact pattern lies towards mid bearing span 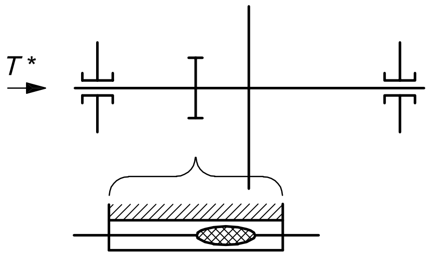	$F_{\beta x}$ in accordance with Equation (53) (compensatory)
b)	Contact pattern lies away from mid bearing span 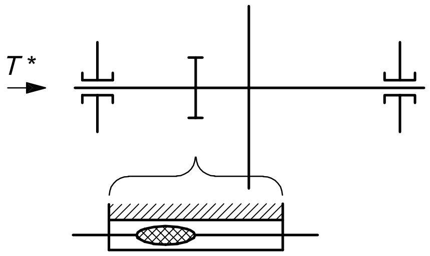	$F_{\beta x}$ in accordance with Equation (52) (additive)
c)	Contact pattern lies towards mid bearing span 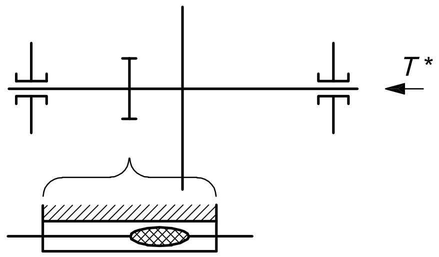	$F_{\beta x}$ in accordance with Equation (52) $\lvert K' \rvert \cdot l \cdot s / d_1^2 \left(d_1 / d_{sh} \right)^4 \leqslant B^*$ (additive) $F_{\beta x}$ in accordance with Equation (53) $\lvert K' \rvert \cdot l \cdot s / d_1^2 \left(d_1 / d_{sh} \right)^4 > B^*$ (compensatory)
d)	Contact pattern lies away from mid bearing span 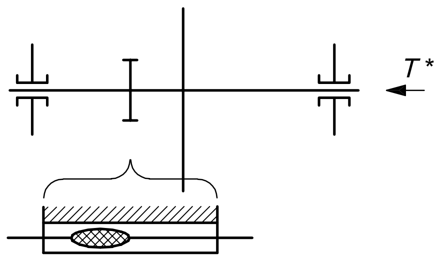	$F_{\beta x}$ in accordance with Equation (52) $\lvert K' \rvert \cdot l \cdot s / d_1^2 \left(d_1 / d_{sh} \right)^4 \geqslant B^* - 0{,}3$ (additive) $F_{\beta x}$ in accordance with Equation (53) $\lvert K' \rvert \cdot l \cdot s / d_1^2 \left(d_1 / d_{sh} \right)^4 < B^* - 0{,}3$ (compensatory)
e)	Contact pattern lies towards the bearing 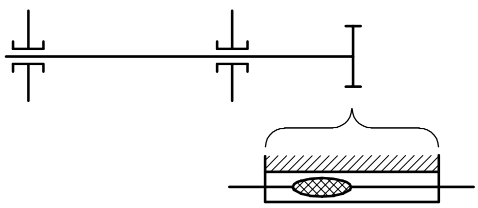	$F_{\beta x}$ in accordance with Equation (52) (additive)

f)	Contact pattern lies away from the bearing 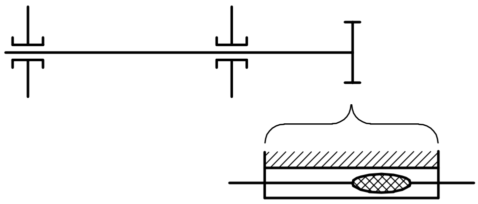	$F_{\beta x}$ in accordance with Equation (53) (compensatory)

a) to d) are the most common mounting arrangements with pinion between bearings.

e) to f) have overhung pinions.

T input or output torqued end, not dependent on direction of rotation.

B^* is equal to 1 for spur and single helical gears and is equal to 1,5 for double helical gears. The peak load intensity occurs on the helix near the torqued end. See also 7.5.2.4.

Figure 12 — Rules for determination of $F_{\beta x}$ with regard to contact pattern position

Factor *K*′ with	**Factor *K*′** without	**Figure**	**Arrangement**
stiffening [a]			
0,48	0,8	a)	with $s/l < 0{,}3$ 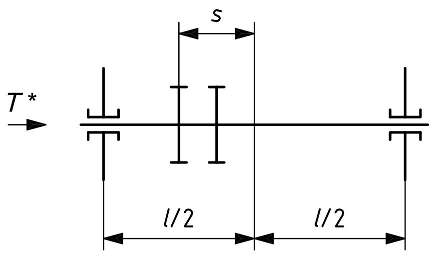
–0,48	–0,8	b)	with $s/l < 0{,}3$ 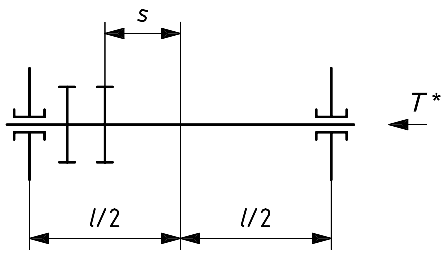
1,33	1,33	c)	with $s/l < 0{,}3$ 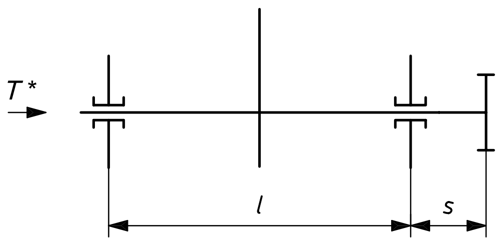
–0,36	–0,6	d)	with $s/l < 0{,}3$ 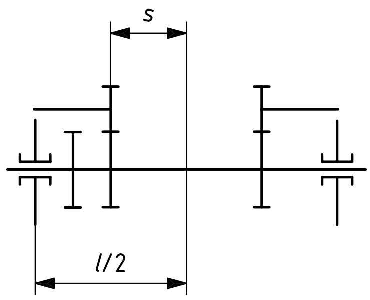

−0,6	−1,0	e)	with $s/l < 0{,}3$ 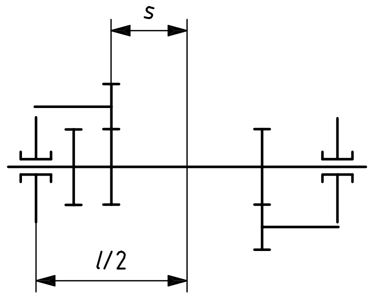

[a] When $d_1/d_{sh} \geqslant 1{,}15$, stiffening is assumed; when $d_1/d_{sh} < 1{,}15$, there is no stiffening; furthermore, scarcely any or no stiffening at all is to be expected when a pinion slides on a shaft and feather key or a similar fitting, nor when normally shrink fitted.

T^* is the input or output torqued end, not dependent on direction of rotation.

Dashed line indicates the less deformed helix of a double helical gear.

Determine f_{sh} from the diameter in the gaps of double helical gearing mounted centrally between bearings.

Figure 13 — Constant K' for the calculation of the pinion offset factor γ

7.5.2.4.4 Specified maximum value for f_{sh}

Sometimes experience with similar gear units enables the choice of an appropriate value of f_{sh} to be made.

EXAMPLE 1 $f_{sh} \approx 0$ µm in the case of a very rigid design; deformations are neglected.

EXAMPLE 2 $f_{sh} = 6$ µm is occasionally specified as a maximum value for some turbine transmissions; the gears are to be designed accordingly.

When calculations are based on such assumptions, the assumptions shall be validated by computations or measurements.

7.5.2.4.5 Value f_{sh} corresponding to gear quality

For certain gears, the value of f_{sh} is specified as a percentage of the allowable helix slope deviation. The gears are to be designed accordingly.

$$f_{sh} = 1{,}0\, f_{H\beta} \tag{59}$$

As for 7.5.2.4.4, assumptions shall be validated by computations or measurements.

7.5.3 Mesh misalignment, f_{ma}

f_{ma} is the maximum separation between the tooth flanks of the meshing teeth of mating gears, when the teeth are held in contact without significant load, the shaft journals being in their working attitudes.

f_{ma} depends on the way in which the deviations of individual components in the plane of action combine, i.e. whether the helix slope deviation $f_{H\beta}$ of each gear and the alignment deviation of the shafts are additive or compensatory, or whether the alignment of the shafts is adjustable (e.g. by means of adjustable bearings).

For purposes of load capacity calculations in accordance with this part of ISO 6336, the methods given in 7.5.3.1 to 7.5.3.6 can be used for the determination of f_{ma}.

It is recommended that the values used for f_{ma} be verified by checking the contact pattern in the working attitude.

7.5.3.1 Derivation of f_{ma} from deviations of individual components

This is to be done after inspection and measurement of gears, bearings and the gear-case.

The maximum mesh misalignment involves the most unfavourable combination of individual deviations:

$$f_{ma\,max} = \left(\left| f_{par\,act} + f_{H\beta 1\ act} + f_{H\beta 2\ act} \right| \right)_{max} \tag{60}$$

The minimum mesh misalignment from the most favorable combination:

$$f_{ma\,min} = \left(\left| f_{par\,act} + f_{H\beta 1act} + f_{H\beta 2\,act} \right| \right)_{min} \tag{61}$$

where $f_{H\beta 1\ act}$ and $f_{H\beta 2\ act}$ are the measured values of helix slope deviation of pinion and wheel (in accordance with ISO 1328-1). The values can vary in size and direction around the circumference.

The combined effect of the helix slope deviation of pinion and wheel, i.e. $\Sigma f_{H\beta} = (f_{H\beta 1\ act} + f_{H\beta 2\ act})$ can be determined as follows.

The pinion and wheel, assembled on their shafts, are mounted on roller blocks which are aligned in parallel pairs and the contact patterns are generated. By moving one of the blocks, the tooth flanks are brought into contact over the entire face width. The $\Sigma f_{H\beta}$ can then be derived from the non-parallelism of the blocks.

$f_{par\ act}$ is the measured value of shaft misalignment, due to in-plane and out-of-plane deviations of either of the shafts. In the event of radial run-out of one or more journals, $f_{par\ act}$ can vary with the angle of rotation. Care shall be taken with the sign of each individual deviation.

A mean value derived from Equation (A.7) is to be used in gear load capacity calculations.

In this procedure, the influence of bearing clearances is neglected.

7.5.3.2 Specified maximum value of f_{ma}

Sometimes permissible limits for the total manufacturing deviation f_{ma}[10)] are specified.

EXAMPLE 1 $f_{ma\ max} = 0$ µm is sometimes demanded for accurate high speed transmissions; due to high precision of manufacturing, deviations can be neglected.

EXAMPLE 2 $f_{ma\ max} = 15$ µm can be a realistic value for certain industrial transmissions.

A mean value derived from Equation (A.6) is to be used in gear load capacity calculations.

7.5.3.3 f_{ma} for a given accuracy

For assembly of gears without any modification or adjustment. Inspection after assembly is recommended in this case. See also 7.5.3.

If, according to ISO 1328-1, for a given gear quality grade helix slope deviation tolerances are given as $f_{H\beta 1}$ and $f_{H\beta 2}$ for pinion and wheel respectively, and if the alignment-of-axes tolerances is given as $f\sigma_{\beta}$, then the most unfavorable combination of deviations (pinion, wheel, case) would be

$$f_{ma} = f_{H\beta 1} + f_{H\beta 2} + f_{\Sigma\beta} \frac{b}{l} \tag{62}$$

---

10) Appropriate control measures should be adopted to ensure that this value is maintained.

Experience has shown that, within many manufacturing environments, aggregate misalignments are close to this value with sufficient frequency for it to be advisable for it to be used in the calculation. However, the distribution of a dimension within its tolerance band is influenced very much by the quality control regime, and in other circumstances the statistical effects mean that a lower aggregate value is appropriate. For example, if controls are in place to ensure that most gears are well within tolerance, with only a small percentage actually near the limit, and to ensure that helix variation *within any single gear* is negligible, then statistical studies show that in only about 10 % of cases will the deviations combine to exceed a total value of 1,0 $f_{H\beta 2}$.

$$f_{ma} = 1{,}0 \; f_{H\beta 2} \tag{63}$$

In most circumstances, the appropriate value to be used lies between these two extremes, and a useful formulation for use in cases of an average quality control regime is

$$f_{ma} = \sqrt{f_{H\beta 1}^2 + f_{H\beta 2}^2} \tag{64}$$

The selection of an appropriate value rests with the user of ISO 6336, but if the chosen value is less than that given by Equation (64), then the user shall be able to justify that selection.

a) For gear pairs with provision for adjustment (lapping or running-in under light load, adjustable bearings or appropriate helix angle modification) and gear pairs suitably crowned, the no-load mesh misalignment can, to a great extent, be compensated for by means of adjustment measures such as re-working of bearings, bearing housings, etc. Satisfactory contact over the face width of the gears can often be achieved by these methods and by means of the other measures mentioned above. See Annex B for guide values for crowning.

   If data from experience are not available, it can be assumed that properly effected adjustments will reduce the value of f_{ma} by 50 %; this is taken into account by the Factor B_2 in Equation (52).

b) For gear pairs with well designed end-relief, in the absence of data from experience and subject to skilled execution, this is taken into account by the factor B_2 in Equation (52). See Annex B for guide values for end relief.

7.5.3.4 Determination of f_{ma} with gears assembled in gear-case

After assembly in the gear-case, it may be possible to measure mesh misalignment directly with the top of the case removed. Values of $f_{ma\ max}$ and $f_{ma\ min}$ are determined from measurements made around the circumference, using feeler gauges; f_{ma} is then derived from Equation (A.7).

For wide gears without helix modification mounted in journal bearings with relatively large clearances, the following procedure may be used. The shaft journals are supported in their working attitudes. The mating gear is clamped to prevent rotation. Bring the working faces into light contact, then insert feeler gauges between the faces at both ends of the mesh. The mesh misalignment f_{ma} is equal to the difference between the thicknesses of the gauges:

$$f_{ma} = \delta_g \left(\frac{b}{l} \right) \tag{65}$$

where δ_g is the difference in the feeler gauge indications, b is the face width and l is the distance between the feeler gauges. When the helices of gears are modified, the amount is included in the difference δ_g, which can also be determined as the difference in thickness of two lead wires which have been inserted between the flanks, where they are subjected to light load.

7.5.4 Component of mesh misalignment caused by case deformation, f_{ca}

Case deformation may be ignored when the gears are assembled in rigid cases. The deflections of other cases f_{ca} may be determined by testing or, approximately, by using the finite element method.

7.5.5 Component of mesh misalignment caused by shaft displacement, f_{be}

In some cases the effects of bearing clearances and bearing deflections are greater than those of shaft and wheel blank deflections.

The components of misalignment in the plane of action as a result of bearing deflections, and journal displacements in bearings clearances, can usually be neglected when the pinion and wheel of spur or double helical gears are positioned midway between bearings of equal stiffness and clearance.

When gears are not positioned in this way, bearing deflections and displacements (clearances) can influence the distribution of load over the face width. This is also valid for single helical or overhung gears.

Since only the relative misalignments due to bearing deflections and displacements of the common axis of the pinion bearings f_{be-1} and that of the wheel f_{be-2} influence the equivalent misalignment, the directions and signs of the misalignments of bearings axes are to be given careful attention. The following equation is valid for the simplest arrangement of a mating pair, with each gear alone on a shaft with two bearings:

$$f_{be} = f_{be1} + f_{be2} \quad \text{or} \quad f_{be} = f_{be1} - f_{be2} \tag{66}$$

For a gear mounted between the bearings, see Figure 14:

$$f_{be} = \frac{b}{l}(\delta_1 - \delta_2) \tag{67}$$

For an overhung gear, see Figure 15:

$$f_{be} = \frac{b}{l}(\delta_1 + \delta_2) \tag{68}$$

where δ_1 and δ_2 are the deflections of bearing 1 and bearing 2 parallel to the plane of action.

The effect of the tilting moment, due to the axial component of the tooth load, of single helical gears, shall be taken into account.

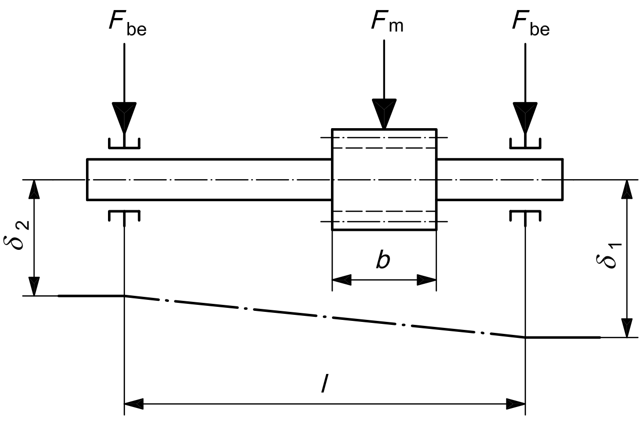

Figure 14 — Loading and deflections for gear mounted between the bearings [see Equation (67)]

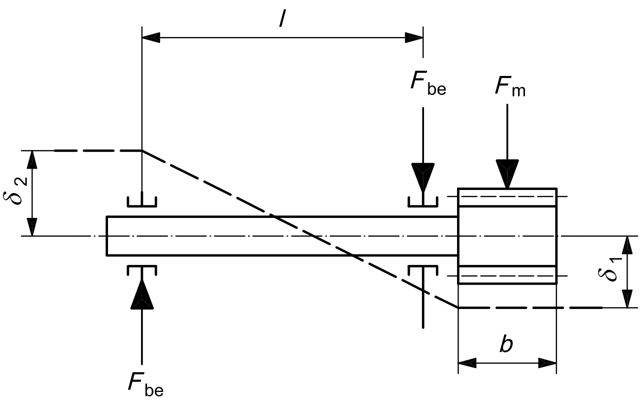

Figure 15 — Loading and deflections for overhung gear [see Equation (68)]

7.6 Determination of face load factor for tooth root stress using Method B or C: $K_{F\beta}$

$K_{F\beta}$ takes into account the effect of the load distribution over the face width on the stresses at the tooth root. It depends on the variables which are determined for $K_{H\beta}$ and also on the face width to tooth depth ratio, b/h.

Determination by calculation:

$$K_{F\beta} = \left(K_{H\beta}\right)^{N_F} \tag{69}$$

$$N_F = \frac{(b/h)^2}{1 + b/h + (b/h)^2} = \frac{1}{1 + h/b + (h/b)^2} \tag{70}$$

The smaller of the values b_1/h_1, b_2/h_2 is to be used as b/h. Boundary condition: when $b/h < 3$, substitute 3 for b/h. For double helical gears, b_B is to be used instead of b.

8 Transverse load factors $K_{H\alpha}$ and $K_{F\alpha}$

8.1 Transverse load distribution

The transverse load factors, $K_{H\alpha}$ for surface stress and $K_{F\alpha}$ for tooth root stress, account for the effect of the non-uniform distribution of transverse load between several pairs of simultaneously contacting gear teeth as follows.

The transverse load factors are defined as the ratio of the maximum tooth load occurring in the mesh of a gear pair at near zero min^{-1} to the corresponding maximum tooth load of a similar gear pair which is free from inaccuracies. The main influences are

a) deflections under load,

b) profile modifications,

c) tooth manufacturing accuracy, and

d) running-in effects.

8.2 Determination methods for transverse load factors — Principles and assumptions

Several methods for the determination of transverse load factors in accordance with the specifications given in 4.1.12 are listed below.

With optimum profile modification appropriate to loading, high manufacture accuracy, even load distribution over the face width and a high specific loading level, the transverse load factor approaches unity.

8.2.1 Method A — Factors $K_{H\alpha\text{-A}}$ and $K_{F\alpha\text{-A}}$

As stated in 6.4.1, the maximum tooth loads (including the inner dynamic tooth loads and the effect of uneven distribution of loading) can be determined directly by measurement or by a comprehensive mathematical analysis. $K_{H\alpha}$ and $K_{F\alpha}$ are then assumed to be unity (as is K_v).

The load distribution, in the tangential direction only, can also be determined by comprehensive analysis of all influence factors. The division of the total tangential load between simultaneously meshing tooth pairs can be derived from strain gauge measurements, made at the tooth roots of gears transmitting load at low speeds.

Information to be stated in the drawing or specification documents is the following:

— maximum (permissible) total tooth load, or

— maximum (permissible) transverse load factor, or

— all data (in particular, information relating to the effective difference of base pitch) necessary for making an accurate analysis.

8.2.2 Method B — Factors $K_{\mathrm{H}\alpha\text{-B}}$ and $K_{\mathrm{F}\alpha\text{-B}}$

This method involves the assumption that the average difference between the base pitches of the pinion and wheel is the major parameter in determining the distribution of load between several pairs of teeth in the mesh zone. See 7.5.2.3 b) and footnote 7).

8.3 Determination of transverse load factors using Method B — $K_{\mathrm{H}\alpha\text{-B}}$ and $K_{\mathrm{F}\alpha\text{-B}}$

According to the conditions and assumptions described in 8.2.2 and footnotes 10 and 11, Method B is suitable for all types of gearing (spur or helical with any basic rack profile and any accuracy). Transverse load factors can be determined by calculation or graphically. The two methods give identical results.

8.3.1 Determination of transverse load factor by calculation [11)]

The calculations are as follows:

a) values $K_{\mathrm{H}\alpha}$ and $K_{\mathrm{F}\alpha}$ for gears with total contact ratio $\varepsilon_\gamma \leqslant 2$

$$K_{\mathrm{H}\alpha} = K_{\mathrm{F}\alpha} = \frac{\varepsilon_\gamma}{2}\left(0{,}9 + 0{,}4\,\frac{c_{\gamma\alpha}\left(f_{\mathrm{pb}} - y_\alpha\right)}{F_{\mathrm{tH}}/b}\right) \tag{71}$$

b) values $K_{\mathrm{H}\alpha}$ and $K_{\mathrm{F}\alpha}$ for gears with total contact ratio $\varepsilon_\gamma > 2$

$$K_{\mathrm{H}\alpha} = K_{\mathrm{F}\alpha} = 0{,}9 + 0{,}4\sqrt{\frac{2\left(\varepsilon_\gamma - 1\right)}{\varepsilon_\gamma}}\,\frac{c_{\gamma\alpha}\left(f_{\mathrm{pb}} - y_\alpha\right)}{F_{\mathrm{tH}}/b} \tag{72}$$

where the following are to be determined:

$c_{\gamma\alpha}$ mesh stiffness in accordance with Clause 9;

f_{pb} the larger of the base pitch deviations of pinion or wheel should be used; 50 % of this tolerance may be used, when profile modifications compensate for the deflections of the teeth at the actual load level [12)];

y_α running-in allowance as specified in 8.3.5;

F_{tH} determinant tangential load in a transverse plane, $F_{\mathrm{tH}} = F_{\mathrm{t}}\,K_{\mathrm{A}}\,K_{\mathrm{v}}\,K_{\mathrm{H}\beta}$.

---

11) Equations (71) and (72) are based on the assumption that the base pitch deviations appropriate to the gear accuracy specified are distributed around the circumference of the pinion and wheel as is consistent with normal manufacturing practice. They do not apply when the gear teeth have some intentional deviation.

12) The base pitch deviation f_{pb} accounts for the total effect of all gear tooth deviations which affect the transverse load factor. If, nevertheless, the profile form deviation $f_{\mathrm{f}\alpha}$ is greater than the base pitch deviation, the profile form deviation is to be taken instead of the base pitch deviation.

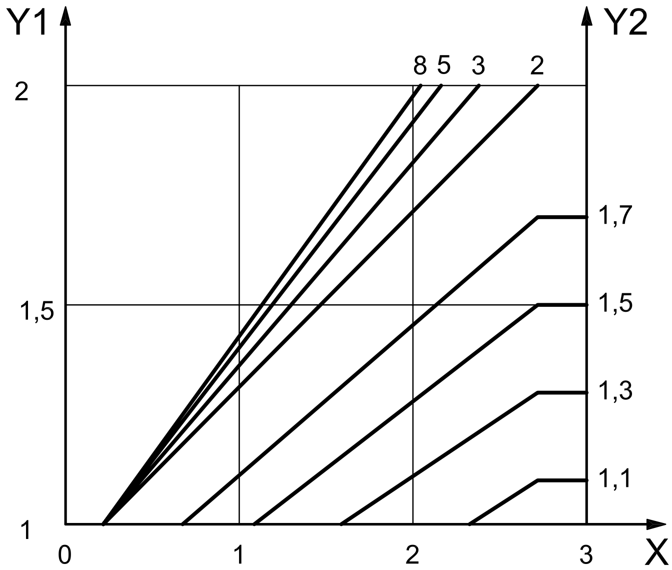

Key

X $q_{\alpha} = \frac{c_{\gamma\alpha}\left(f_{pb} - y_{\alpha}\right)}{F_{tH}/b}$

Y1 $K_{F\alpha}$, $K_{H\alpha}$

Y2 ε_{γ}

Figure 16 — Determination of transverse load factors $K_{H\alpha}$ and $K_{F\alpha}$ by Method B
(see 8.3.3 and 8.3.4 for limiting conditions)

8.3.2 Transverse load factors from graphs

$K_{H\alpha}$ and $K_{F\alpha}$ can be read from Figure 16; the curves are consistent with Equations (71) and (72).

8.3.3 Limiting conditions for $K_{H\alpha}$

When, in accordance with Equation (71) or (72)

$$K_{H\alpha} > \frac{\varepsilon_{\gamma}}{\varepsilon_{\alpha} Z_{\varepsilon}^2} \tag{73}$$

then for $K_{H\alpha}$ substitute $\frac{\varepsilon_{\gamma}}{\varepsilon_{\alpha} Z_{\varepsilon}^2}$, and when $K_{H\alpha} < 1{,}0$, then for $K_{H\alpha}$ substitute as the limit value 1,0.

See 8.3.4.

8.3.4 Limiting conditions for $K_{F\alpha}$

When, in accordance with Equation (71) or (72)

$$K_{F\alpha} > \frac{\varepsilon_{\gamma}}{0{,}25\,\varepsilon_{\alpha} + 0{,}75} \tag{74}$$

then for $K_{F\alpha}$ substitute $\frac{\varepsilon_{\gamma}}{0{,}25\,\varepsilon_{\alpha} + 0{,}75}$ and when $K_{F\alpha} < 1{,}0$ then for $K_{F\alpha}$ substitute as limit value 1,0.

With limiting values in accordance with Equations (71) and (72), the least favourable distribution of load is assumed, implying that the entire tangential load is transferred by only one pair of mating teeth. Furthermore, it is recommended that the accuracy of helical gears be so chosen that $K_{H\alpha}$ and $K_{F\alpha}$ are not greater than ε_α. As a consequence, it may be necessary to limit the base pitch deviation tolerances of gears of coarse accuracy grade.

8.3.5 Running-in allowance y_α

The value y_α is the amount by which the initial base pitch deviation is reduced by running-in from the start of operation. See 7.5.2 for the main influences. y_α does not account for an allowance due to any extent of running-in as a controlled measure, being part of the production process, e.g. lapping. This adjustment is to be taken into consideration when considering the gear accuracy.

y_α may be determined in accordance with 8.3.5.1 or 8.3.5.2 (Method B) where direct, verified values from experimentation or experience are lacking (Method A).

The value for the base pitch deviation f_{pb} determined in accordance with 8.3.1 or 6.4.3 should be used in both methods. The equations and graphs should also be applied analogously for the profile form deviation $f_{f\alpha}$.

8.3.5.1 Determination by calculation

The running-in allowance y_α may be calculated using Equations (75) to (78). These are consistent with the curves in Figures 17 and 18 (see Table 2 for abbreviations used).

a) For St, St(cast), V, V(cast), GGG(perl., bai.) and GTS(perl.):

$$y_\alpha = \frac{160}{\sigma_{H\,lim}}\, f_{pb} \tag{75}$$

where

for $v \leqslant 5$ m/s there is no restriction;

for 5 m/s $< v \leqslant 10$ m/s the upper limit of y_α is 12 800/$\sigma_{H\,lim}$ corresponding to $f_{pb} = 80$ µm;

for $v > 10$ m/s the upper limit of y_α is 6400/$\sigma_{H\,lim}$ corresponding to $f_{pb} = 40$ µm;

b) For GG and GGG(ferr.):

$$y_\alpha = 0{,}275\, f_{pb} \tag{76}$$

where

for $v \leqslant 5$ m/s there is no restriction;

for 5 m/s $< v \leqslant 10$ m/s the upper limit of y_α is 22 µm corresponding to $f_{pb} = 80$ µm;

for $v > 10$ m/s the upper limit of y_α is 11 µm corresponding to $f_{pb} = 40$ µm;

c) For Eh, IF, NT(nitr.), NV(nitr.) and NV(nitrocar.): for all velocities but with the restriction that the upper limit of y_α is 3 µm corresponding to $f_{pb} = 40$ µm

$$y_\alpha = 0{,}075\, f_{pb} \tag{77}$$

When the materials differ, $y_{\alpha 1}$ should be determined for the pinion material and $y_{\alpha 2}$ for the wheel. The average value is used for the calculation:

$$y_\alpha = \frac{y_{\alpha 1} + y_{\alpha 2}}{2} \quad (78)$$

8.3.5.2 Graphical values

y_α may be read from Figures 17 and 18 as a function of the base pitch deviation f_{pb} and the material value $\sigma_{H\ lim}$ (see Table 2 for abbreviations used).

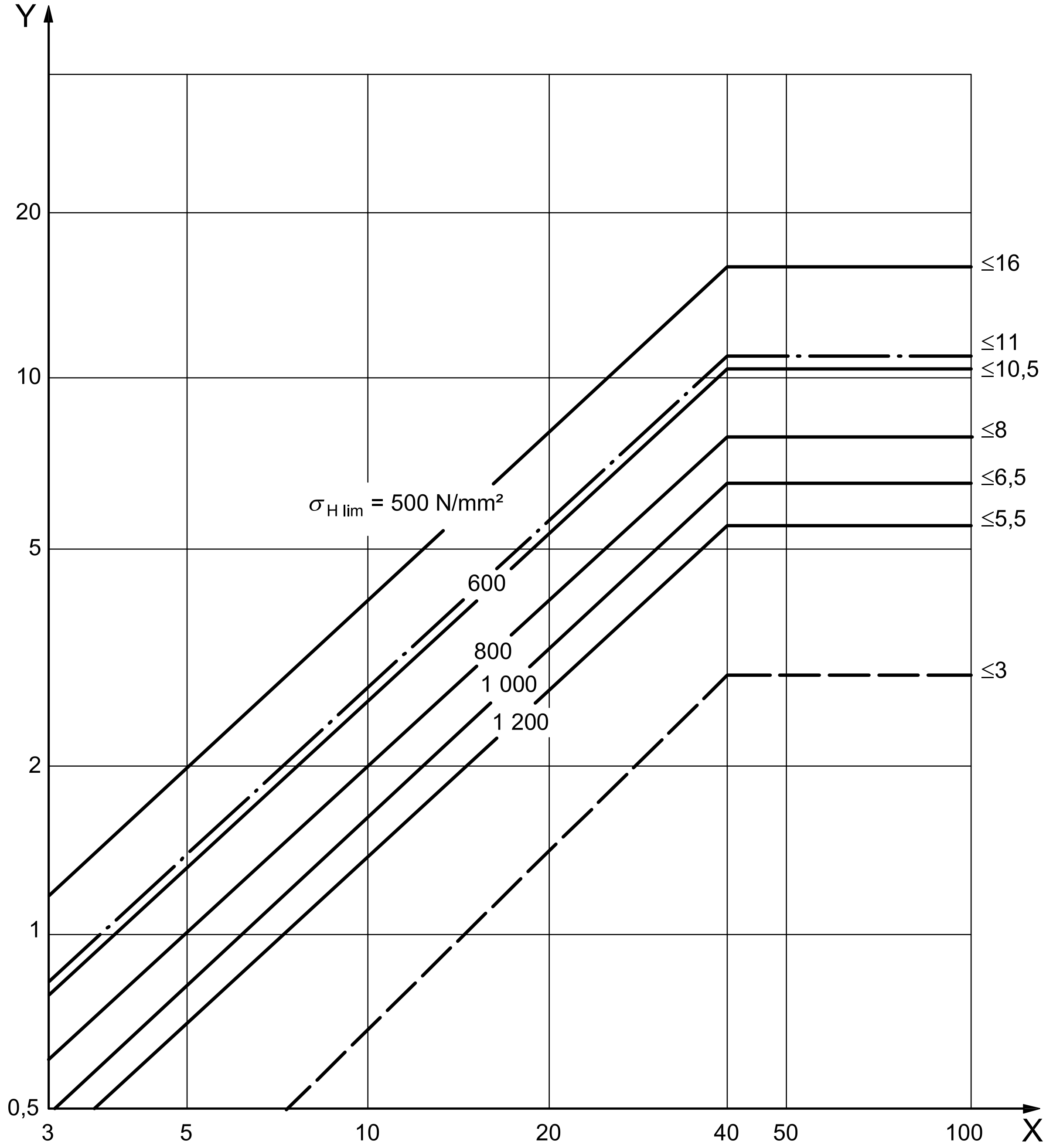

Key

X base pitch deviation, f_{pb}, µm

Y running-in allowance, y_{α}, µm

———— (solid line)	St, St (cast), V, GGG (perl., bai.), GTS (perl.)	tangential velocity $v > 10$ m/s
—·— (dash-dot line)	GG, GGG (ferr.)	
— — — (dashed line)	Eh, IF, NT (nitr.), NV (nitr.), NV (nitrocar.)	all tangential speeds

This graph is derived from Figure 10. If the materials of the pinion and the wheel are different, y_{α} shall be determined in accordance with Equation (78).

Figure 17 — Determination of running-in allowance y_{α} of gear pair (see also Figure 18)

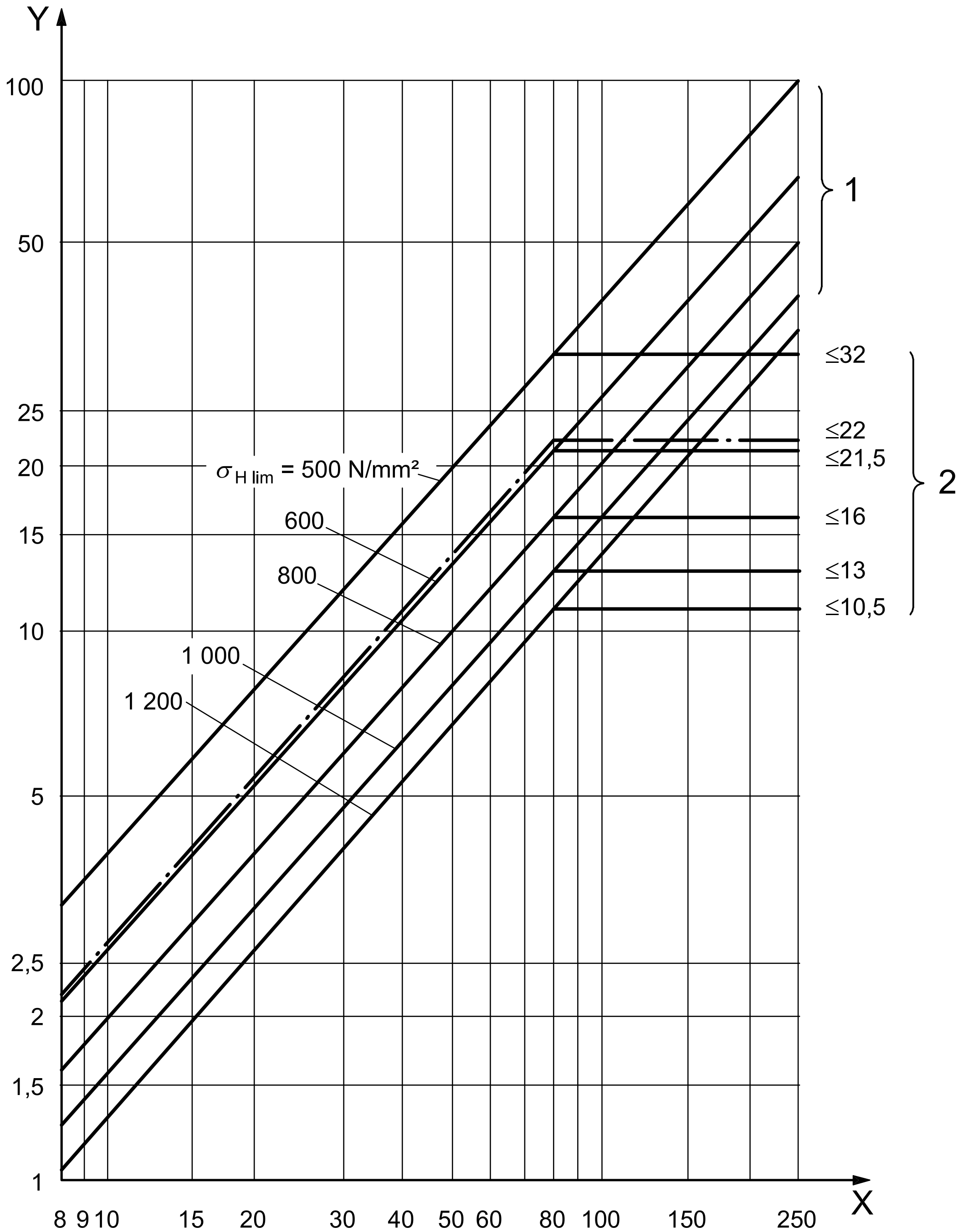

Key

X base pitch deviation, f_{pb}, µm

Y running-in allowance, y_α, µm

1 circumferential speed at reference circle $v \leqslant 5$ m/s

2 circumferential speed at reference circle $5 < v \leqslant 10$ m/s

———————	St, St (cast), V, GGG (perl., bai.), GTS (perl.)	tangential velocity $v \leqslant 10$ m/s
——— · ———	GG, GGG (ferr.)	

This graph is derived from Figure 11. If the materials of the pinion and the wheel are different, y_α shall be determined in accordance with Equation (78).

Figure 18 — Determination of running-in allowance y_α of gear pair (see also Figure 17)

9 Tooth stiffness parameters c' and c_γ

9.1 Stiffness influences

A tooth stiffness parameter represents the requisite load over 1 mm face width, directed along the line of action [13] to produce, in line with the load, the deformation amounting to 1 µm of one or more pairs of deviation-free teeth in contact. This deformation is equal to the base circle length of arc, corresponding to the load-induced rotation angle of one gear of the pair when the mating gear is held fast.

Single stiffness, c', is the maximum stiffness of a single pair of spur gear teeth. It is approximately equal to the maximum stiffness of a tooth pair in single pair contact [14]. The value c' for helical gears is the maximum stiffness normal to the helix of one tooth pair; c' is needed for the calculation of the dynamic factor K_v.

Mesh stiffness, c_γ, is the mean value of stiffness of all the teeth in a mesh. For the determination of the dynamic factor K_v and transverse load factors $K_{H\alpha}$ and $K_{F\alpha}$, the tangent of the load-deflection curve at the pertinent load is used for evaluation of c_γ (see 9.3.2.1). For the determination of the face load factors $K_{H\beta}$ and $K_{F\beta}$, the slope of a line drawn in the load-deflection graph between the original and the pertinent load point is used for evaluation of c_γ (see 9.3.2.2).

The main influences affecting tooth stiffness are

a) tooth data (number of teeth, basic rack profile, addendum modification, helix angle, transverse contact ratio),

b) blank design (rim thickness, web thickness),

c) specific load normal to the tooth flank,

d) shaft-hub connection,

e) roughness and waviness of the tooth surface,

f) mesh misalignment of the gear pair, and

g) modulus of elasticity of the materials.

9.2 Determination methods for tooth stiffness parameters — Principles and assumptions

Several methods of determining tooth stiffness parameters in accordance with the rules given in 4.1.12 are described in 9.2.1 to 9.2.2. For Method B, these stiffness values apply for accurate gears; lower values can be expected for less accurate gears.

9.2.1 Method A — Tooth stiffness parameters c'_A and $c_{\gamma\text{-}A}$

In this method, the tooth stiffness is determined by comprehensive analysis including all influences. This can be done by making direct measurements on the gear pair of interest. Values based on the theory of elasticity can be calculated or determined by finite element methods.

---

13) The tooth deflection can be determined approximately using F_t (F_m, F_{tH}, ...) instead of F_{bt}. Conversion from F_t to F_{bt} (load tangent to the base cylinder) is covered by the relevant factors, or the modifications resulting from this conversion can be ignored when compared with other uncertainties (e.g. tolerances on the measured values).

14) c' at the outer limit of single pair tooth contact can be assumed to approximate the maximum value of single stiffness when $\varepsilon_\alpha > 1{,}2$.

9.2.2 Method B — Tooth stiffness parameters c'_B and $c_{\gamma\text{-}B}$

This method is based on studies of the elastic behaviour of solid disc spur gears.

With the help of a series expansion, a sample expression was derived for cylindrical gears conjugate to a standard basic rack profile according to ISO 53; see Note in 9.3.1.1. This was based on an assumed specific loading of $F_t/b = 300$ N/mm. Using this method, theoretical single stiffnesses, c'_{th}, are obtained.

Differences between these theoretical results and the results of measurements are adjusted by means of a correction factor, C_M, and extension section to adjust for low specific loading.

Additional correction factors, determined by measurement and theoretical means, allow this method to be applied to gears consisting of rims and webs (factor C_R), similar to gears conjugate to other basic rack profiles (factor C_B) and helical gears (factor cos β).

By superposition of the single stiffness of all tooth pairs simultaneously in contact, an expression for the calculation of c_γ was developed. Its accuracy was verified by measurement results.

9.3 Determination of tooth stiffness parameters c' and c_γ according to Method B

Subject to the conditions and assumptions described in 9.2.2, c' and c_γ as determined by Method B are, in general, sufficiently accurate for the calculation of the dynamic factor and face load factors as well as for the determination of profile and helix modifications for gears in accordance with the following:

a) external gears;

b) any basic rack profile;

c) spur and helical gears with $\beta \leqslant 45°$;

d) steel/steel gear pairs;

e) any design of gear blank;

f) shaft-hub fitting spreads the transfer of torque evenly around the circumference (pinion integral with shaft, interference fit or splined fitting);

g) specific load $(F_t K_A) / b \geqslant 100$ N/mm.

NOTE The numbers of teeth of virtual spur gears in the normal section can be calculated approximately as:

$$z_{n1} \approx \frac{z_1}{\cos^3 \beta} \text{ and } z_{n2} \approx \frac{z_2}{\cos^3 \beta} \quad (79)$$

Method B can also be used, either approximately or with further auxiliary factors, for gears in accordance with the following:

— internal gears;

— materials combination other than steel/steel;

— shaft-hub assembly other than under f), e.g. with fitted key;

— specific load $(F_t K_A) / b < 100$ N/mm.

9.3.1 Single stiffness, c'

For gears having features listed under 9.3 a) to g) the following equation provides acceptable average values:

$$c' = c'_{th} \, C_M \, C_R \, C_B \cos\beta \tag{80}$$

9.3.1.1 Theoretical single stiffness, c'_{th}

c'_{th} is appropriate to solid disc gears and to the specified standard basic rack tooth profile. c'_{th} for a helical gear is the theoretical single stiffness relevant to the appropriate virtual spur gear (see Note in 9.3, above).

c'_{th} can be calculated for gear teeth having the basic rack profile specified in the following Note using Equations (81) and (82).

$$c'_{th} = \frac{1}{q'} \tag{81}$$

where

q' is the minimum value for the flexibility of a pair of teeth (compare with definition of c' in 9.1);

$$q' = C_1 + \frac{C_2}{z_{n1}} + \frac{C_3}{z_{n2}} + C_4 \, x_1 + \frac{C_5 \, x_1}{z_{n1}} + C_6 \, x_2 + \frac{C_7 \, x_2}{z_{n2}} + C_8 \, x_1^2 + C_9 \, x_2^2 \tag{82}$$

See Table 9 for coefficients C_1 to C_9.

NOTE Series progression in accordance with 9.2.2 for gears with basic rack profile: $\alpha_P = 20°$, $h_{aP} = m_n$, $h_{fP} = 1,2\ m_n$, and $\rho_{fP} = 0,2\ m_n$. Equations (81) and (82) apply for the range $x_1 \geqslant x_2$; $-0,5 \leqslant x_1 + x_2 \leqslant 2,0$. Deviations of actual values from calculated values in range $100 \leqslant F_{bt} / b \leqslant 1600$ N/mm are between +5 % and −8%.

Table 9 — Coefficients for Equation (82)

C_1	C_2	C_3	C_4	C_5	C_6	C_7	C_8	C_9
0,047 23	0,155 51	0,257 91	−0,006 35	−0,116 54	−0,001 93	−0,241 88	0,005 29	0,001 82

9.3.1.2 Correction factor, C_M

C_M accounts for the difference between the measured values and the theoretical calculated values for solid disc gears:

$$C_M = 0,8 \tag{83}$$

9.3.1.3 Gear blank factor, C_R

C_R accounts for the flexibility of gear rims and webs. The following provides mean values of C_R, suitable for use when the mating gear body is equally stiff or stiffer.

For solid disc gears:

$$C_R = 1,0 \tag{84}$$

NOTE The adoption of these average values is permissible considering the other uncertainties. Thus, for instance, the tooth stiffness of a gear of webbed design is not constant over the face width.

a) Determination by calculation: C_R can be calculated using Equation (85). It is consistent with curves in Figure 19, within −1% to +7%.

$$C_R = 1 + \frac{\ln\left(b_s / b\right)}{5\,e^{s_R / (5\,m_n)}} \quad (85)$$

Boundary conditions: when $b_s / b < 0{,}2$ substitute $b_s / b = 0{,}2$

when $b_s / b > 1{,}2$ substitute $b_s / b = 1{,}2$

when $s_R / m_n < 1$ substitute $s_R / m_n = 1$

b) Graphical values: C_R can be read from Figure 19 as a function of gear rim thickness s_R and central web thickness b_s.

9.3.1.4 Basic rack factor, C_B

C_B accounts for the deviations of the actual basic rack profile of the gear, from the standard basic rack profile (see ISO 53).

$$C_B = [1{,}0 + 0{,}5\,(1{,}25 - h_{fP} / m_n]\,[1{,}0 - 0{,}02\,(20° - \alpha_{Pn})] \quad (86)$$

When the pinion basic rack dedendum is different from that of the wheel, the arithmetic mean of C_{B1} for a gear pair conjugate to the pinion basic rack and C_{B2} for a gear pair conjugate to the basic rack of the wheel is used:

$$C_B = 0{,}5\,(C_{B1} + C_{B2}) \quad (87)$$

9.3.1.5 Additional information

The following is also relevant:

a) Helical gearing

The theoretical single stiffness of the teeth of virtual spur gears of a helical gear pair is transformed by the term $\cos\beta$ in Equation (80) from the normal into the transverse theoretical single stiffness c'_{th} of the teeth of the helical gears.

b) Internal gearing

Approximate values of the theoretical single stiffnesses of internal gear teeth can also be determined from Equations (81) and (82), by the substitution of infinity for z_{n2}.

c) Material combinations

For material combinations other than steel with steel, the value of c' can be determined from the following equation:

$$c' = c'_{St/St}\left(\frac{E}{E_{St}}\right) \quad (88)$$

where

$$E = \left(\frac{2\,E_1\,E_2}{E_1 + E_2}\right) \quad (89)$$

(E/E_{St}) is equal to 0,74 for steel/grey cast iron, and is equal to 0,59 for grey cast iron/grey cast iron.

d) Shaft and gear assembly

If the pinion or the wheel or both are assembled on the shaft(s) with a fitted key, the single stiffness, under constant load, varies between maximum and minimum values twice per revolution.

The minimum value is approximately equal to the single stiffness with interference or spline fits.

When one gear of a pair is press fitted onto a shaft with a fitted key, and the mating gear is assembled with its shaft by means of an interference or splined fitting, the average value of single stiffness is about 5 % greater than the minimum. When both gears of a pair are push fitted onto shafts with fitted keys, the average single stiffness is about 10 % greater than the minimum.

e) Specific load $(F_t K_A / b) < 100$ N/mm

At low specific loading, the single stiffness decreases with reduced load [15]. By way of approximation, when $(F_t K_A)/b < 100$ N/mm:

$$c' = c'_{th} C_M C_B C_R \cos\beta \left(\frac{F_t K_A / b}{100} \right)^{0,25} \tag{90}$$

9.3.2 Mesh stiffness, c_γ

9.3.2.1 Mesh stiffness, $c_{\gamma\alpha}$

$c_{\gamma\alpha}$ is used for the calculation of the internal dynamic factor K_v, see Clause 6, and the transverse load factors $K_{H\alpha}$ and $K_{F\alpha}$, see Clause 8.

Following the methods quoted in 9.2.2 for spur gears with $\varepsilon_\alpha \geqslant 1,2$ and helical gears with $\beta \leqslant 30°$, the mesh stiffness:

$$c_{\gamma\alpha} = c' (0,75\, \varepsilon_\alpha + 0,25) \tag{91}$$

with c' according to Equation (80). The value $c_{\gamma\alpha}$ can be up to 10 % less than values from Equation (91) when for spur gears $\varepsilon_\alpha < 1,2$.

9.3.2.2 Mesh stiffness, $c_{\gamma\beta}$

$c_{\gamma\beta}$ is used for the calculation of the face load factors $K_{H\beta}$ and $K_{F\beta}$, see Clause 7.

For $c_{\gamma\beta}$, a value as follows is used:

$$c_{\gamma\beta} = 0,85\, c_{\gamma\alpha} \tag{92}$$

with $c_{\gamma\alpha}$ according to Equation (91).

15) When $(F_t K_A) / b > 100$ N/mm, c' can be assumed to be constant.

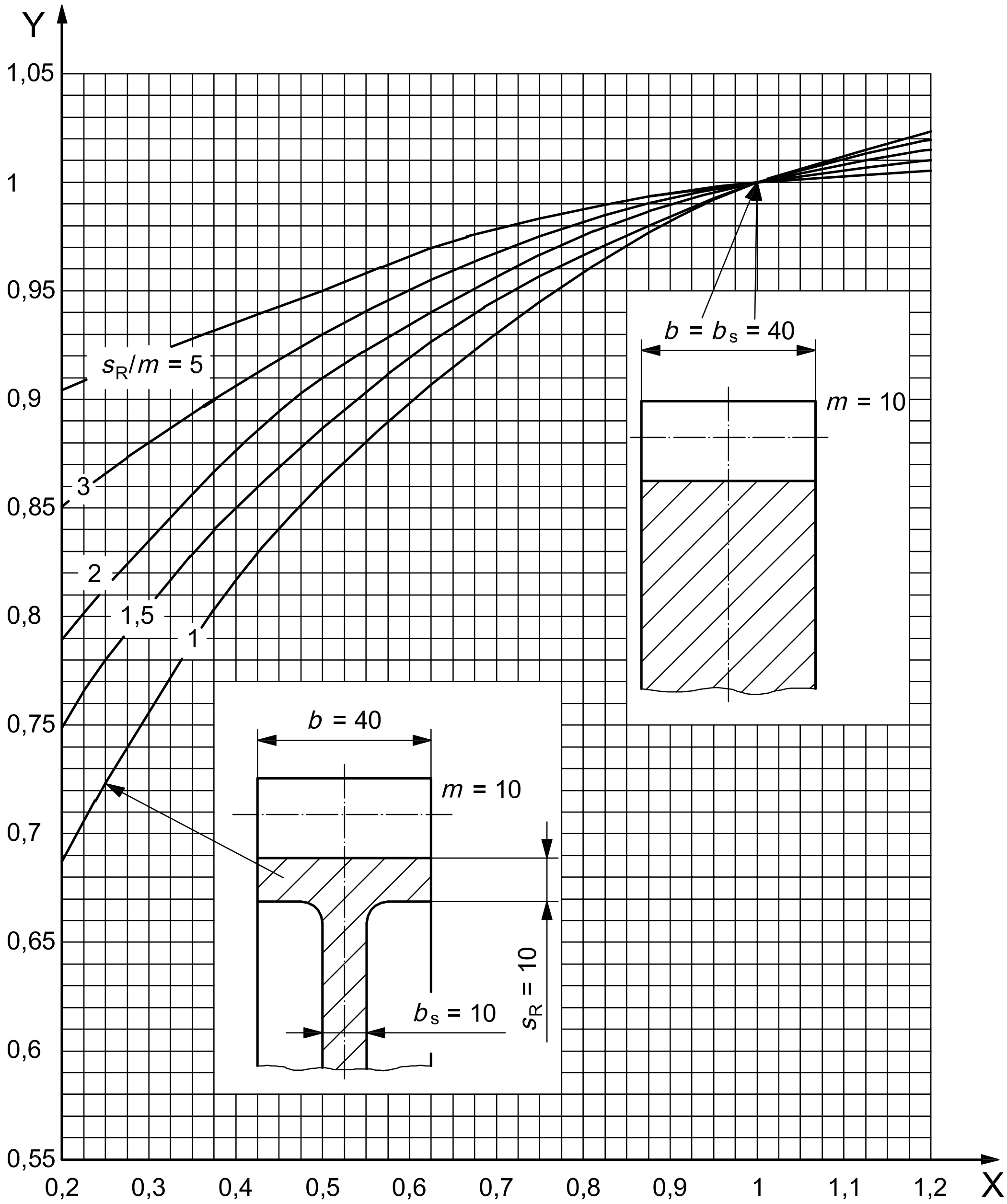

Key

X b_s/b

Y wheel blank factor, C_R

Figure 19 — Wheel blank factor C_R — Mean values for mating gears of similar or stiffer wheel blank design

Annex A
(normative)

Additional methods for determination of f_{sh} and f_{ma}

A.1 Determination of f_{sh} from contact pattern

Once the transmission has been assembled, the equivalent misalignment, f_{sh}, can be calculated for gears with or without helix modification from the width of the contact pattern without load and with part load. Equipment suitable for the application of part load shall be available.

Since the mesh stiffness falls off sharply at low specific loading, the specific loading at partial load should be at least 100 N/mm.

Care shall be taken to ensure that the pinion and wheel-shaft journals are in their working attitudes during contact pattern development (appropriate bearing clearances).

The procedure is as follows:

a) Determine the mesh misalignment f_{ma}, in accordance with 7.5.3.1.

b) Measure contact pattern length $b_{cal\,T}$ under partial load F_{mT} and calculate $b_{cal\,T} / b$.

It is necessary that the part load be chosen such that the contact pattern dimension b_{cal} is less than the face width ($b_{cal}/b < 1$); however, the smallest load should not be less than 10 % of the full load. The maximum length of contact pattern should not exceed 85 % of the face width ($b_{cal}/b < 0{,}85$), in order to ensure that the contact pattern width is less than the face width (the type of load distribution for $b_{cal} = b$ is not clearly defined, see Figures 7 and 8).

c) Determine the equivalent misalignment $F_{\beta x\,T}$ under partial load (see Clause 9 for tooth stiffness $c_{\gamma\beta}$):

$$F_{\beta x T} = \frac{2\,F_{mT}}{\left[b \left(\frac{b_{calT}}{b} \right)^2 c_{\gamma\beta} \right]} \tag{A.1}$$

d) Calculate $f_{sh\,T}$ under partial load:

$$f_{shT} = \left| F_{\beta\,xT} - f_{ma} \right| \tag{A.2}$$

e) Compute f_{sh} under full load (linear extrapolation):

$$f_{shT} = f_{shT} \left(\frac{F_m}{F_{mT}} \right) \tag{A.3}$$

NOTE Depending on the design, the accuracy of the method can be seriously impaired when the non-linear deflection components are induced at larger partial loads.

A.2 Determination of f_{ma}

A.2.1 Determination of f_{ma} on basis of no-load contact pattern

Under ideal conditions f_{ma} can be derived from

$$f_{ma} = \left(\frac{b}{b_{c0}} \right) s_c \qquad (A.4)$$

where b_{c0} is the length, at low loading, of the contact pattern of the assembled gears and s_c is the thickness of the coating of marking compound (see Figure A.1) [16]. If gears are crowned or end-relieved, an accurate analysis is necessary.

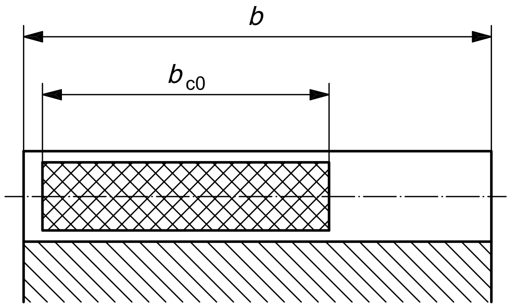

Figure A.1 — Length of contact pattern b_{c0} and face width b

The coating thickness of common marking compounds is in the range 2 µm to 20 µm; 6 µm can be used as a mean value consistent with good working practice.

If the minimum length of contact pattern is stated on the drawing, it is convenient to determine the maximum permissible mesh misalignment.

$$f_{ma\,max} = \frac{b\, s_c}{b_{c0\,min}} \qquad (A.5)$$

A mean value suitable for use in preliminary design calculations is

$$f_{ma} = \frac{2}{3} f_{ma\,max} \qquad (A.6)$$

After final assembly in the gear case, maximum and minimum values of mesh misalignment, $f_{ma\ max}$ and $f_{ma\ min}$, can be determined from the minimum or the maximum lengths of the contact pattern respectively. These values enable recalculation of preliminary rated load capacity:

$$f_{ma} = 0{,}5 \left(f_{ma\,max} + f_{ma\,min} \right) \qquad (A.7)$$

$$f_{ma\,max} = \left(\frac{b}{b_{c0\,min}} \right) s_c \qquad (A.8)$$

16) Precise knowledge of the coating thickness is of great importance. In case of doubt, the actual coating thickness should be determined.

$$f_{\mathrm{ma\,min}} = \left(\frac{b}{b_{\mathrm{c0\,max}}}\right) s_{\mathrm{c}} \quad \text{(A.9)}$$

The contact patterns shall be created with pinion and wheel shaft journals in their working attitudes.

A.2.2 Determination of f_{ma} from length of the contact pattern under partial load and theoretically determined deformations

The following conditions are necessary for application:

The elastic deflections of pinion, wheel, shafts, gears and bearings, f_{sh}, f_{sh2}, f_{ca} and f_{be} (see 7.5.2.3), are to be determined using an accurate calculation method. As a rule, Method C is not sufficiently accurate for the purpose. As indicated, the individual deflections shall be carefully considered.

The length of the contact pattern, $b_{\mathrm{cal\ T}}$, at partial loading, F_{mT} (see A.1), is measured and the equivalent misalignment, $F_{\beta xT}$, at partial loading is determined using Equation (A.10):

$$F_{\beta\,\mathrm{xT}} = \frac{2\,F_{\mathrm{mT}}}{\left[b\left(\frac{b_{\mathrm{calT}}}{b}\right)^2 c_{\gamma\beta}\right]} \quad \text{(A.10)}$$

When calculating mesh misalignment, it is necessary to distinguish between two cases.

Case 1: the elastic deflections augment the mesh misalignment (see, for example, Figure 12):

$$f_{\mathrm{ma}} = F_{\beta\,\mathrm{xT}} - \left|\left(f_{\mathrm{sh}} + f_{\mathrm{sh2}} + f_{\mathrm{ca}} + f_{\mathrm{be}}\right)_{\mathrm{T}}\right| \quad \text{(A.11)}$$

Case 2: the elastic deflections tend to compensate for the mesh misalignment (see, for example, Figure 12):

$$f_{\mathrm{ma}} = F_{\beta\,\mathrm{xT}} + \left|\left(f_{\mathrm{sh}} + f_{\mathrm{sh2}} + f_{\mathrm{ca}} + f_{\mathrm{be}}\right)_{\mathrm{T}}\right| \quad \text{(A.12)}$$

When gears are crowned or end-relieved, an accurate analysis is necessary.

When the length of the contact pattern varies around the circumference, $f_{\mathrm{ma\ max}}$ shall be derived from the minimum length, $f_{\mathrm{ma\ min}}$ shall be derived from the maximum length, and then f_{ma} shall be derived from Equation (A.7).

Annex B
(informative)

Guide values for crowning and end relief of teeth of cylindrical gears

B.1 General

Well-designed crowning and end relief have a beneficial influence on the distribution of load over the face width of a gear (see Clause 7). Design details should be based on a careful estimate of the deformations and manufacturing deviations of the gearing of interest. If deformations are considerable, helix angle modification might be superposed over crowning or end relief, but well-designed helix modification is preferable.

B.2 Amount of crowning C_β

The following non-mandatory rule is drawn from experience; the amount of crowning which is necessary to obtain acceptable distribution of load can be determined as follows:

Subject to the limitations, 10 µm $\leqslant C_\beta \leqslant$ 40 µm plus a manufacturing tolerance of 5 µm to 10 µm, and that the value b_{cal}/b would have been greater than 1 had the gears not been crowned, $C_\beta = 0{,}5\ F_{\beta x\ cv}$ [see Figure 8)].

The initial equivalent misalignment, $F_{\beta x\ cv}$, should be calculated as though the gears were not crowned, using a modified version of Equation (52) in which 1,0 f_{sh} is substituted for 1,33 f_{sh} — see Equation (B.1).

Furthermore, f_{sh} shall be determined as though the gears were not crowned in accordance with 7.5.2.4.

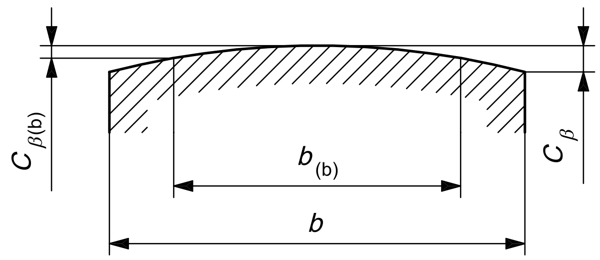

Figure B.1 — Amount of crowning $C_{\beta(b)}$ and width $b_{(b)}$ (see 7.5.2.4)

So as to avoid excessive loading of tooth ends, instead of deriving f_{ma} from 7.5.3, the value shall be calculated as

$$f_{ma\,c} = 1{,}5\ f_{H\beta} \tag{B.1}$$

Thus the crowning amount:

$$C_\beta = 0{,}5\left(f_{sh} + 1{,}5\ f_{H\beta}\right) \tag{B.2}$$

When the gears are of such stiff construction that f_{sh} can for all practical purposes be neglected, or when the helices have been modified to compensate for deformation at mid-face width, the following value can be substituted:

$$C_\beta = f_{H\beta} \tag{B.3}$$

Subject to the restriction 10 µm $\leqslant C_\beta \leqslant$ 25 µm plus a manufacturing tolerance of about 5 µm, 60 % to 70 % of the above values are adequate for extremely accurate and reliable high speed gears.

B.3 Amount $C_{I(II)}$ and width $b_{I(II)}$ of end relief

Method B.3.1

This method is based on an assumed value for the equivalent misalignment of the gear pair, without end relief and on the recommendations for the amount of gear crowning. The following is non-mandatory.

a) Amount of end relief

For through hardened gears, $C_{I(II)} = F_{\beta x\,cv}$ plus a manufacturing tolerance of 5 to 10 µm.

Thus, by analogy with $F_{\beta x\,cv}$ in B.1, $C_{I(II)}$ should be approximately

$$C_{I(II)} = f_{sh} + 1{,}5\ f_{H\beta} \tag{B.4}$$

For surface hardened and nitrided gears: $C_{I(II)} = 0{,}5\ F_{\beta x\,cv}$ plus a manufacturing tolerance of 5 to 10 µm.

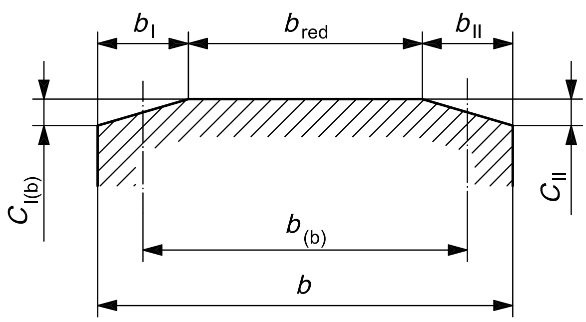

Figure B.2 — Amount $C_{I(II)\,(b)}$ and width $b_{(b)}$ of end relief (see 7.5.2.4)

Thus, by analogy with $F_{\beta x\,cv}$ in A.1, $C_{I(II)}$ should be approximately

$$C_{I(II)} = 0{,}5\,(f_{sh} + 1{,}5\ f_{H\beta}) \tag{B.5}$$

When the gears are of such stiff construction that f_{sh} can for all practical purposes be neglected, or when the helices have been modified to compensate deformation, proceed in accordance with Equation (B.2).

60 % to 70 % of the above values is appropriate for very accurate and reliable gears with high tangential velocities.

b) Width of end relief

For approximately constant loading and higher tangential velocities, $b_{I(II)}$ is the smaller of the values (0,1 b) or (1,0 m).

The following is appropriate for variable loading, low and average speeds:

$$b_{red} = (0{,}5 \text{ to } 0{,}7)\ b \tag{B.6}$$

Method B.3.2

This method is based on the deflection of gear pairs assuming uniform distribution of load over the face width:

$$\delta_{\text{bth}} = F_{\text{m}} / (b\ c_{\gamma\beta}), \text{ where } F_{\text{m}} = F_{\text{t}}\ K_{\text{A}}\ K_{\text{v}} \tag{B.7}$$

For highly accurate and reliable gears with high tangential velocities, the following are appropriate:

$$C_{\text{I(II)}} = (2 \text{ to } 3)\ \delta_{\text{bth}} \tag{B.8}$$

$$b_{\text{red}} = (0{,}8 \text{ à } 0{,}9)\ b \tag{B.9}$$

For similar gears of lesser accuracy:

$$C_{\text{I(II)}} = (3 \text{ to } 4)\ \delta_{\text{bth}} \tag{B.10}$$

$$b_{\text{red}} = (0{,}7 \text{ to } 0{,}8)\ b \tag{B.11}$$

Annex C
(informative)

Guide values for $K_{H\beta\text{-}C}$ for crowned teeth of cylindrical gears

C.1 General

The purpose of this annex is to allow the analysis of the more general (non-optimum) crowning condition.

C.2 $K_{H\beta\text{-}C}$ for crowned gears

Clause 7 covers the calculation of $K_{H\beta}$ for crowned gears where the crowning height C_β is one of two precise values. This annex covers the more general crowning condition.

C.2.1 Non-dimensional crowning height, C_β^*

This is calculated as follows:

$$C_\beta^* = \frac{c_\beta \; c_{\gamma\beta}}{F_m/b} \quad \text{(C.1)}$$

C.2.2 Non-dimensional mesh misalignment, $F_{\beta x}^*$

This is calculated as follows:

$$F_{\beta x}^* = (1{,}33\, B_3\ f_{sh} + f_{ma}) \frac{c_{\gamma\beta}}{F_m/b} \quad \text{(C.2)}$$

where

B_3 is equal to 0,1 if a helix modification carefully calculated to match the torque being analysed is applied

B_3 is otherwise equal to 1,0.

C.2.3 Graphical values

The value of $K_{H\beta}$ can be read from Figure C.1.

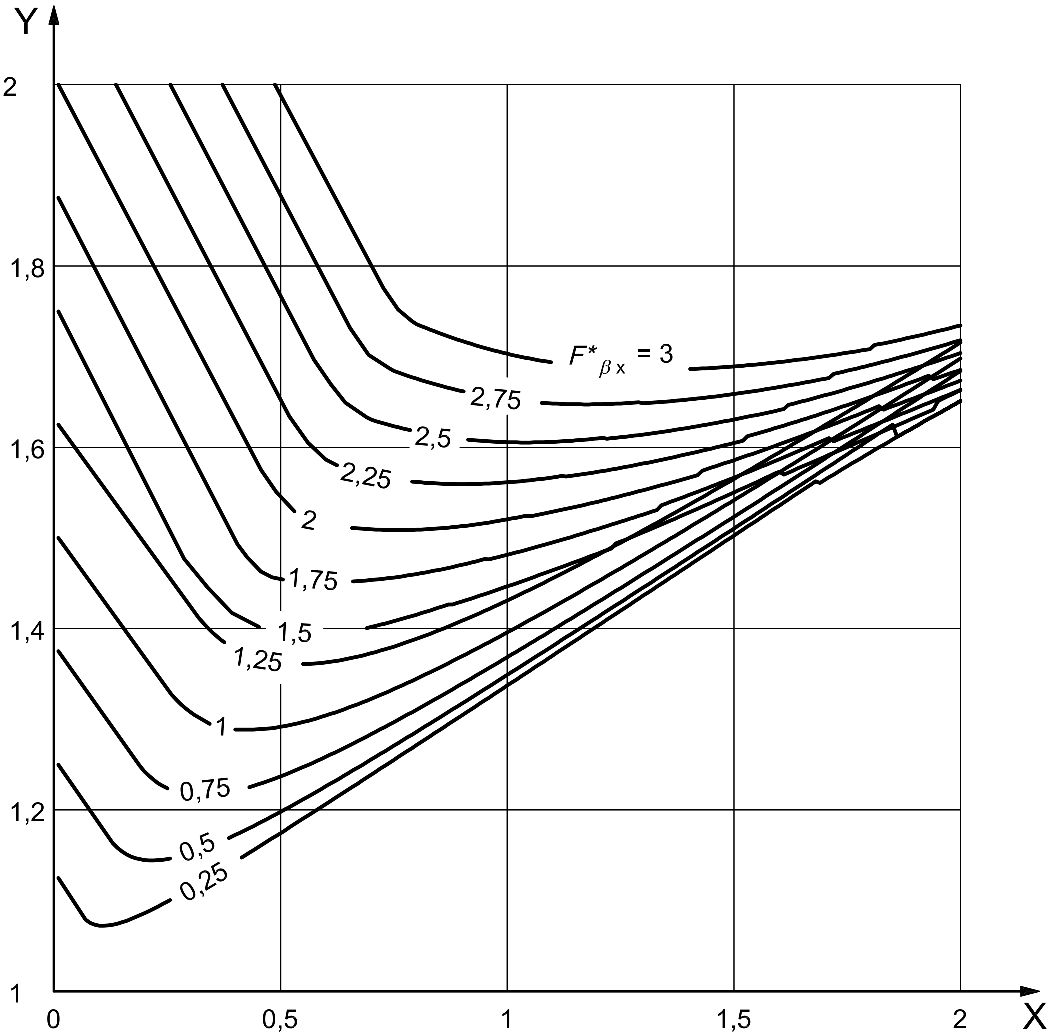

Key

X crowning height, C_β^*

Y face load factor, $K_{H\beta}$

Figure C.1 — Face load factors $K_{H\beta}$ for crowned gears

C.2.4 Determination by calculation

If $C_\beta^* = 0$, then:

$$\begin{aligned} &\text{if } F_{\beta x}^* < 2 \text{ then } K_{H\beta} = 1 + \frac{F_{\beta x}^*}{2} \\ &\text{if } F_{\beta x}^* \geqslant 2 \text{ then } K_{H\beta} = \sqrt{2 F_{\beta x}^*} \end{aligned} \quad \text{(C.3)}$$

If $C_\beta^* > 1{,}5$ and $F_{\beta x}^* < \left\{ 4\, C_\beta^* \left[1 - \left(\frac{1{,}5}{C_\beta^*} \right)^{1/3} \right] \right\}$, then:

$$K_{H\beta} = (2{,}25\, C_\beta^*)^{1/3} \quad \text{(C.4)}$$

If $C_\beta^* > (0{,}25\ F_{\beta x}^*)$ and $F_{\beta x}^* < 1{,}5$, then:

$$K_{H\beta} = 1 + \frac{C_\beta^*}{3} + \frac{\left(F_{\beta x}\right)^2}{16\ C_\beta^*} \tag{C.5}$$

If none of the above applies, and $C_\beta^* > (0{,}25\ F_{\beta x}^*)$, then use iteration as follows.

Set $q = 1{,}0$ as the seed value

$$k = \sqrt{\frac{q}{C_\beta^*}} \tag{C.6}$$

$$m = \frac{F_{\beta x}^*}{8\ C_\beta^*} + \frac{k-1}{2} \tag{C.7}$$

$$t = 4\ C_\beta^*\ m\left(k - m\right) \tag{C.8}$$

$$A = \frac{2\ q\ k - C_\beta^*\ m^3}{3} - \frac{m\ t}{2} \tag{C.9}$$

$$q = q - \frac{1{,}5\,(A-1)}{k} \tag{C.10}$$

Continue until A is close to unity, then $K_{H\beta} = q$.

If none of the above applies, then obtain value by linear interpolation.

Annex D
(informative)

Derivations and explanatory notes

D.1 General

The explanatory notes in this annex are intended to assist the user's understanding of formulae used in this part of ISO 6336.

D.2 Derivation of $K_{H\beta}$ from elastic torsional and bending deflections of pinion

Figure D.1 shows the deformation of a pinion due to bending and torsion when the load is distributed uniformly.

The following is the equation of torsional deflection under uniform load distribution:

$$f_t(\xi) = \frac{8}{\pi} \frac{F_m/b}{0{,}39\, E} \left(\frac{b}{d_1}\right)^2 \xi \left(1 - \frac{\xi}{2}\right) \quad \text{(D.1)}$$

The maximum value of f_t occurs at $\xi = 1$ and is

$$f_{tmax}(\xi) = \frac{4}{\pi} \frac{F_m/b}{0{,}39\, E} \left(\frac{b}{d_1}\right)^2 \quad \text{(D.2)}$$

Mean value

$$f_m = \int_0^1 f_1(\xi)\, d\xi = \frac{2}{3} f_{t\,max} \quad \text{(D.3)}$$

The following is the equation of the bending deflection when the load is evenly distributed across the face width.

$$f_b = \frac{8}{3\pi} \frac{F_m/b}{E} \left(\frac{b}{d_1}\right)^4 \left[\xi^4 - 2\xi^3 + 3\left(1 - \frac{l}{b}\right)\xi^2 + 2\left(\frac{3}{2}\frac{l}{b} - 1\right)\xi\right] \quad \text{(D.4)}$$

The maximum value of f_b occurs at $\xi = 1/2$ and is

$$f_{b\,max} = \frac{2}{\pi} \frac{F_m/b}{E} \left(\frac{b}{d_1}\right)^4 \left(\frac{l}{b} - \frac{7}{12}\right) \quad \text{(D.5)}$$

Mean value

$$f_{bm} = \frac{4}{3\pi} \frac{F_m/b}{E} \left(\frac{b}{d_1}\right)^4 \left(\frac{l}{b} - \frac{3}{5}\right) \quad \text{(D.6)}$$

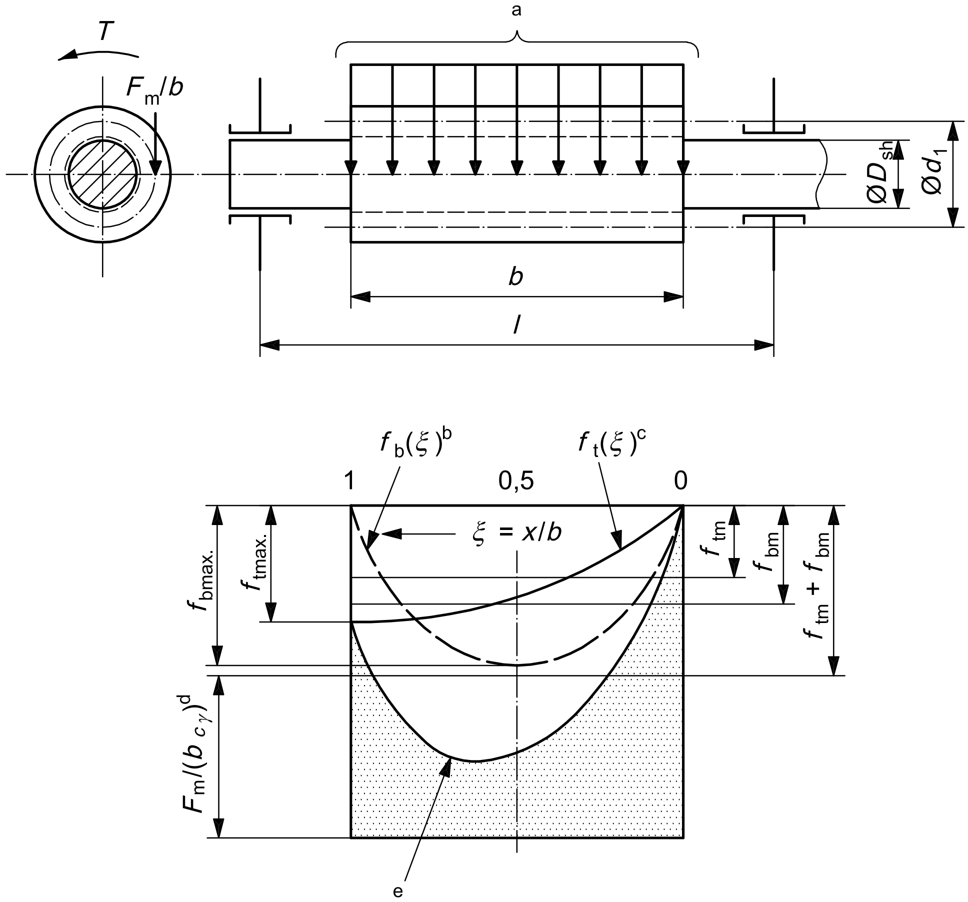

Key

f_{tm} mean value for torsional deflection

f_{bm} mean value for bending deflection

f_{tmax} maximum torsional deflection of the pinion

f_{bmax} maximum bending deflection of the pinion

a F_m/b under a uniform load distribution.

b Bending component only.

c Torsional component only.

d Mean value of tooth deflection.

e Torsional and bending component.

Figure D.1 — Deflection of pinion shaft and pinion teeth

From which follows as an approximation:

$$f_{bm} = \frac{2}{3} f_{b\,max} \tag{D.7}$$

The total deformation component of equivalent misalignment is the sum of the mean values of torsional and bending deflections.

$$\frac{1}{2} F_{\beta x} = f_{bm} + f_{tm} = \frac{2}{3}(f_{b\,max} + f_{t\,max}) \tag{D.8}$$

To obtain the deformation component of $F_{\beta y}$ inclusive of a proportional amount of the running-in allowance, it is necessary to multiply the deformation component of equivalent misalignment by the factor χ_β.

The face load factor $K_{H\beta}$ is as defined in 7.3.1:

$$K_{H\beta} = \frac{(F / b)_{max}}{F_m / b} \tag{D.9}$$

If the deflections calculated above are introduced into Equation (D.9), the following is obtained:

$$\begin{aligned} K_{H\beta} &= \frac{c_{\gamma\beta}\left[\dfrac{F_m}{b\,c_{\gamma\beta}}(f_{tm} + f_{bm} - y_\beta)1000\right]}{c_{\gamma\beta}\,\dfrac{F_m / b}{c_{\gamma\beta}}} \\ &= 1 + \frac{c_{\gamma\beta}\,\chi_\beta\,(f_{tm} + f_{bm})1000}{F_m / b} \\ &= 1 + \frac{2}{3}\,\frac{c_{\gamma\beta}}{F_m / b}\,\chi_\beta\,(f_{t\,max} + f_{b\,max})1000 \end{aligned} \tag{D.10}$$

D.3 Explanatory notes to Equations (52) and (53)

The factor 1,33 in Equations (52), (53) and (54) corrects the error arising from the assumption that the elastic deformation f_{sh} is linear. Using the linear deformation formulation with 1,33 f_{sh}, the same value of $K_{H\beta}$ is calculated as with the actual parabolic deformation and 1,0 f_{sh} (see Figure D.2).

The following applies to Equation (53):

When correct patterns which are suitable in both size and position are obtained, one or more of the following is implied:

a) components have been correctly manufactured and assembled in accordance with an adequate design specification;

b) manufacturing deviations of the assembled components partially cancel each other and the deviations may be less than the permissible values according to ISO 1328-1;

c) manufacturing component f_{ma} and the deformation component f_{sb} of mesh alignment are mutually compensatory.

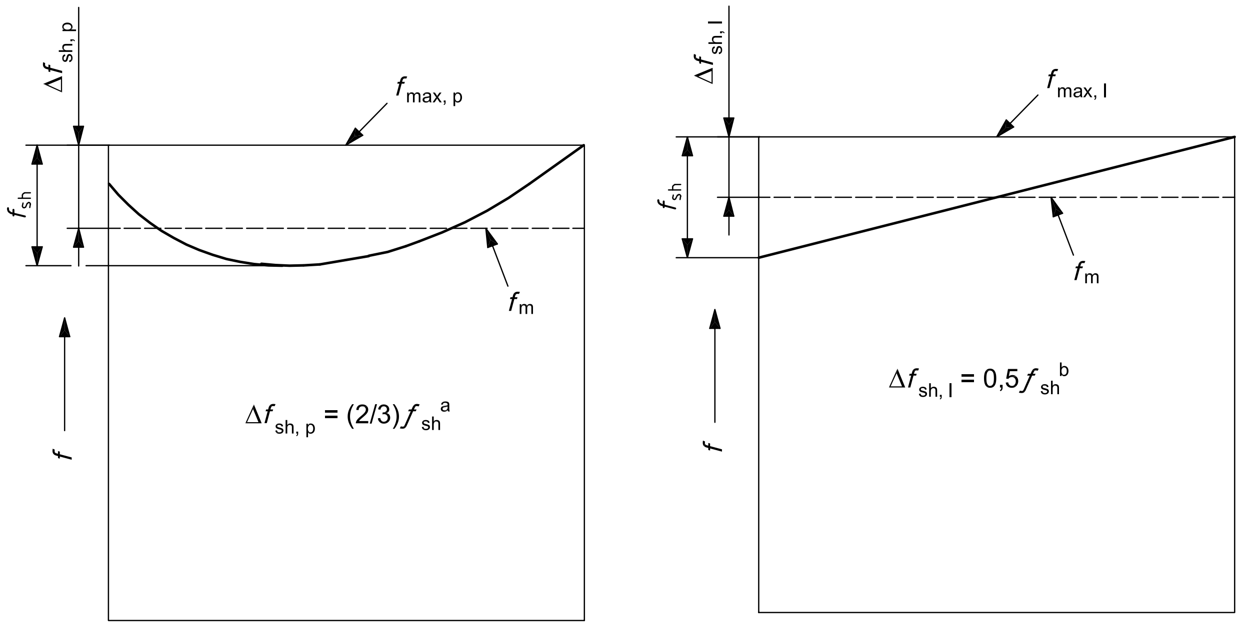

a) Actual deflection occuring **b) Assumed deflection**

$$K_{H\beta} = \frac{F_{max} / b}{F_m / b} = \frac{f_{max,p}}{f_m} = 1 + \frac{\Delta f_{sh,p}}{f_m} = 1 + \frac{1,33\,\Delta f_{sh,l}}{f_m}$$

where f ($f = w / c_\gamma$) is the tooth deflection.

[a] Parabolic deflection.

[b] Linear deflection.

Figure D.2 — Elastic deflection of the pinion f_{sh} (principle) — Comparison of actual and assumed progression

Annex E
(informative)

Analytical determination of load distribution

E.1 General

In this annex a method for the evaluation of the load distribution across the teeth of parallel axis gears is described. This method covers the most important deflections such as shaft bending and torsional deflections, and tooth deflections. Other deflections can be taken into account by a similar approach. The determination of the deflections is demonstrated by the example shown in Figure E.1.

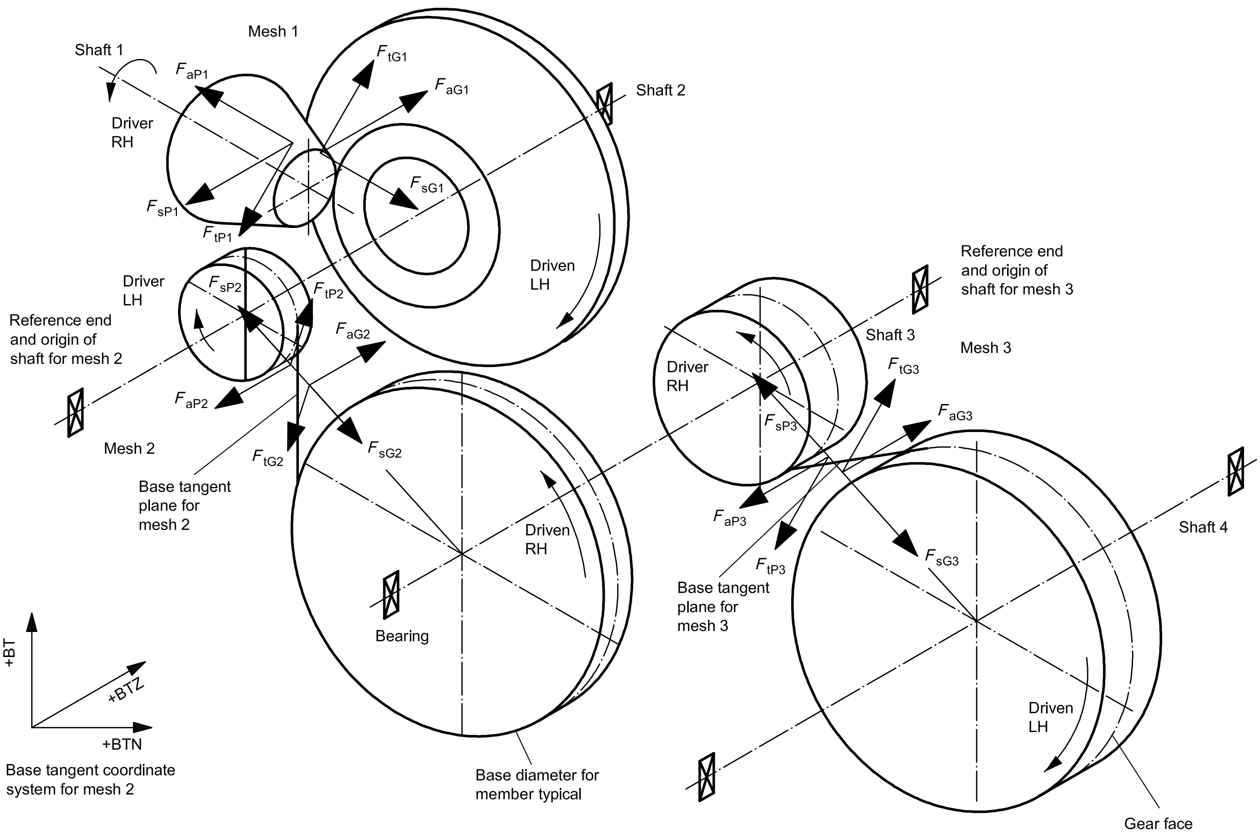

+BT axis along tangent plane of target mesh

+BTN axis normal to base tangent plane of target mesh

Figure E.1 — Example general case gear arrangement (base tangent coordinate system)

E.2 Shaft bending deflections

Gears transmitting power will impose loads and moments on their shafts, which will cause elastic deflections. These deflections can affect the alignment of the gear teeth and therefore affect the load distribution across the gear face width.

A simplified computer program integration method for calculating the bending deflection of a stepped shaft with radial loads imposed and two bearing supports is presented as follows. Rules for calculating bending deflection when calculating load distribution factor are also presented.

E.2.1 Simplified bending calculation routine

As explained in Clause 7, when calculating shaft deflections, the area of the gear teeth is broken into 10 separate load application sections. However, to simplify the explanation of the deflection calculation method the following model and explanation will be of a stepped shaft with two supports, three changes in diameter, and two point loads, as shown in Figure E.2 and Table E.1.

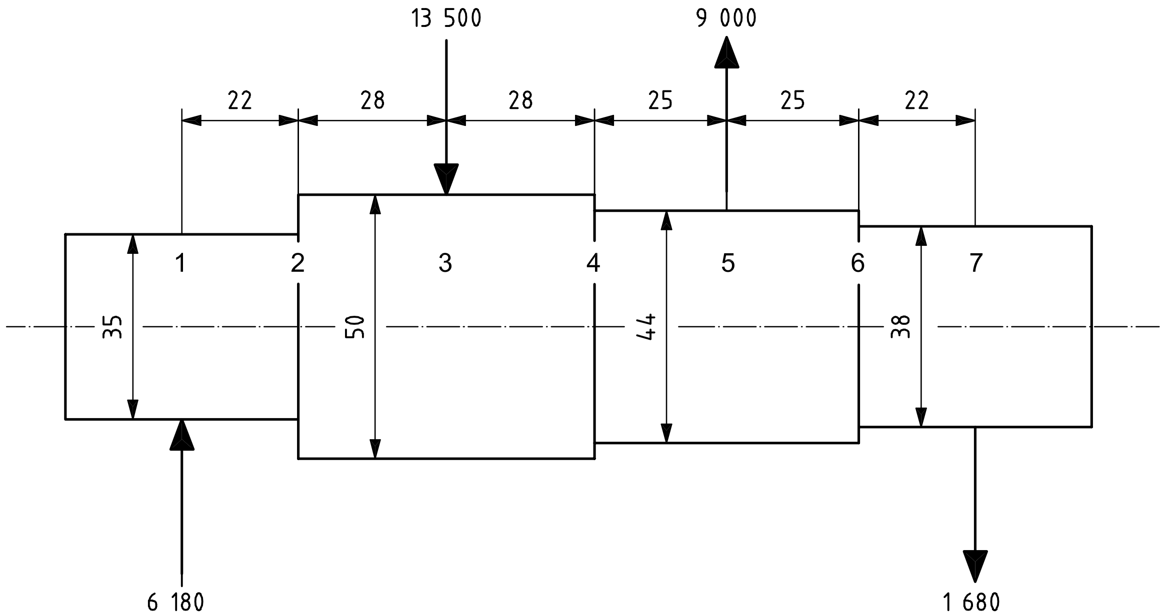

Figure E.2 — Example shaft

Table E.1 — Calculation data and results

1	2	3	4	5	6	7	8	9
Station number from left	**Outside shaft diameter**	**Inside shaft diameter**	**Force or reaction**	**Shear at preceding station**	**Distance between stations**	**Bending moment**	**Moment of inertia**	EI, EI_u, EI_l
i	d_{sh}	d_{in}	F or R	V	x	M	I	$EI/10^3$
—	mm	mm	N	N	mm	N·mm	mm^4	$N{\cdot}mm^2$
1	35	0	6 180	0	—	0	73 662	15 174 322
2	35 50	0	0	6 180	22	135 960	73 662 306 796	15 174 322 63 200 008
3	50	0	–13 500	6 180	28	309 000	306 796	63 200 008
4	50 44	0	0	–7 320	28	104 040	306 796 183 984	63 200 008 37 900 752
5	44	0	9 000	–7 320	25	–78 960	183 984	37 900 752
6	44 38	0	0	1 680	25	–36 960	183 984 102 354	37 900 752 21 084 898
7	38	0	–1 680	1 680	22	0	102 354	21 084 898

Table E.1 (*continued*)

1	9	10	11	12	13	14	15	16
Station number from left	EI, EI_u, EI_l	M/EI, M/EI_u, M/EI_l	**Average column 10**	**Slope**	**Average slope**	**Deflection increment**	**Integration constant**	**Calculated deflection**
i	$EI/10^3$	MEI	$AMEI$	SL	ASL	DI	ICS	y
—	N·mm^2	µm^{-1}	µm^{-1}	µrad	µrad	µm	µm	µm
1	15 174 322	0		0				0
			0,004 48		0,492 79	1,084 14	–4,659 02	
2	15 174 322 63 200 008	0,008 96 0,002 151		0,098 56				–3,574 9
			0,003 52		0,147 84	4,139 58	–5,929 66	
3	63 200 008	0,004 889		0,197 13				–5,365
			0,003 27		0,242 87	6,800 47	–5,929 66	
4	63 200 008 37 900 752	0,001 646 0,002 745		0,288 62				–4,494 2
			0,000 33		0,292 76	7,318 94	–5,294 34	
5	37 900 752	–0,002 083		0,296 89				–2,469 6
			–0,001 53		0,277 78	6,944 44	–5,294 34	
6	37 900 752 21 084 898	–0,000 975 –0,001 753		0,258 66				–0,819 4
			–0,000 88		0,249 02	5,478 46	–4,659 02	
7	21 084 898	0,0		0,239 38				0
					S_y = **31,766** IC = **–0,211 8**			

All modelling will be from the left-hand support moving toward the right-hand support. Deflection at supports is zero. The gearing loads and any other external loads are used to obtain the free body load diagram. In the load diagram the loads, F_i, and the distances, X_{fi}, from left support to load location are specified.

Using standard static load analyses, calculate the reaction, R_R, at the right side support by summing the moments about the left support:

$$R_R = \frac{\sum\left[\left(F_i\right)\left(X_{fi}\right)\right]}{L_S} \quad \text{(E.1)}$$

where

F is the load applied, in newtons (N);

L_S is the distance between the two supports, in millimetres (mm);

X_{fi} is the distance from left support to load location, F_i, in millimetres (mm)

$$X_{fi} = x_i + X_{f(i\ 1)} \ldots i = 1, 2, 3, \ldots, n \tag{E.2}$$

Then calculate the reaction at the left using the total sum of the loads:

$$R_L = \sum F_i - R_R \tag{E.3}$$

It is critical that sign convention be maintained during the calculations with the preceding formulae. The basic equation for small deflection of a stepped shaft is

$$\frac{d^2 y}{dx^2} = \frac{M}{EI} \tag{E.4}$$

where

x is the distance between stations, in millimetres (mm);

M is the bending moment, in newton metres (N·m);

I is the moment of inertia, in millimetres to the power of four (mm^4);

E is the modulus of elasticity, in newtons per square millimetre (N/mm^2);

Y is the deflection, in micrometres (µm).

Integrating Equation (E.4) twice gives the deflection. The following step-by-step procedure applied to the stepped shaft as shown in Figure E.2 will illustrate the procedure evaluating shaft deflection. A tabulated form as shown in Table E.1 lends itself to the process.

Step 1: Divide the shaft into lengths with intervals beginning at each force and at each change in section (see Figure E.2).

Step 2: Label the ends of intervals with station numbers beginning at the left support with station $i = 1$ and ending at the right support with station $i = n$.

Step 3: List station numbers, i, on alternate lines in column 1 of the calculation sheet (see Table E.1).

Step 4: List free body forces in column 4 on the same lines as the station numbers at which they occur. Care should be taken to designate proper signs to forces (upward forces are considered positive in this example).

Step 5: Calculate the shear, V_i, at each station by summing the values in column 4. Tabulate each shear value in column 5, one station below the station for which it is calculated. The last shear value should be numerically equal, but opposite in sign, to the last force listed in column 4.

$$V_{i+1} = V_i + F_i \ldots i = 1, 2, 3, \ldots, n - 1 \tag{E.5}$$

where

V is the shear, in newtons (N);

i is the station number;

n is the station number at right support.

Step 6: In column 6, on the same line as the station number, list the distance to the preceding station.

Step 7: Calculate bending moment, M_i, at each station and list the value in column 7. The value at the first station is zero. Values at succeeding stations are obtained by summing the products of shear force, V_i (column 5), and distance between stations, x_i (column 6). The moment at the first and last station, $i = 1$ and $i = n$, should be zero (i.e. $M_1 = 0{,}0$ and $M_n = 0{,}0$).

$$M_{i+1} = M_i + \left(V_{i+1}\right)\left(x_{i+1}\right) \ldots i = 1, 2, 3, \ldots, n \tag{E.6}$$

Step 8: Calculate the moment of inertia, I_i, in bending for each interval and each diameter. Place the I value in column 8.

$$I_i = \frac{\pi\left(d_{sh\ i}^4 - d_{in\ i}^4\right)}{64} \ldots i = 1, 2, 3, \ldots, n \tag{E.7}$$

where

d_{sh} is the outside shaft diameter — bending, in millimetres (mm);

d_{in} is the inside shaft dimeter — bending, in millimetres (mm).

Step 9: Multiply each I_i value by the modulus of elasticity, E, and insert the EI_i value in column 9 on the same lines as the corresponding I_i values. Dividing the EI_i values by 10^3 before tabulating them in column 9 results in units of µm for the rest of the tabulation.

$$EI_i = (E)(I_i) \ldots i = 1, 2, 3, \ldots, n-1 \tag{E.8}$$

Step 10: Divide each bending moment M_i value in column 7 by the EI_i value in column 9 which precedes and follows it. List these values, MEI_{ui} and MEI_{li}, in column 10.

$$MEI_{ui} = \frac{M_i}{EI_i} \ldots i = 1, 2, 3, \ldots, n-1 \tag{E.9}$$

$$MEI_{li} = \frac{M_{i+1}}{EI_i} \ldots i = 1, 2, 3, \ldots, n-1 \tag{E.10}$$

Step 11: Obtain the average MEI values, $AMEI_i$, for each interval by averaging the values on the lines on which the station is listed and the following line. List the average values on the lines between stations in column 11.

$$AMEI_i = \frac{MEI_{ui} + MEI_{li}}{2} \ldots i = 1, 2, 3, \ldots, n-1 \tag{E.11}$$

Step 12: Calculate the slope value, SL_i, in column 12 starting with zero at station 1 (i.e., $SL_1 = 0$). Succeeding values are obtained by summing the products of $AMEI_i$ from column 11 and the x_i value on the next lower line of column 6. These values are listed on the same lines as the stations.

$$SL_i + 1 = SL_i + (AMEI_i)(x_i + 1) \ldots, i = 1, 2, 3, \ldots, n-1 \tag{E.12}$$

Step 13: Average the slope values in column 12 at the beginning and end of each interval. These values, ASL_i, are listed on the lines between stations in column 13.

$$ASL_i = \frac{SL_i + SL_{i+1}}{2} \ldots i = 1, 2, 3, \ldots, n-1 \tag{E.13}$$

Step 14: Obtain the deflection increment values, DI_i, in column 14 by multiplying the average slope value in column 13 and the x_i value from the next lower line in column 6.

$$DI_i = (ASL_i)(x_i + 1) \ldots i = 1, 2, 3, \ldots, n-1 \tag{E.14}$$

Step 15: Evaluate the integration constant, which depends on the type of shaft. For the simply supported shaft with no load outside of the supports as shown in Figure E.2, the constant is obtained by summing the deflection increment values in column 14 to obtain S_y. The sign of S_y is changed and the sum divided by the distance between the reaction, L_s, to obtain the integration constant per millimetre of length.

$$S_y = \sum_{i=1}^{n-1} DI_i \tag{E.15}$$

$$L_s = \sum_{i=1}^{n} x_i \tag{E.16}$$

$$IC = \frac{S_y}{L_s} \tag{E.17}$$

Other shaft configurations will change the integration constant.

Step 16: The integration constant for each section, ICS_i, is now calculated. Multiply integration constant IC calculated in step 15, by x_i value on the next lower line from column 6 to obtain the constant for each section. List these values in column 15 on the same line as the average slope and deflection increments.

$$ICS_i = (IC)(x_{i+1}) \ldots i = 1, 2, 3, \ldots, n-1 \tag{E.18}$$

Step 17: Column 16 is the calculated deflection. Place zero at left support location, i.e. $y_1 = 0{,}0$, because support locations must have zero deflection. For all other stations the deflection values are obtained by summing together the deflection increment and integration constant values from columns 14 and 15. These deflection values are inserted on the same line as the station. As a math check when summing the values of y_i, the calculated value at the right support location, y_n, should be very close to zero.

$$y_{i+1} = y_i + DI_i + ICS_i \ldots i = 1, 2, 3, \ldots, n-1 \tag{E.19}$$

E.2.2 Assumptions

When using the shaft bending deflection routine explained in E.2.1 to calculate load distribution, the following assumptions apply.

— This is a two-dimensional deflection analysis.

— Shear deflections are not included.

— The length between any two stations is critical to the accuracy of this calculation. Rules for station length are: no longer than 1/2 diameter of the station; no longer than 3 times the shortest section of the non-gear tooth portion of the shaft; no longer than 30 mm.

When in doubt about the number of stations, if adding more does not significantly change the calculation results, the number of original stations is adequate.

When calculating bending deflection for load distribution factor, the following rules also apply.

- Only forces acting in the base tangent plane of the subject mesh are considered.
- When calculating shaft deflections, the area of the gear teeth is broken into ten equal sections.
- The effective bending outside diameter of the teeth is the (tip diameter minus root diameter)/2 plus the root diameter.
- The moment couple applied to single helical gears due to the thrust component of tooth loading can be modelled as equal positive and negative forces at a location just to the left and right of the gear tooth area.

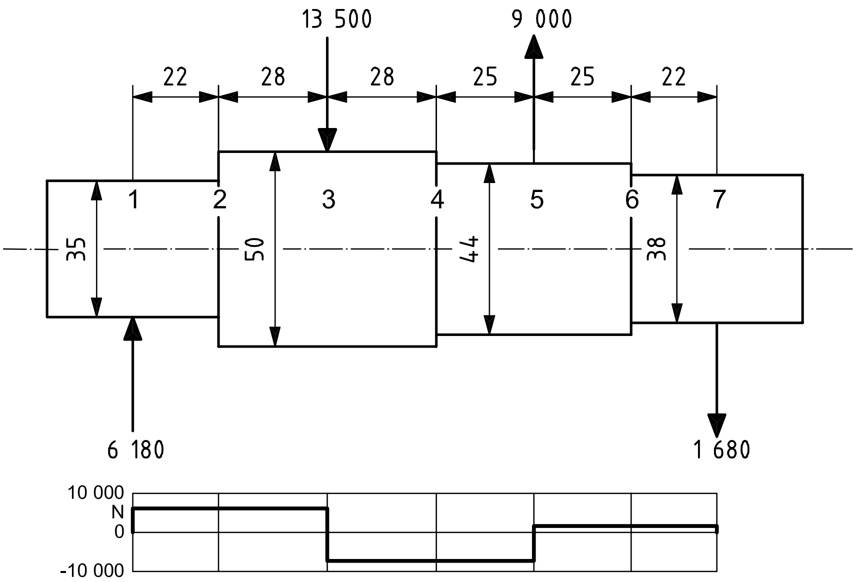

a) Shear diagram, V

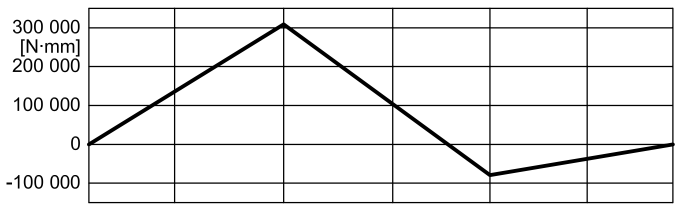

b) Moment diagram M

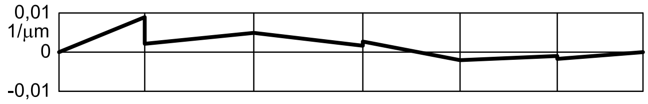

c) M / EI **diagram**

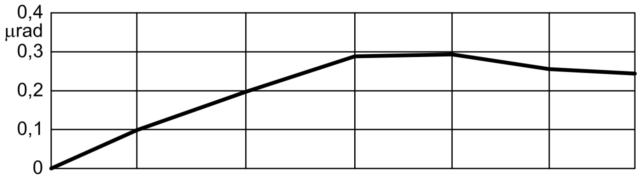

d) Slope curve

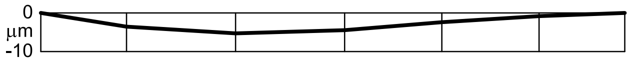

e) Deflection curve

Figure E.3 — Calculated shaft diagrams

E.3 Shaft torsional deflection

Meshing gear sets transmitting torque will also twist the shafts that carry the gear elements. The twist will cause deflection at the teeth that will affect the load distribution across their face width.

E.3.1 Torsional deflection

The torque input end is subjected to full torque. The torque value decreases along the face until it becomes zero at the other end. Hence the direction of torque path is of importance.

Consider a cylindrical shaft with circular cross section with outside effective twist diameter, d, inside diameter, d_{in}, and incremental length, X_{j}, as shown in Figure E.4.

The equation for torsional twist can be found in machinery design text. The torsional deflection must be calculated over the length of the tooth face. The twist must be converted from radians to a deflection in the base tangent plane. Equation (E.20) is in a form that allows summation using the discrete stations used in this document. This results in the equation:

$$t_{\delta \mathrm{i}} = \frac{\left(10^3\right)\left(\sum_{j=1}^{i} L_{\mathrm{j}}\right)\left(\sum_{j=1}^{i-1} X_{\mathrm{j}}\right) 4\, d^2}{G\pi\left(d^4 - d_{\mathrm{in}}^4\right)} \qquad \text{(E.20)}$$

where

- $t_{\delta\mathrm{i}}$ is the torsional deflection at a station, in micrometres (µm);
- L_{j} is the load at a station, in newtons (N);
- X_{j} is the distance between adjacent stations, in millimetres (mm);
- d is the effective twist diameter (see E.2.2), in millimetres (mm);
- d_{in} is the inside diameter, in millimetres (mm);
- i is the station number;
- G is the shear modulus (83 000 N/mm^2 for steel).

At the first point of interest on the tooth where $j = 1$, the summation of X_j will be zero and the torsional deflection is zero. Continued calculation of the torsional twist toward the end of the tooth face where torque is being applied results in a maximum torsional deflection, see Figure E.4.

Equation (E.20) is an approximation which yields reasonable results for gearing. The theoretically correct equation would be an integration.

A slightly more accurate approximation is found in Equation (E.21).

$$f_{\delta i} = \frac{\left(10^3\right)\left[\sum_{k=1}^{i-1}\left(\sum_{j=1}^{k} L_j X_k\right)\right] 8\, d^2}{G\pi\left(d^4 - d_{in}^4\right)} \qquad \text{(E.21)}$$

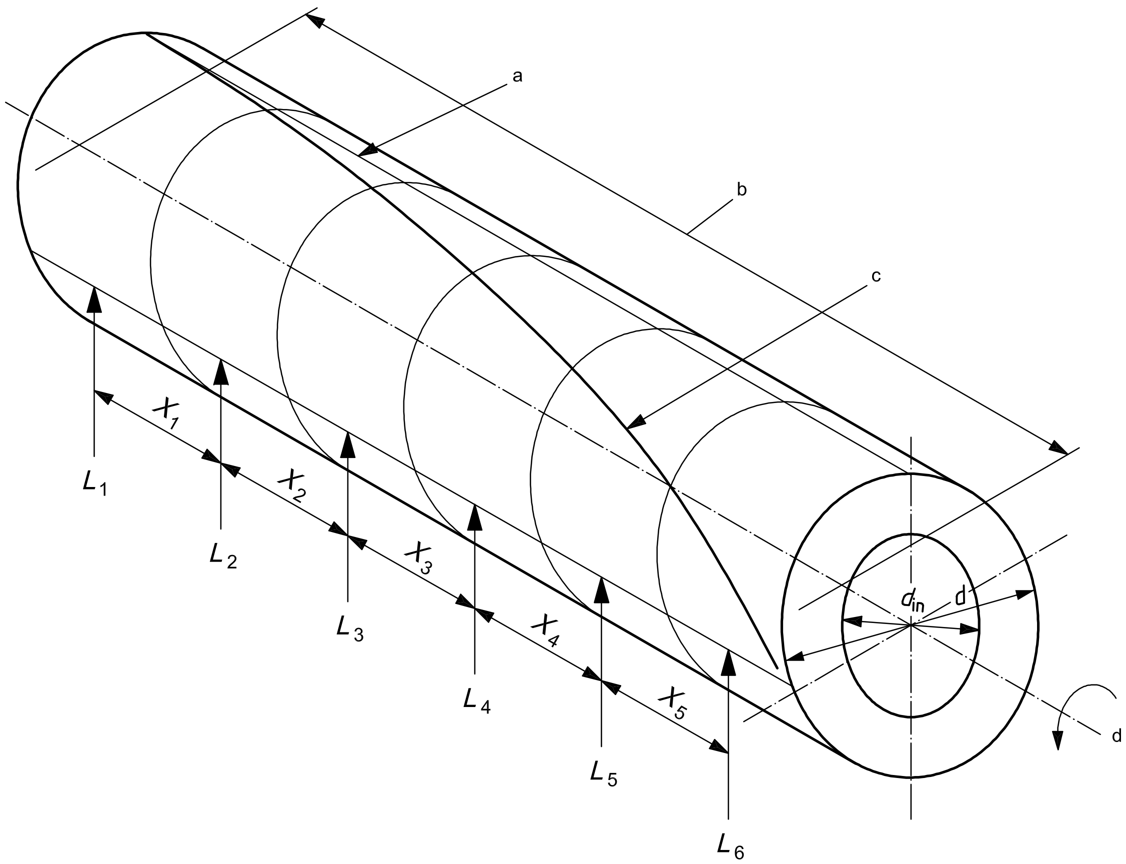

Key

L_i load on teeth

a Undeformed position.

b Face width.

c Torsional deflection.

d Torque input.

Figure E.4 — Torsional increments

E.3.2 Rules

Since the angle is small, it is assumed that the deflection in the base tangent plane is proportional to the twist angle.

The rules that apply to this shaft torsional deflection are

— the outside effective twist diameter of tooth section is the root diameter plus 0,4 times the normal module, and

— the twist of all elements except the target mesh being analyzed is ignored.

CAUTION — Equations (E.20) and (E.21) only cover torques in the target mesh that arise from gear tooth loading. Other torques may require additional modelling.

E.4 Gap analysis

Elastic bending and torsional deflections, tooth modifications, lead variations and shaft misalignments cause the gear teeth to not be in contact across the entire face width. The distance between non-contacting points along the face width of the mating teeth is defined as the gap. This gap is closed to some degree when the gear set is loaded due to the compliance of the gear teeth along the face width of the target mesh.

Bending deflection

Use the values obtained from the bending analysis for each shaft increment of the target mesh. Retain the positive or negative sign of the bending deflection.

Torsional deflection

Use the values from the torsional analysis for each shaft increment of the target mesh. Retain the positive or negative sign of torsional deflection.

Tooth modification

Tooth modification accounts for lead modification and crowning. The sign convention for tooth modification as illustrated in Table E.2 is the following: if the load direction on the teeth is positive, removal of metal at an individual station is entered as a positive value; if the direction of load on the teeth is negative, the removal of metal at an individual station is entered as a negative value.

Lead variation

The actual lead variation of the gear set is not available at the design stage. At this stage, lead variation based on the expected ISO 1328-1 tolerance of the gear set may be used. The lead variation must be incorporated so as to increase the total mesh gap (check both directions).

At final verification stage use actual lead variation measured for the gear set. The lead variation corresponding to material removal from the tooth flank has the same sign as the load on the tooth flank when it is entered in Table E.2.

Shaft misalignment

Shaft misalignment accounts for the error in concentricity of the bearing diameters on the shaft, bearing clearance, housing bore non-parallelism, etc. At design stage, values should be based on expected manufacturing accuracy. Incorporate expected shaft misalignment so as to increase mesh gap (check both directions).

Unless otherwise determined, values of f_{ma} described in 7.5.3 may be used.

At final verification stage, use actual shaft misalignment. The shaft misalignment that corresponds to material removal on the tooth flank has the same sign as the load on the tooth flank when entered in Table E.2.

Use the deflections, modifications, variations and misalignment values with proper positive or negative signs for each shaft of the target mesh to form Table E.2. In Table E.2 the shaft gap is the algebraic sum of all deflections, tooth modifications, lead variation and misalignment. The difference between the individual shaft gap positions is the total mesh gap. To evaluate load distribution by the iterative method, the relative gap is used. Relative mesh gap at each station of interest is obtained by subtracting the least total mesh gap from the total mesh gap at the station. The last column in Table E.2 reflects the relative mesh gap.

Table E.2 is an example of the mesh gap evaluated for mesh number 3 of general arrangement shown in Figure E.1.

Table E.2 — Evaluation of mesh gap for mesh No. 3, in micrometres (μm)

Station number	Shaft No. 3						Shaft No. 4						Total mesh gap	Relative mesh gap
	Bending deflection	Torsional deflection	Tooth modification	Lead variation	Shaft misalign-ment	Shaft No. 3 gap	Bending deflection	Torsional deflection	Tooth modification	Lead variation	Shaft misalign-ment	Shaft No. 4 gap		
8	11,8	–9,1	5,0	0,0	0,0	7,7	–12,8	8,6	0,0	0,0	0,0	–4,2	11,9	0,0
9	11,7	–8,9	3,5	0,3	0,8	7,4	–12,7	8,4	0,0	–0,3	–0,8	–5,4	12,8	0,9
10	11,5	–8,5	2,7	0,6	1,3	7,6	–12,6	8,0	0,0	–0,6	–1,3	–6,5	14,1	2,2
11	11,3	–7,9	2,0	0,8	1,8	8,0	–12,4	7,4	0,0	–0,8	–1,8	–7,6	15,6	3,7
12	11,0	–7,1	1,3	1,0	2,3	8,5	–12,1	6,6	0,0	–1,0	–2,3	–8,8	17,3	5,4
13	10,7	–6,1	0,7	1,3	2,8	9,4	–11,8	5,6	0,0	–1,3	–2,8	–10,3	19,7	7,8
14	10,3	–4,9	0,0	1,5	3,3	10,2	–11,4	4,4	0,0	–1,5	–3,3	–11,8	22,0	10,1
15	9,9	–3,5	0,0	1,7	3,8	11,9	–11,0	3,0	0,0	–1,7	–3,8	–13,5	25,4	13,5
16	9,5	–2,1	1,0	2,0	4,3	14,7	–10,5	1,6	0,0	–2,0	–4,3	–15,2	29,9	18,0
17	9,1	–0,8	3,5	2,2	4,8	18,8	–9,9	0,8	0,0	–2,2	–4,8	–16,1	34,9	23,0

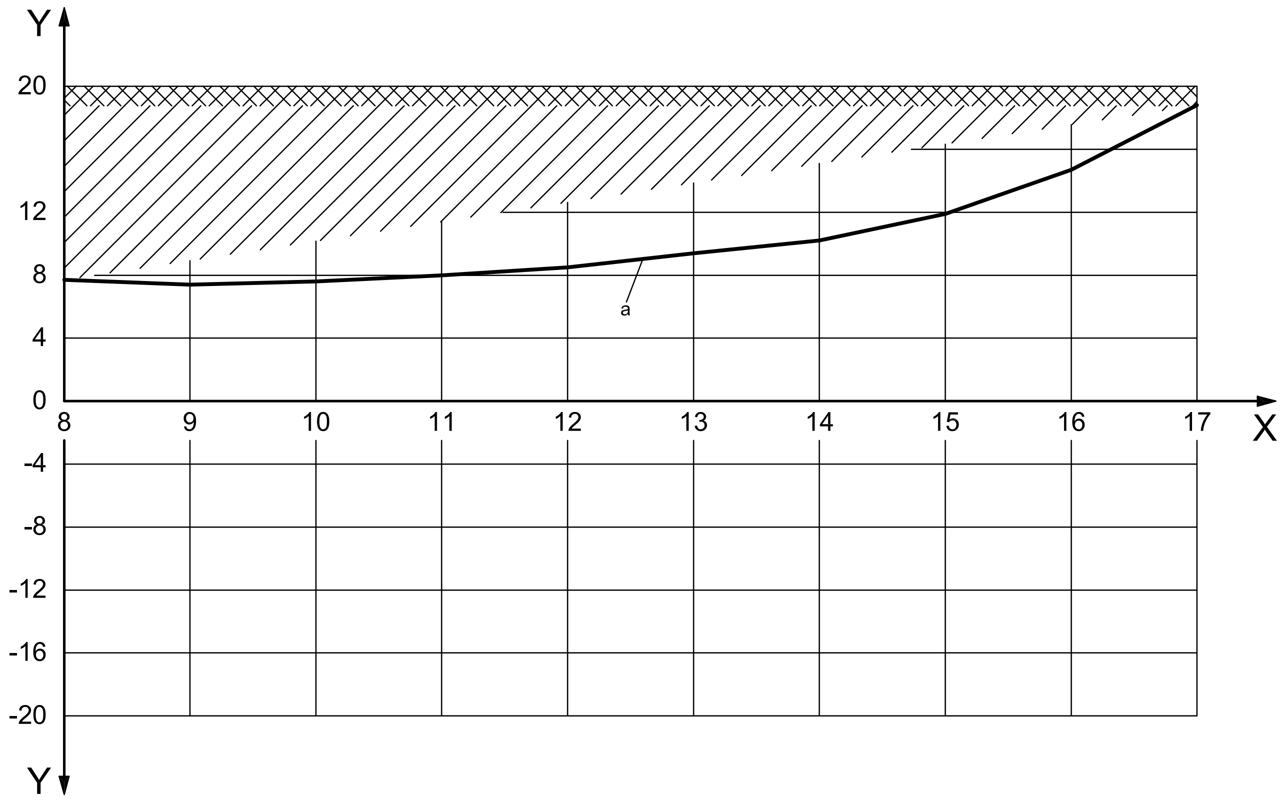

Key

X station number

Y mesh gap, µm

a Shaft No. 3.

Figure E.5 — Shaft No. 3 gap

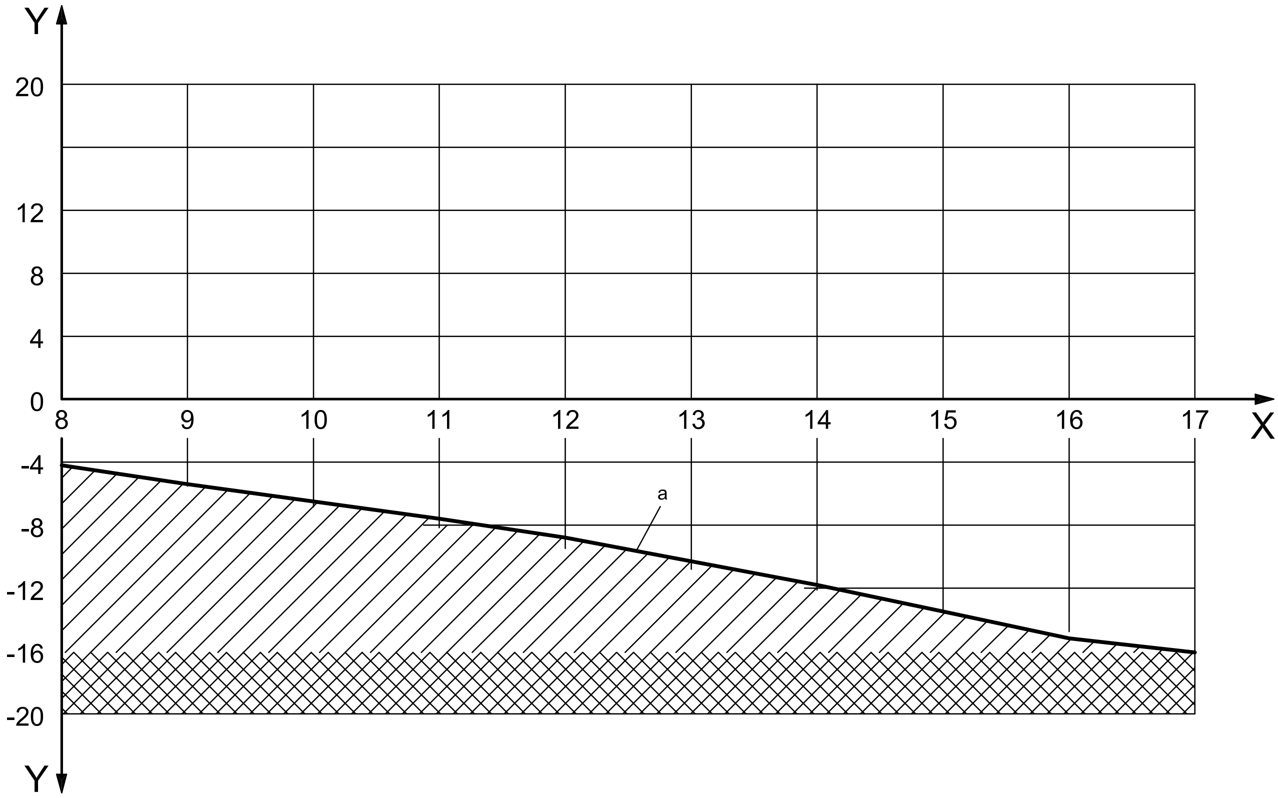

Key

X station number

Y mesh gap, µm

a Shaft No. 4.

Figure E.6 — Shaft No. 4 gap

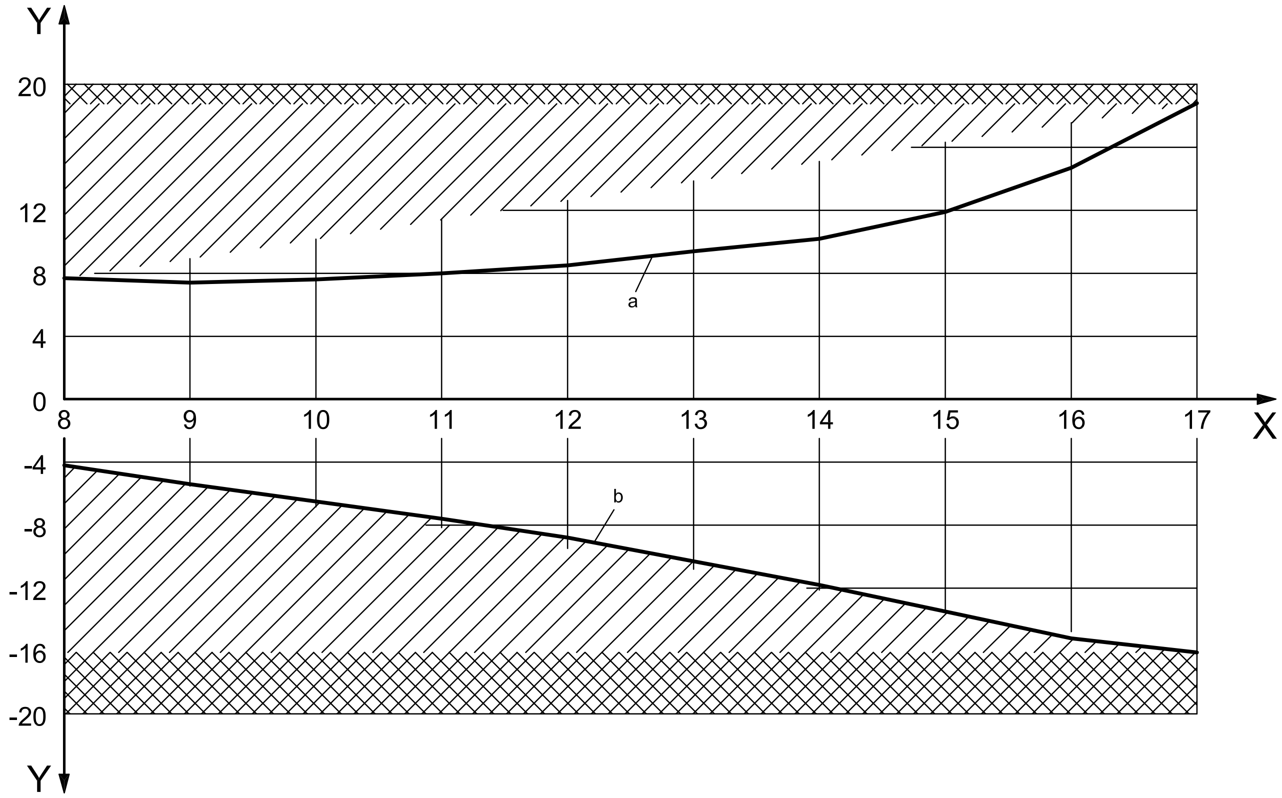

Key

X station number

Y mesh gap, µm

a Shaft No. 3.

b Shaft No. 4.

Figure E.7 — Total mesh gap

E.5 Load distribution

E.5.1 Tooth deflection

This method uses the concept of a tooth mesh stiffness constant, $C_{\gamma m}$, to compare the tooth load intensity and tooth deflection with the total load and overall mesh gap. For simplicity, the base tangent plane along the line of action is used and multiple teeth in contact are ignored. Effectively, the mesh is analyzed as if it were a spur set. For the purpose of illustrating this concept, this clause will use only 6 sections in the mesh area. Hertzian contact and tooth bending deflections are combined to produce a single mesh stiffness constant, $C_{\gamma m}$, and the mesh is assumed to be a set of independent springs (as shown in Figure E.8).

The tooth deflection at a given point is a linear function of the load intensity at that point and the tooth mesh stiffness as shown in Equation (E.22) below.

$$L_{\delta i} = \delta_{ti} \, C_{\gamma m} \tag{E.22}$$

where

$L_{\delta i}$ is the load intensity, in newtons per millimetre (N/mm);

δ_{ti} is the tooth deflection at a load point "i", in micrometres (µm);

$c_{\gamma m}$ is the stiffness constant, in newton millimetres per micrometre (N·mm/µm).

E.3 explains the methods used to calculate the mesh gap. This gap in the mesh must be accommodated by deflection of the teeth, δ_t, as shown in Figure E.8 and Equation (E.22).

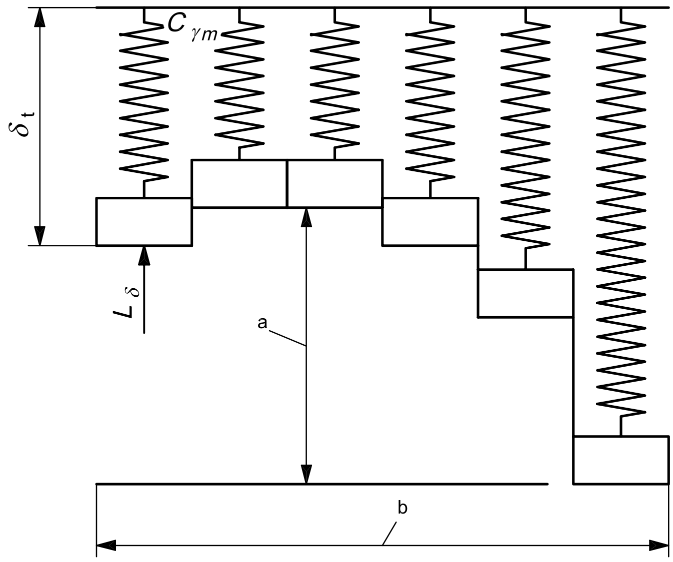

a Mesh gap, δ_i.

b Face width.

Figure E.8 — Tooth section with spring constant $C_{\gamma m}$, load L, and deflection δ

E.5.2 Mesh gap analysis

The mesh gap analysis divides the target mesh into discreet equal length sections, X_i, with point loads, L_i, applied in the centre of each of these sections (see Figure E.9). For double helical, analyze each helix separately. Since the method for calculating mesh gap uses point loads, while the tooth deflections per Equation (E.22) are based on load intensity, the point loads must be converted to load intensity. This is shown in Equation (E.23).

$$L_{\delta i} = \frac{L_i}{X_i} \qquad \text{(E.23)}$$

where

X_i is the length of face where the point load is applied;

L_i is the load at a specific point "i", in newtons (N);

$L_{\delta i}$ is the load intensity, in newtons per millimetre (N/mm).

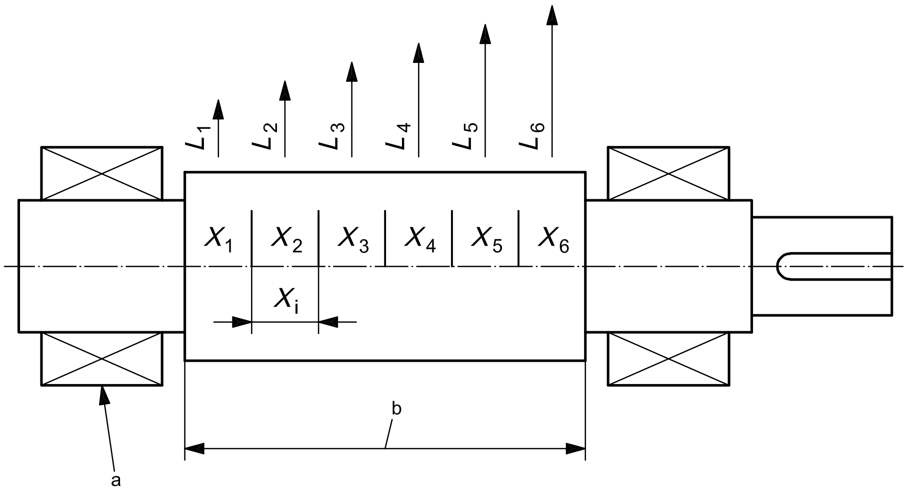

a Bearing.

b Face width.

Figure E.9 — Deflection sections

Note that load is not applied directly on the ends of the tooth. This should improve accuracy as mesh stiffness is generally lower at the ends of the teeth, but it is assumed constant in this analysis. Also note that the tooth is divided into equal-length sections such that all values of X_i are equal. In addition, the sum of the individual loads must equal the total load on the gearset as shown in Equation (E.24).

$$L_1 + L_2 + L_3 + ... + L_n = F_g \tag{E.24}$$

where

F_g is the total load in the plane of action, *BTP*, in newtons (N);

n is the total number of discrete sections across the face width.

The difference in load intensity between any two points, i and j, is proportional to the difference in mesh gap between these two points multiplied by the tooth stiffness constant. Notice the switch in terms. The absolute tooth deflection is not used, rather the change in mesh gap which is equal to the change in tooth deflection is used. Therefore, Equation (E.25) below can be derived from Equation (E.22) (see Figure E.10):

$$L_{\delta i} - L_{\delta j} = (\delta_i - \delta_j)\, C_{\gamma m} \tag{E.25}$$

In terms of the point loads used in the mesh gap analysis, Equation (E.25) may be rewritten as

$$\frac{L_i}{X_i} - \frac{L_j}{X_j} = (\delta_i - \delta_j)\, C_{\gamma m} \tag{E.26}$$

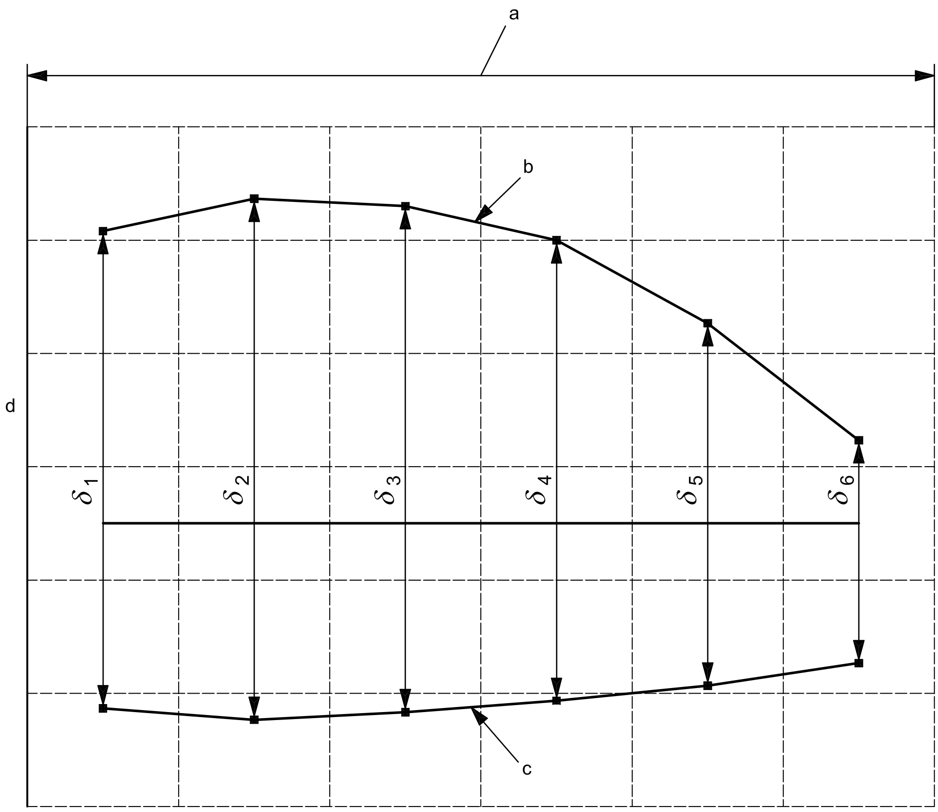

a Face width.

b Total pinion deflection.

c Total gear deflection.

d Mesh gap, δ_i.

Figure E.10 — Mesh gap section grid

E.5.3 Summation and load solution

Areas with greater mesh gap have lower tooth load and areas with lower mesh gap have higher tooth load. Using Figure E.10 as a guide, note that in Equation (E.26) as mesh gap, δ_i, gets larger, the load, L_i, must get smaller.

One location is selected as a reference, in this example it is location "1" (see Figure E.10). A sum of the values for all locations referenced to location "1" can then be created. This is done by setting term "j" in Equation (E.26) to location "1" and rearranging the equation as shown below:

$$\frac{L_i}{X_i} - \frac{L_j}{X_j} = (\delta_i - \delta_1)\, C_\gamma \tag{E.27}$$

or:

$$L_1 = X_1 \left(\frac{L_i}{X_i} - (\delta_i - \delta_1)\, C_{\gamma\,m} \right) \tag{E.28}$$

and:

$$L_i = X_i \left(\frac{L_1}{X_1} - (\delta_i - \delta_1)\, C_{\gamma m} \right) \tag{E.29}$$

Sum up the values for all locations using Equation (E.27) and obtain Equation (E.30) below. Remember, only one value of tooth stiffness, $C_{\gamma m}$, is used and the tooth face width is broken into equally spaced segments:

$$\left(\frac{L_1}{X_1}-\frac{L_1}{X_1}\right)+\left(\frac{L_2}{X_2}-\frac{L_1}{X_1}\right)+\ldots+\left(\frac{L_n}{X_n}-\frac{L_1}{X_1}\right)=\left[(\delta_1-\delta_1)+(\delta_2-\delta_1)+\ldots+(\delta_n-\delta_1)\right]C_{\gamma m} \quad \text{(E.30)}$$

Simplifying Equation (E.30) gives

$$\left(\frac{L_1}{X_1}+\frac{L_2}{X_2}+\ldots\frac{L_n}{X_n}\right)-\frac{nL_1}{X_1}=[(\delta_i-\delta_1)+(\delta_2-\delta_1)+\ldots(\delta_n-\delta_1)]\,C_{\gamma m} \quad \text{(E.31)}$$

The sum of all loads always equals the base tangent plane load, F_g, and all values of X_i are equal, so:

$$\left(\frac{L_1}{X_1}+\frac{L_2}{X_2}+\ldots\frac{L_n}{X_n}\right)=\frac{F_g}{X_n} \quad \text{(E.32)}$$

Solving the equations for the value of L_1 gives:

$$L_1=\frac{F_g}{i}-\frac{C_{\gamma m}\,X_i}{i}\left[(\delta_1-\delta_1)+(\delta_2-\delta_1)+\ldots+(\delta_n-\delta_1)\right] \quad \text{(E.33)}$$

Using Equation (E.29), the rest of the values for loads can be calculated.

E.5.4 K_H evaluation from loads

For the first iteration, a uniform load distribution across the mesh is assumed and gaps are calculated. From these initial gaps, an uneven load distribution is calculated. This new load distribution is then used to calculate a new set of gaps. This iteration process is continued until the newly calculated gaps differ from the previous ones by only a small amount. Usually only a few, 2 or 3, iterations are required to get an acceptable error (less than 3,0 µm change in gaps calculated).

The loads that correspond to the final iteration that results in negligible change in gaps calculated are then used to calculate the load distribution factor, $K_{H\beta}$. This is defined as the highest or peak load divided by the average load.

$$K_{H\beta}=\frac{L_{i\,peak}}{L_{i\,ave}} \quad \text{(E.34)}$$

where:

$$L_{i\,ave}=\frac{F_g}{n} \quad \text{(E.35)}$$

E.5.5 Partial face contact

Initially, all loads on the face width are assumed to be in the same direction, i.e. have the same sign. If there is not full contact across the face width some stations will have their load value change sign. This indicates tooth separation and there is no tooth contact at that location and, therefore, the load must be zero at that location. The method used to correct this condition relies on the difference in load between stations being a function of the change in deflection between stations. Therefore, even if a change in sign is calculated, the difference in load between stations with tooth contact will be correct.

To find the actual loads at these stations, do the following. Sum all the loads that had a change in sign and divide by the total number of loads that had a change in sign. Subtract this value from each load that did not have a change in sign. Set the value of load to zero at all stations that had a change in sign. The sum of loads at all stations that have contact will now equal the total load on the face width and the difference in load between these stations will not have changed.

E.5.6 Restatement of rules

The rules that govern the loads on the face width are the following.

— The sum of the individual loads on the face width, L_i, must equal the total load on the gearset, F_g.

— The change in load intensity, $L_i - L_j$, between any two locations on the face width must equal the change in tooth deflection, $\delta_{ti} - \delta_{tj}$, or change in mesh gap, $\delta_i - \delta_j$, between those locations.

— Areas on the face width with more mesh gap (mesh misalignment) have lower tooth load and areas with lower mesh gap (mesh misalignment) have higher tooth load.

— Areas where load changes sign represent areas where the teeth are not in contact and their sum must be included in the loads that did not change sign, i.e., $\sigma L_i = F_g$.

— The face width shall be divided into 18 sections for the actual gap analysis and load distribution factor calculations.

Bibliography

[1] HIRT M. *Einfluß der Zahnfußausrundung auf Spannung und Festigkeit von Geradstirnrädern*, Doctoral dissertation, Technische Universität München, 1976

[2] STRASSER, H. *Einflüsse von Verzahnungsgeometrie, Werkstoff und Wärmebehandlung auf die Zahnfußtragfähigkeit*, Doctoral dissertation, Technische Universität München, 1984.

[3] BROSSMANN, U. *Über den Einfluß der Zahnfußausrundung und des Schrägungswinkels auf Beanspruchung und Festigkeit schrägverzahnter Stirnräder*, Doctoral dissertation, Technische Universität München, 1979

[4] ANSI/AGMA 2001-C95, *Fundamental Rating Factors and Calculation Methods for Involute Spur and Helical Gear Teeth*, January 1995

[5] DIN 3990, *Grundlagen für die Tragfähigkeitsberechnung von Gerad- und Schrägstirnrädern*, Beuth Verlag GmbH, Berlin, Köln, 31, Dezember 1987

[6] JGMA 6101-01, *Calculation of Bending Strength for Spur and Helical Gears*, March 1988 (only in Japanese)

[7] JGMA 6102-01, *Calculation of Surface Durability (Pitting Resistance) for Spur and Helical Gears*, March 1989 (only in Japanese)

[8] TGL 10545, *Tragfähigkeitsberechnung von außenverzahnten Stirnrädern*, November 1988

[9] ISO 54:1977, *Cylindrical gears for general engineering and for heavy engineering — Modules and diametral pitches*

[10] ISO 701:1998, *International gear notation — Symbols for geometrical data*

[11] ISO/TR 10064-1, *Cylindrical gears — Code of inspection practice — Part 1: Inspection of corresponding flanks of gear teeth*

ICS 21.200

Price based on 109 pages